Interleukin-1 signaling in the blood-brain barrier influences the behavioral response to chronic social stress

Dissertation

Zur Erlangung des Grades

Doktor der Naturwissenschaften

Am Fachbereich Biologie

Der Johannes Gutenberg-Universität Mainz

Vorgelegt von

Eva Charlotte Schramm-Hermann

Geboren am 19. Juni 1993 in Darmstadt, Deutschland

Mainz, 2025

Dekan: Prof. Dr. Eckhard Thines

1. Berichterstatter:

2. Berichterstatter:

Tag der mündlichen Prüfung: 05.06.2025

TABLE OF CONTENTS

LIST OF ABBREVIATIONS

Abbreviation	Full name
ACK	Ammonium-chloride-potassium
ACTH	Adrenocorticotropic hormone
APCs	Antigen-presenting cells
BBB	Blood-brain barrier
BCSFB	Blood-CSF barrier
BDNF	Brain-derived neurotrophic factor
BECs	Blood-brain barrier endothelial cells
BSA	Bovine serum albumin
CCR	CC chemokine receptor
CLDN5	Claudin-5
COX	Cyclooxygenase
CRH	Corticotropin-releasing hormone
CSD	Chronic social defeat
CSF	Cerebrospinal fluid
CUS	Chronic unpredictable stress
CVS	Chronic variable stress
DAMPs	Damage-associated molecular patterns
DEGs	Differentially expressed genes
DPBS	Dulbecco's modified phosphate buffered saline
EAE	Experimental autoimmune encephalomyelitis
EDTA	Ethylendiaminetetraacetic acid
FACS	Fluorescence-activated cell sorting
FBS	Fetal bovine serum
FMO	Fluorescence minus one
FST	Forced swim test

GCs	Glucocorticoids
GFAP	Glial fibrillary acidic protein
GO	Gene ontology
h	hours
HBSS	Gibco Hank’s buffered saline solution
HPA	Hypothalamic-pituitary-adrenal
HPRT	Hypoxanthin-guanin-phosphoribosyltransferase
ICAM	Intercellular adhesion molecule
IFN	Interferon
IL	Interleukin
IL-1R1	Interleukin 1 receptor type I
IL-1R2	Interleukin 1 receptor type II
IL-1RAcP	Interleukin 1 receptor accessory protein
JAMs	Junctional adhesion molecules
KO	Knockout
LDPT	Light-dark preference test
LPS	Lipopolysaccharide
LRG1	Leucine rich alpha-2-glycoprotein-1
MACS	Magnetic-activated cell sorting
MAPK	Mitogen-activated protein kinase
max	maximum
MDD	Major depressive disorder
MFG-E8	Milk fat globule-EGF factor 8 protein
MFI	Mean fluorescence intensity
min	minutes
mPRα	Membrane progesterone receptor alpha
NA	Noradrenaline

NF-κB	Nuclear factor 'kappa-light-chain-enhancer' of activated B cells
No.	Number
NVU	Neurovascular unit
PAMPs	Pathogen-associated molecular patterns
PCR	Polymerase chain reaction
PECAM	Platelet endothelial cell adhesion molecule
PFA	Paraformaldehyde
PRR	Pattern recognition receptors
PTSD	Post-traumatic stress disorder
qPCR	Quantitative real-time PCR
REVs	Reactive endothelial venules
RSD	Repeated social defeat
SAS	Subarachnoid space
SEM	Standard error of the mean
SI	Social interaction
SNP	Single-nucleotide polymorphism
SNS	Sympathetic nervous system
SPF	Specific pathogen-free
SSRIs	Selective serotonin reuptake inhibitors
TAE	Tris-acetate-EDTA
TAP	Transporter associated with antigen processing
TARC	Translational animal research center
TLR	Toll-like receptor
TNF	Tumor necrosis factor
VCAM	Vascular cell adhesion molecule
VE-cadherin	Vascular endothelial cadherin
ZO	Zonula occludens

1 INTRODUCTION

1.1 Major depressive disorder (MDD)

Mental disorders are a major global health burden, with depressive and anxiety disorders ranking among the top 25 health burdens worldwide in 2019 [1]. Furthermore, it was predicted that by 2030, major depressive disorder (MDD), the classic, most common form of depression, would become the leading cause of disability worldwide [2]. In 2021, 6.4% of the population of over 27 European countries reported to be currently suffering from a depressive disorder [3]. MDD is therefore affecting one out of six adults at some point during their lifetime [4]. MDD is characterized by persistent sadness and feelings of hopelessness, worthlessness, or guilt, as well as by anhedonia, a reduced ability to experience pleasure [5]. Other common symptoms include difficulties in concentrating, disturbed sleep and appetite, low energy levels and recurrent thoughts of death and suicide [5, 6]. In addition to the burden of these disease symptoms themselves as well as the risk of suicide, MDD is associated with a higher risk for the development of other medical conditions such as cardiovascular diseases and stroke [2]. The etiology of MDD remains incompletely understood, with genetics being estimated to contribute only 35% [4]. Social and environmental factors increase the risk of developing depression, among them are e.g., childhood adversity [7], illness or loss of close relatives or friends, financial problems and unemployment, low socioeconomic status and low social support [8, 9]. It is well established that depressive episodes often occur in the context of stressful life events [5]. However, stress alone is not necessarily sufficient to cause MDD, which is rather caused by the interplay between environmental factors and genetic predisposition [5]. In contrast, post-traumatic stress disorder (PTSD) is directly caused by the exposure to extremely stressful life event such as combat, sexual abuse, or natural disasters [10]. Nevertheless, also in PTSD, genetic and social factors, previous stressful life events and biological processes influence individual disease susceptibility [10].

Patients suffering from MDD show chronically increased activity in specific brain region such as the amygdala, the prefrontal cortex, and the nucleus accumbens, which is restored to normal levels upon successful antidepressant treatment [6]. Furthermore, structural and functional alterations of the hippocampus and the prefrontal cortex were observed in depressed patients [11, 12]. These brain regions have in common that they receive monoamine projections, namely dopamine, serotonin and noradrenaline input, which explains why many antidepressants act by acutely increasing the availability of monoamines [13]. Another biological mechanism associated with depression is a reduction in neurotrophins, growth factors that regulate

plasticity in the adult brain such as brain-derived neurotrophic factor (BDNF) [14]. Interestingly, one of the mechanisms of action of antidepressants is to increase adult hippocampal neurogenesis, a process also influenced by BDNF [6].

1.2 Chronic stress as a major risk factor for depression

Chronic stress is defined by the National Institute of Mental Health as part of the research domain criteria [15] as the "sustained threat" construct [16] which is described as the following: "An aversive emotional state caused by prolonged (i.e., weeks to months) exposure to internal and/or external condition(s), state(s), or stimuli that are adaptive to escape or avoid. The exposure may be actual or anticipated; the changes in affect, cognition, physiology, and behavior caused by sustained threat persist in the absence of the threat, and can be differentiated from those changes evoked by acute threat." [17]. As already indicated in this definition, exposure to chronic stress often leads to pathological changes in the behavior of an individual which persist even after the end of chronic stress exposure. A substantial body of evidence links the onset of MDD to the previous occurrence of major stress events with 80% of depression cases being preceded by stressful life events [18]. Furthermore, exposure to chronic stress events (ongoing for more than 12 months) was more strongly correlated with the development of depression than the exposure to acute stressors [19]. Similarly, chronic adverse or challenging situations, such as poverty, medical disabilities or having a disabled child, were also linked to an increased risk of developing depression [20, 21]. Along the same lines, the exposure to childhood trauma is one of the strongest risk factors for developing MDD, with estimations that between 25% to 75% of MDD patients have experienced childhood trauma [22, 23]. Therefore, exposure to chronic social, psychological, or physical stress is commonly used as a model to study the mechanisms underlying depression [24].

The exact mechanism by which chronic stress leads to the development of depression is not yet fully understood. However, it seems to be an interplay of different mechanisms in which the sympathetic nervous system (SNS) and the hypothalamic–pituitary–adrenal (HPA) axis play a major role (Fig. 1). Exposure to stress activates components of the limbic system such as the amygdala, prefrontal cortex, hippocampus, and hypothalamus leading to the activation of the SNS [25]. Nerve fibers of the SNS stimulate the medulla of the adrenal gland to release adrenaline into the circulation and also directly release noradrenaline into primary and secondary lymphoid organs and peripheral tissues [26]. In addition, stress exposure activates neurons in the hypothalamus which secrete vasopressin and corticotropin-releasing hormone

(CRH), which in turn stimulate the secretion of adrenocorticotropic hormone (ACTH) from the pituitary gland [27, 28]. ACTH stimulates the release of glucocorticoid hormones, cortisol in humans and corticosterone in rodents, from the adrenal cortex into the circulation [27]. This process is known as HPA axis activation. Therefore, the experience of stressful situations has two main outcomes: (1) increases in systemic levels of adrenaline and noradrenaline and (2) release of glucocorticoid hormones from the adrenal gland into the bloodstream [28] (Fig. 1). Glucocorticoids can then bind to glucocorticoid receptors and induce gene expression changes important for the stress response, and, in addition, also terminate the stress response by initiating a negative feedback loop that inhibits HPA axis activity [29]. However, during chronic stress and in stress-induced psychiatric disorders, a glucocorticoid receptor resistance develops leading to HPA axis hyperactivity and chronically elevated cortisol levels in the majority of MDD patients [30]. Increased glucocorticoid levels affect brain neuroplasticity [29], since glucocorticoids are known to be involved in the regulation of neuronal survival, neuronal excitability and neurogenesis [31]. Therefore, glucocorticoid receptor antagonists are currently being tested as a treatment for MDD patients with childhood trauma [22]. Another potential link between stress and depression is BDNF, since BDNF levels are decreased in the hippocampus after stress exposure thereby negatively affecting neuroplasticity [14]. Interestingly, this stress effect was reversed by antidepressant treatment [14]. Furthermore, glucocorticoid resistance also seems to be linked to increased levels of inflammation in depressed patients [32]. Signs of glucocorticoid resistance and higher levels of pro-inflammatory cytokines were found in the blood of depressed patients compared to healthy controls [33]. This increased inflammation seems to correlate directly with the exposure to chronic stress, e.g., the exposure to early-life adversities leads to a pro-inflammatory state during adulthood [34, 35].

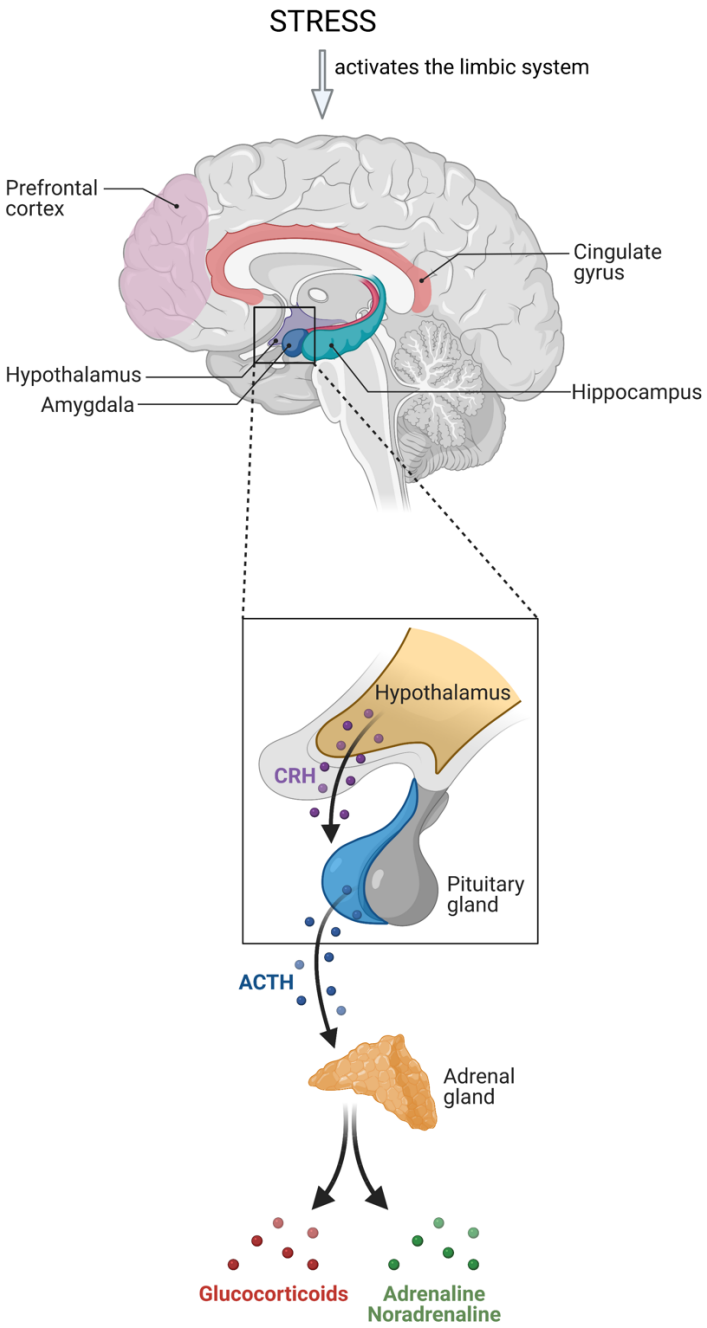

Figure 1: Stress exposure induces activation of the sympathetic nervous system (SNS) and the hypothalamic-pituitary-adrenal (HPA) axis

In stressful situations, brain regions of the limbic system become activated, leading to the activation of the SNS. The SNS then induces the release of adrenaline and noradrenaline from the adrenal gland into the circulation. Furthermore, stress induces the release of corticotropin-releasing hormone (CRH) from neurons in the hypothalamus, which stimulates the release of adrenocorticotropic hormone (ACTH) from the pituitary gland. ACTH then induces the release of glucocorticoids (GCs) from the adrenal cortex into the circulation.

Figure from Schramm & Waisman, 2022 [28]

1.3 The link between chronic stress, depression and inflammation

1.3.1 Mechanisms by which chronic stress induces inflammation

Direct evidence for the activation of inflammatory pathways in human subjects in stressful situations was provided by a study in which the activity of the nuclear factor 'kappa-light-chain-enhancer' of activated B-cells (NF-κB) was analyzed in the peripheral blood mononuclear cells of volunteers that were subjected to a short stress test [36]. In most volunteers, stress exposure caused rapid NF-κB activation together with increases in catecholamine and cortisol levels [37].

The two neuroendocrine pathways induced by stress, namely the SNS and the HPA axis, both have immunomodulatory functions [26] (Fig. 2). Noradrenaline and adrenaline released by the SNS can bind to adrenergic receptors on leukocytes, which induces pro-inflammatory programs via the NF-κB pathway [26]. Furthermore, noradrenaline released into the bone marrow during chronic stress induces hematopoietic stem cell proliferation leading to a higher release of neutrophils and inflammatory monocytes into the circulation [38]. Similarly, also glucocorticoid signals seem to contribute to the enhanced release of monocytes from the bone marrow into the circulation during chronic stress [39]. Glucocorticoids are traditionally regarded as anti-inflammatory molecules and have been widely used as treatments for inflammatory disorders. However, under steady-state conditions, glucocorticoids also play a role in priming the innate immune system to ensure its readiness to respond to pathogens [40]. The effects of glucocorticoids therefore seem to be influenced by the duration of exposure and basal state of the immune system at the time of exposure [41]. Under physiological conditions, glucocorticoids can have pro-inflammatory functions and ensure proper immune system function, while during pathological inflammation, they function as anti-inflammatory molecules to restrict inflammatory processes [41]. This also seems to explain why glucocorticoids can have pro-inflammatory functions in the context of stress [41].

In addition to the activation of the SNS and the HPA axis, stress can also cause inflammation via the activation of the inflammasome pathway by “sterile” stressors, the endogenous damage-associated molecular patterns (DAMPs), such as ATP, heat shock proteins, uric acid, high mobility group box 1 (HMGB1) and molecules linked to oxidative stress [42]. These DAMPs are induced by psychological and physiological stressors, e.g., by stressors used in animal models of stress [43], which leads to inflammasome activation and cleavage of the precursor forms of interleukin (IL)-1β and IL-18 into the active cytokines.

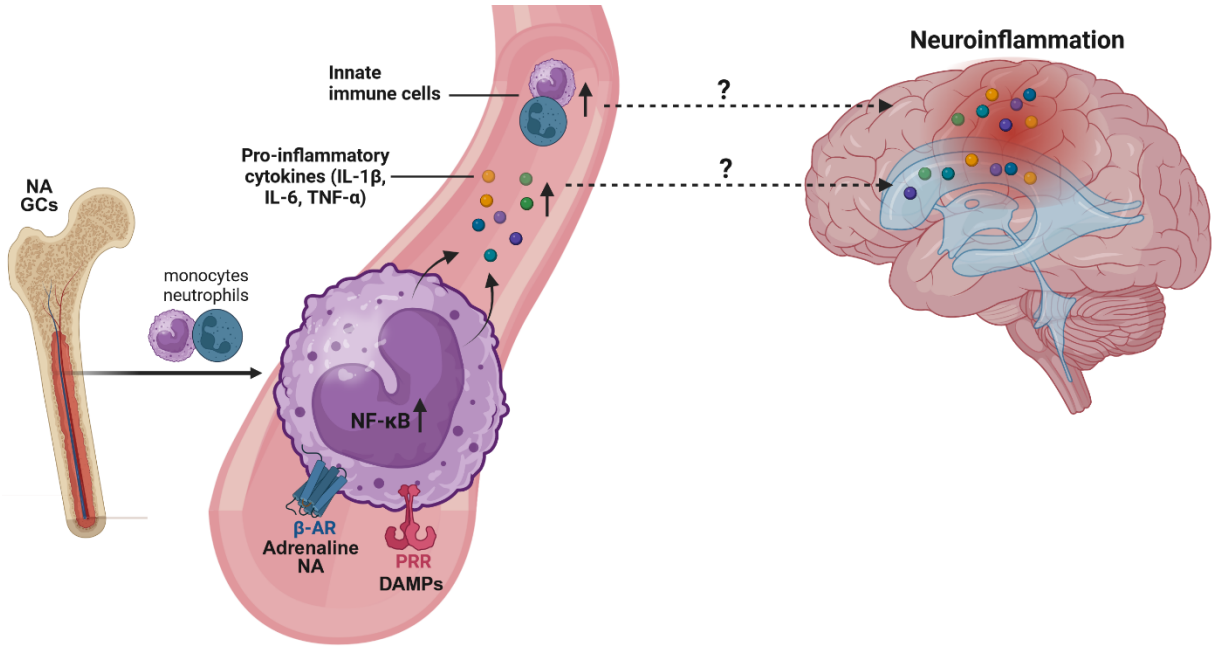

Figure 2: Adrenaline, noradrenaline, and glucocorticoids induce pro-inflammatory responses during stress
Noradrenaline (NA) and glucocorticoid (GC) signals in the bone marrow induce an enhanced release of monocytes and neutrophils into the circulation during chronic stress. Furthermore, noradrenaline and adrenaline can directly bind to β-adrenergic receptors (β-AR) on leukocytes which causes an activation of the pro-inflammatory NF-κB pathway. Also endogenous damage-associated molecular patterns (DAMPs) contribute to the inflammatory response during stress via the activation of pattern-recognition receptors (PRRs) on myeloid cells. Overall, chronic stress exposure thereby leads to an increased abundance of monocytes and neutrophils in the circulation, as well as to elevated levels of the pro-inflammatory cytokines interleukin (IL)-1β, IL-6, and tumor necrosis factor (TNF)-α. The exact cause of neuroinflammation during chronic stress remains incompletely understood.

1.3.2 Evidence for inflammation in depression

MDD patients exhibit increased levels of the pro-inflammatory cytokines IL-1β, IL-6 and tumor necrosis factor (TNF)-α in the blood, show increases in the relative abundance of innate immune cells and exhibit decreased adaptive immune responses [44]. In addition, pro-inflammatory cytokines are increased in the cerebrospinal fluid (CSF) of MDD patients, either by penetration of cytokines through the blood-brain barrier (BBB) or by direct production from glia cells within the brain, and microglia show increased levels of activation [44, 45]. In post-mortem brain samples of depressed individuals who committed suicide, elevated levels of IL-1β, IL-6, TNF-α, Toll-like receptor (TLR)-3 and TLR-4 were found [42]. Furthermore, several longitudinal human studies showed that high levels of inflammation (high IL-6 or C-reactive protein (CRP) levels) could predict that these patients were more likely to develop depression in the following years [46-48]. Interestingly, patients with the highest IL-6 levels were also found to be the least likely to respond to antidepressant treatment [49]. Along the same lines,

treatment with pro-inflammatory cytokines, such as with interferon-α (IFN-α) for the treatment of chronic hepatitis, often causes the development of depressive symptoms [50, 51]. In a genome-wide association study, the analysis of single-nucleotide polymorphisms (SNPs) from a MDD patient cohort revealed an enrichment of 19 pathways, including genes involved in cytokine and immune response [52]. SNPs in the IL-6 receptor promoter region and in *P2RX7,* a mediator of innate immune activation, have been associated with altered susceptibility to the development of depression [53, 54]. Nevertheless, up to now, it is still debated whether immune system activation is causal for the development of depression, or whether depression rather causes impairment of the immune system which in turn leads to an increased vulnerability to infectious diseases [55]. Furthermore, only a subgroup of MDD patients shows elevated levels of inflammatory markers [56, 57] questioning a general role of the immune system in the etiology of depression.

1.3.3 Potential mechanisms by which inflammation could lead to depression

For peripheral inflammation to influence behavior, it must first be translated into the brain. Three pathways of how peripheral inflammatory signals could be transmitted into the brain have been described in the literature: (1) Cytokines can pass through leaky regions in the BBB, such as the circumventricular organs, or can be transported into the CNS by transporters on the BBB. (2) Cytokines can bind to peripheral nerves such as the vagus nerve which causes stimulation of catecholaminergic fibers in the brain. (3) Activated immune cells, such as monocytes can traffic to the brain vasculature and, potentially, into the brain parenchyma [42]. Interestingly, a similar observation was made in post-mortem MDD brain tissue, in which the proportion of blood vessels surrounded by a high density of macrophages was much higher in the dorsal anterior cingulate cortex of depressed patients who committed suicide than in healthy controls [58]. In addition, microglia also get activated during the stress response, probably by a combination of direct effects of adrenergic signals, pro-inflammatory cytokines and DAMPs released locally within the CNS [28].

The ability of the immune system to modulate behavior is nicely illustrated by the so-called “sickness behavior”, a behavioral response to infection or, as an animal model, to the administration of lipopolysaccharide (LPS), leading to behavioral symptoms such as anhedonia, decreased activity and social withdrawal caused by pro-inflammatory cytokines such as IL-1β, IL-6 and TNF-α [55]. This sickness behavior most likely represents an evolutionary strategy to ensure survival, since it ensures saving energy resources for infection and wound healing [42].

Mechanistically, pro-inflammatory cytokines seem to modulate behavior via different processes. They can reduce the levels of available monoamines (serotonin, noradrenaline and dopamine) by increasing the reuptake of serotonin [59] or by decreasing the synthesis of monoamines [60]. Cytokines such as IFN-γ and TNF-α also increase the expression of indoleamine 2,3-dioxygenase (IDO) which metabolizes tryptophan to kynurenine at the expense of serotonin synthesis leading to an imbalance of these metabolites that is associated with depression [44]. Altogether, these mechanisms lead to a reduced availability of serotonin which has been linked to the development of depression since the 1960s [61] and constitutes a major target of antidepressants. Other mechanisms by which pro-inflammatory cytokines can modulate mood and behavior include: (1) influences on neuroplasticity through inhibition of neurogenesis and by the induction of neurotoxicity [62-65], (2) the remodeling of dendrites [44], and (3) the modulation of neuron-glia cell interactions [44].

1.4 Immunomodulatory drugs as a treatment option for MDD

Current treatments for MDD only lead to remission in about one third of patients and to partial remission in another third of the patients leaving about one third of the patients unresponsive [66, 67]. In general, patients are treated for MDD with psychotherapy, pharmacotherapy, lifestyle interventions such as exercise, or brain stimulation through electroconvulsive therapy [68, 69]. In many cases, a combination of these approaches leads to a greater treatment efficacy than one treatment alone [68]. The most used pharmacological agents to treat depression are tricyclic antidepressants and monoamine reuptake inhibitors including selective serotonin reuptake inhibitors (SSRIs) and reuptake inhibitors targeting noradrenaline and dopamine, as well as second-generation psychotics [68]. SSRIs such as fluoxetine and citalopram remain the gold-standard for the treatment of depression and are recommended as the first-line treatment for patients with MDD, since they show a high efficacy and fewer side effects than tricyclic antidepressants [69]. In addition, neurotransmitter reuptake inhibitors that target not only serotonin, but also other monoamines (noradrenaline and dopamine), are commonly prescribed to patients who do not respond to SSRIs [69]. For patients suffering from treatment-resistant depression, alternative therapies that modulate neuronal activity are available or being tested [70]. These include transcranial electrical stimulation and deep brain stimulation, as well as magnetic field therapy which often impact the circuitry of the prefrontal cortex [70].

Several immune system-targeting compounds have been evaluated for their potential antidepressant effects; this was often done by analyzing changes in depressive symptoms in

patients treated for a primary immunological disorder [44]. Among the immune system targets tested to date are prostaglandins, TNF-α, IL-6, IL-12/23, IL-23, p38 mitogen-activated protein kinase (MAPK) and B cell-related targets such as CD20 [44]. In a mega-analysis of patient data from 18 randomized clinical trials, anti-IL-6 antibodies and an anti-IL-12/23 antibody showed a good efficacy for the improvement of depressive symptoms in a cohort of patient with high depressive symptoms [71]. Some of the other immunomodulatory drugs have also successfully improved depressive symptoms; however, the analysis of comorbid depressive symptoms in the presence of a primary immunological disorder in these studies makes it difficult to draw clear conclusions [44].

To avoid these difficulties, studies are needed in which the effects of immunomodulatory drugs are directly tested in MDD patients. Unfortunately, to date, these studies have been rather scarce. In a clinical trial of a monoclonal anti-TNF-α antibody to treat MDD, the TNF-α antibody showed an effect similar to that of standard antidepressants; however, only in a subgroup of patients with high levels of inflammation, indicating that immune system-targeting compounds will most likely only be effective in MDD patients who exhibit elevated baseline inflammatory markers [57]. Similarly, also treatment with an anti-IL-6 antibody slightly improved anhedonia symptoms in a MDD patient cohort with high plasma CRP levels [44]. Minocycline, a brain-penetrant anti-inflammatory molecule that inhibits the activation of T cells, neutrophils and microglia and the release of pro-inflammatory cytokines, has also been tested for its potential antidepressant effects in several studies, but with very heterogeneous results [44]. Taken together, immunomodulatory treatments are a promising option for MDD patients with evidence of immune dysfunction related to the pathway targeted by the immunomodulatory drug and for patients suffering from comorbid depressive symptoms [44].

1.5 Central nervous system barriers

1.5.1 The different barriers of the central nervous system

The CNS has historically been regarded as an “immune-privileged site”, based on early observations that tissue grafts implanted in the CNS survive without being rejected by the immune system [204]. This immune privilege is attributed to the inability of antigen-presenting cells (APCs) to migrate from the CNS parenchyma to local lymph nodes for antigen presentation [72], since the complex barrier system of the CNS only allows clearance of small, soluble compounds, including small antigens, from the CNS parenchyma into the CSF [73]. From the CSF, fluid and immune cells can reach deep cervical lymph nodes through CNS-draining lymphatic vessels, which were rediscovered in recent years [74]. Despite these barriers, certain immune surveillance mechanisms are active in the CNS. They are carried out at the CNS interfaces by myeloid cells positioned in the meninges, perivascular spaces and the choroid plexus, as well as by memory T cells circulating through the CSF [72].

The CNS is enclosed by three membranous layers called the meninges, which shield the CNS parenchyma from the CSF and the surrounding skull (Fig. 3). The outermost layer, the dura mater, is a fibrous membrane containing blood vessels and lymphatics. Beneath it lies the arachnoid mater, which is impermeable for liquids and interfaces with the CSF in the subarachnoid space (SAS). The pia mater, the innermost meningeal layer, lines the other side of the SAS and envelops blood vessels that run through the subarachnoid space. Below the pia mater, the CNS surface is coated by the glia limitans, a structure composed of astrocyte endfeet and a basement membrane. The movement of solutes, molecules and immune cells from blood vessels into the CNS parenchyma is tightly regulated by the specialized properties of the BBB. In addition, a blood-CSF barrier (BCSFB) regulates the passage of substances and cells between the blood and the CSF.

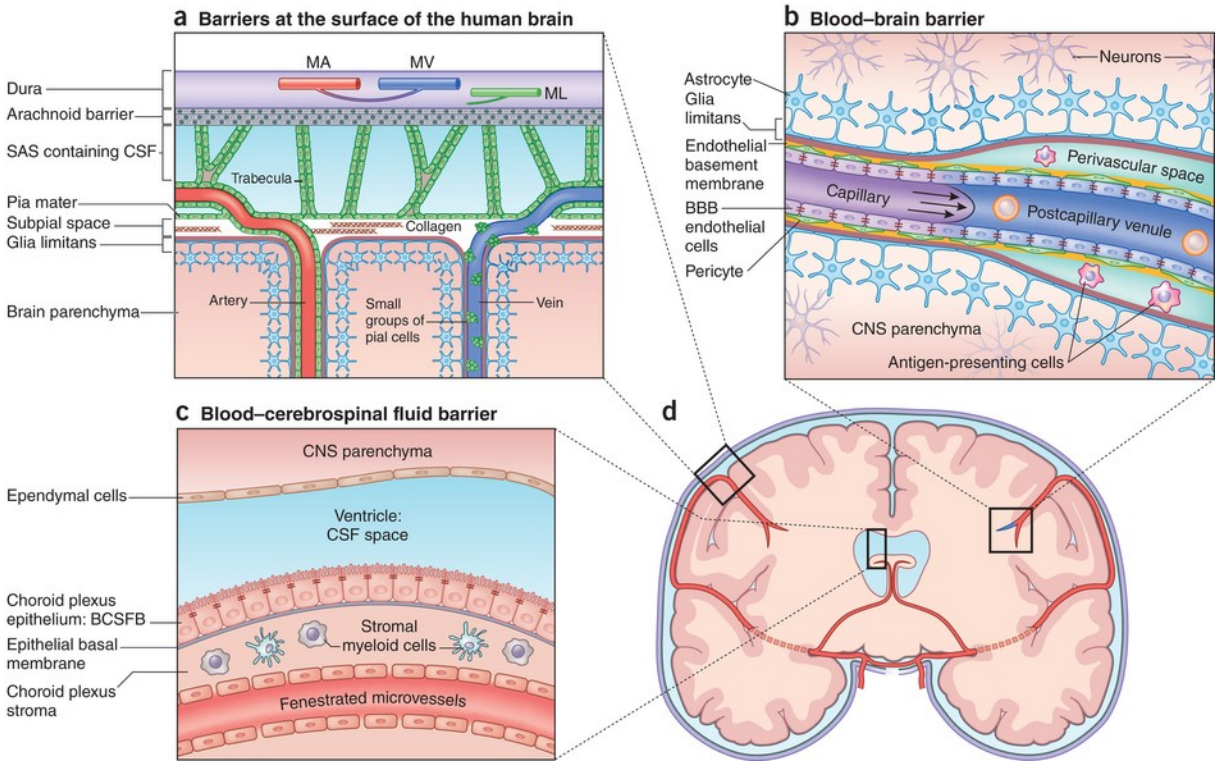

Figure 3: Barriers of the CNS

(a) The dura mater separates the brain from the skull and contains meningeal arteries (MA), meningeal veins (MV) and meningeal lymphatics (ML). The arachnoid mater separates the dura from the cerebrospinal fluid (CSF) in the subarachnoid space (SAS). The pia mater is the inner border between the SAS and the CNS parenchyma and coats the blood vessels in the SAS and the arteries that enter the brain. The glia limitans is as an additional border shielding the CNS parenchyma from blood vessels and the surface. (b) The blood-brain barrier (BBB) is located in capillaries and postcapillary venules and is formed by endothelial cells, an endothelial basement membrane containing pericytes, and the glia limitans. (c) The blood-CSF barrier (BCSFB) in the choroid plexus separates the CSF-containing brain ventricles from the blood. The BCSFB consist of the choroid plexus epithelium and its basement membrane. The choroid plexus stroma contains different myeloid cell populations. (d) Coronal brain section shows the image areas that are magnified in a, b, and c.

Figure from Engelhardt *et al*., 2017 [75]

1.5.2 The blood-brain barrier (BBB)

The term “blood-brain barrier” describes the specialized characteristics of CNS blood vessels rather than a discrete anatomical structure [76]. It is established by the unique properties of BBB endothelial cells in CNS microvessels, which tightly regulate the selective exchange of solutes and cells between the blood and the CNS. This regulation protects the CNS from harmful substances while ensuring optimal neuronal function.

Endothelial cells, the most critical cell type of the BBB, interact with mural, glial, neural and immune cells within the “neurovascular unit” (NVU). Unlike endothelial cells in other tissues,

BBB endothelial cells are tightly interconnected by tight junctions and adherens junctions (Fig. 4B), strongly restricting paracellular diffusion. Additionally, transcellular transport is minimal due to very low rates of transcytosis [77]. BBB endothelial cells also express a unique combination of ion channels and transporters, which play a crucial role in maintaining the CNS environment essential for optimal synaptic function [78].

Adherens junctions are the basic adhesions between endothelial cells and are formed by vascular endothelial cadherin (VE-cadherin) and catenins [76]. Platelet endothelial cell adhesion molecule (PECAM)-1, also known as CD31, is critical for adherens junction formation [79] and BBB integrity, as evidenced by increased BBB leakiness in PECAM-1-deficient mice in experimental autoimmune encephalomyelitis (EAE), a mouse model for Multiple Sclerosis [80]. Tight junctions are cell adhesions formed by multiple transmembrane proteins that interact with each other. CNS endothelial cells have a specific combination of tight junction proteins that are responsible for the low paracellular permeability of the BBB. Claudins are an important family of tight junction proteins, with claudin-5 (CLDN5) being the predominant claudin at the BBB [81]. Other key tight junction components are claudin-12, occludin and junctional adhesion molecules (JAMs) [76]. Cytoplasmic scaffolding proteins like zonula occludens (ZO)-1, ZO-2, ZO-3 and cingulin anchor the tight junction proteins to the cytoskeleton, thereby supporting tight junction formation [76].

The abluminal side of endothelial cells is surrounded by a vascular basement membrane, which also contains pericytes arranged in a discontinuous layer. Both endothelial cells and pericytes secrete structural proteins such as laminins, fibronectins and collagens that form the basement membrane [76]. Beyond the basement membrane, astrocyte endfeet and an astrocyte-secreted glial basement membrane form the glia limitans, providing an additional barrier separating the blood from the CNS parenchyma (Fig. 4A). While endothelial cells are the most critical component for BBB function, pericytes contribute to its integrity by regulating endothelial and astrocyte function. Pericyte-deficient mice exhibit increased BBB permeability, underlining the importance of this cell type in BBB maintenance [82]. Astrocytes further support BBB stability by secreting paracrine mediators. *In vitro*, astrocyte-conditioned medium induces an increased expression of tight junction proteins by brain endothelial cells and decreases paracellular permeability [83]. *In vivo*, astrocyte ablation leads to decreased expression of the tight junction protein ZO-1 and compromises BBB integrity [84].

Collectively, the CNS barrier system tightly regulates the exchange of substances and cells between the blood and the CNS, thereby protecting the neural tissue from the infiltration of peripheral substances and immune cells to maintain CNS homeostasis.

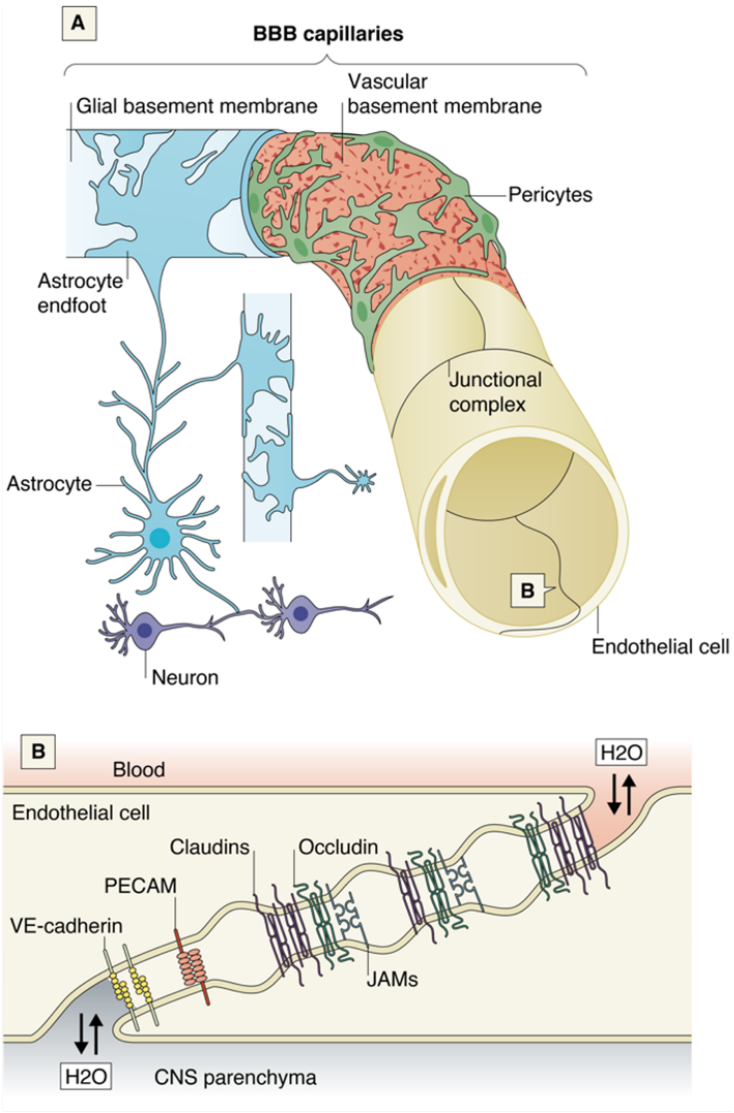

Figure 4: The blood-brain barrier (BBB)

(A) Endothelial cells in the CNS are surrounded by a pericyte-containing vascular basement membrane. The glia limitans, consisting of astrocyte endfeet and a glial basement membrane, forms an additional barrier between the CNS parenchyma and the blood. **(B)** Endothelial cells in the CNS form a monolayer and are tightly stitched together by adherens and tight junctions. Adherens junctions are formed by vascular endothelial cadherin (VE-cadherin) and supported by platelet endothelial cell adhesion molecule (PECAM). Tight junction proteins include claudins, occludins and junctional adhesion molecules (JAMs).

Figure modified from Profaci *et al.*, 2020 [76]

1.5.3 Immune cell migration across the CNS barriers

In the steady state in the absence of neuroinflammation, peripheral immune cells rarely cross the CNS barriers and immune cell entry into the CNS is restricted to activated T cells [75]. Immune cells that surveil the CNS cross the outer barriers and reach the CSF in the brain ventricles, the perivascular spaces and the SAS, but they do not cross the glia limitans and therefore remain separated from the CNS parenchyma [85]. Potential entry sites for infiltrating immune cells are thus from the SAS across the walls of leptomeningeal venules, across the BBB in parenchymal postcapillary venules and across the BCSFB in the choroid plexus [75]. These entry points are minimally accessible under normal conditions but become increasingly permissive during neuroinflammation, when immune cells cross the glia limitans and enter the CNS parenchyma.

The entry of circulating immune cells into tissues involves a multistep process to traverse the endothelial cell barrier [85]. First, selectins on the immune cell interact with their ligands (e.g., P-selectin glycoprotein ligand (PSGL-)1) on the endothelial cell, or α4-integrins on the immune cell bind to their ligands, such as vascular cell adhesion molecule (VCAM)-1 and mucosal addressin cell adhesion molecule (MAdCAM)-1), on the endothelial cell. This initial interaction slows the rolling of the immune cell along the vascular wall. Next, chemokines presented on the endothelial cell surface bind to G-protein-coupled receptors on the immune cell, inducing conformational changes in the immune cell's integrins. These changes increase integrin affinity, enabling binding to VCAM-1, MAdCAM-1, intercellular adhesion molecule (ICAM)-1, and ICAM-2 on the endothelial cell. The immune cell then crawls along the endothelium, a process regulated by leukocyte function-associated antigen (LFA)-1 and endothelial ICAM-1 and ICAM-2, before crossing the endothelium via either the paracellular or transcellular pathway [85]. After reaching the CSF-filled spaces behind the endothelial wall, in MS and EAE, T cells need to be reactivated by local APCs presenting the T cell's antigen in order to cross the glia limitans and infiltrate the CNS parenchyma [86, 87]. The reactivation also induces the production of pro-inflammatory cytokines by T cells which further promotes immune cell infiltration into the CNS.

1.5.4 The BBB in chronic stress and depression

Unlike neuroinflammatory conditions such as MS and EAE, chronic stress does not involve adaptive immune responses against a specific antigen, as no such antigens are present. However, the BBB and its alterations during chronic stress remain a critical area of research, as neurovascular dysfunction is implicated in driving the adverse effects of chronic stress exposure [88]. In a seminal study, Menard *et al.* investigated the effects of chronic social defeat (CSD) stress – a mouse model that uses prolonged social stress to induce depression-like behavior in mice – on the neurovasculature [89]. Following CSD exposure, stressed mice were categorized based on their behavior in a social interaction test, with resilient mice behaving similarly to unstressed controls, while susceptible mice exhibited stress-induced social avoidance. Notably, the tight junction component claudin-5 was significantly downregulated in the nucleus accumbens and hippocampus of susceptible mice compared to resilient mice and unstressed controls, which was accompanied by increased BBB permeability and abnormalities in blood vessel ultrastructure [89]. In contrast, no differences in claudin-5 expression were observed in the prefrontal cortex or hypothalamus of male mice. Furthermore, the expression of other tight junction components remained unchanged. Interestingly, Menard *et al.* could also confirm claudin-5 downregulation in the nucleus accumbens in the chronic variable stress (CVS) model, another rodent model of chronic stress, as well as in patients with MDD [89]. These findings suggest that chronic stress compromises BBB integrity by downregulating claudin-5 in specific brain regions, leading to increased BBB permeability and the establishment of depression-like behaviors.

Interestingly, a follow-up study using a modified CSD protocol in female mice revealed sex-dependent effects. In contrast to males, claudin-5 expression in the nucleus accumbens of stress-susceptible female mice remained unaltered. Instead, significant downregulation of claudin-5 was observed in the prefrontal cortex [90]. This sex-specific pattern was further confirmed in MDD patients, where claudin-5 mRNA was downregulated in the prefrontal cortex of female patients but not males [90]. These results collectively indicate that the downregulation of the key BBB tight junction molecule claudin-5 in stress-susceptible mice is not ubiquitous but occurs in specific brain regions in a sex-dependent manner. In contrast, increased BBB leakiness, indicated by the deposition of blood products such as erythrocytes, IgG and fibrinogen in the parenchyma and perivascular spaces, is observed throughout the brain in susceptible mice [91-93].

Increased BBB permeability may facilitate immune cell infiltration into the CNS parenchyma, a process that requires upregulation of adhesion molecules on BBB endothelial cells. Indeed, increased expression of ICAM-1, VCAM-1 and E-selectin was reported in various brain regions after CSD [94]. Migration of transplanted bone marrow-derived cells into the hippocampal parenchyma was initially described in a model of foot shock stress [95]. In subsequent studies, increased proportions of $CD45^{high}$ peripheral immune cells were observed in the brains of mice exposed to CSD in flow cytometry analyses [96-99]. However, the majority of these cells was located in the perivascular spaces, with only few cells infiltrating into the parenchyma of the hippocampus, prefrontal cortex and amygdala [96]. In other studies, peripheral immune cell infiltration was restricted to the perivascular spaces [89] and the meninges and choroid plexus [100], while in a more recent study, immune cells were not even detected at these brain borders [93].

Similar to what was observed in mouse models, alterations of the BBB have also been described in MDD. In women with MDD, evidence of increased vascular permeability was reported [101]. Furthermore, claudin-5 downregulation seems to occur in specific brain regions in a sex-dependent manner also in MDD patients. In the study by Menard *et al.,* claudin-5 was downregulated in the nucleus accumbens but not in the prefrontal cortex or hippocampus of MDD patients [89]. In contrast, another study observed significantly lower claudin-5 levels in the prefrontal cortex of an all-female MDD cohort [90]. A third study reported reduced claudin-5 expression in the hippocampal grey matter of MDD patients [102]. These partially conflicting findings underscore the need for further research to clarify the role of BBB pathology in the context of chronic stress and MDD.

1.6 The pro-inflammatory cytokine interleukin-1 (IL-1)

1.6.1 Overview of the function of IL-1α and IL-1β

The interleukin-1 family consists of 11 cytokine members and 10 receptor members [103]. IL-1α and IL-1β, which are often referred to in simplified form as IL-1, bind to the cell surface receptor interleukin 1 receptor type I (IL-1R1) [104] which associates with the IL-1R accessory protein (IL-1RAcP) [105] to induce downstream signaling (Fig. 5). Upon ligand binding to IL-1R1, the adaptor protein MyD88 is recruited which leads to the coupling of downstream protein kinases (IRAK and TRAF6), and finally, to the activation of the NF-κB pathway or to the activation of MAPK leading to inflammatory responses (Fig. 5) [106]. IL-1ra is a selective, competitive receptor antagonist [107] which also binds to IL-1R1 but fails to trigger the

association with IL-1RAcP, thereby preventing downstream signaling. An additional receptor, the interleukin 1 receptor type II (IL-1R2) [108], can also bind IL-1α, IL-1β and IL-1ra, but lacks an intracellular domain, thereby preventing downstream signaling. IL-1R2 can act in a membrane-bound form, in a released form and directly in the cytoplasm [109]. The two negative regulatory systems are essential for the strict regulation of IL-1 signaling under physiological and pathological conditions [109]. Other closely related molecules that belong to the interleukin-1 family are other receptor agonists (IL-18, IL-33, IL-36α, IL-36β, and IL-36γ), other receptor antagonists (L-36Ra, and IL-38), as well as an anti-inflammatory cytokine (IL-37) [103].

IL-1α and IL-1β are both synthesized as precursor proteins. IL-1α is constitutively expressed and stored intracellularly by mesenchymal cells such as keratinocytes and lung epithelial cells, as well as by astrocytes and endothelial cells [109]. In contrast, in monocytes and macrophages, IL-1α is only produced after stimulation [110]. When cells undergo necrosis, the intracellularly stored IL-1α gets released in its precursor form and can act as a DAMP [103]. The IL-1α precursor protein is also integrated into the cell membrane of several cell types such as monocytes, macrophages and B cells [103, 109], and can bind to IL-1R1 on neighboring cells to induce downstream signaling [109]. In addition, cleavage of the IL-1α precursor protein liberates a cleavage product that can enter the nucleus and acts as a transcription factor [110]. However, even during inflammation, IL-1α is rarely detected in the circulation, indicating that IL-1α predominantly acts as local mediator within tissues [109].

In contrast to IL-1α, IL-1β is not constitutively expressed and is mostly produced by monocytes, macrophages and dendritic cells, as well as to some extent by B cells and NK cells, after stimulation [111]. Microbial products induce IL-1β expression via the activation of TLRs, in addition, also IL-1 itself is a potent inducer of IL-1β expression [111]. The precursor of IL-1β requires cleavage by caspase-1 which gets activated in the inflammasome. In a first step, the expression of NLRP3 and other inflammasome components is induced upon recognition of DAMPs, pathogen-associated molecular patterns (PAMPs) or pro-inflammatory cytokines by pattern recognition receptors (PRRs) [112]. In a second step, NLRP3 gets activated by another stimulus such as bacterial toxins or ATP leading to the assembly of the NLRP3 inflammasome and the activation of caspase-1 which cleaves the IL-1β precursor protein into its mature form [112]. The mechanisms underlying IL-1β secretion are not completely understood, and most likely, several mechanisms exist that are induced by different stimuli [113].

IL-1 cytokines are key regulators of inflammatory reactions by regulating diverse processes and are able to activate innate immunity [114]. IL-1β induces fever via the induction of cyclooxygenase (COX)-2, prostaglandin-E2, platelet activating factor, and nitric oxide production [111]. Furthermore, IL-1β upregulates the expression of the cell adhesion molecules ICAM-1 and VCAM-1 on mesenchymal and endothelial cells, thereby promoting the infiltration of immune cells from the circulation into tissues and has pro-angiogenic effects on blood vessel formation [111]. IL-1α and IL-1β also stimulate T cell function, are important for the generation of Th17 cell responses and induce the expression of numerous pro-inflammatory cytokines and chemokines [111].

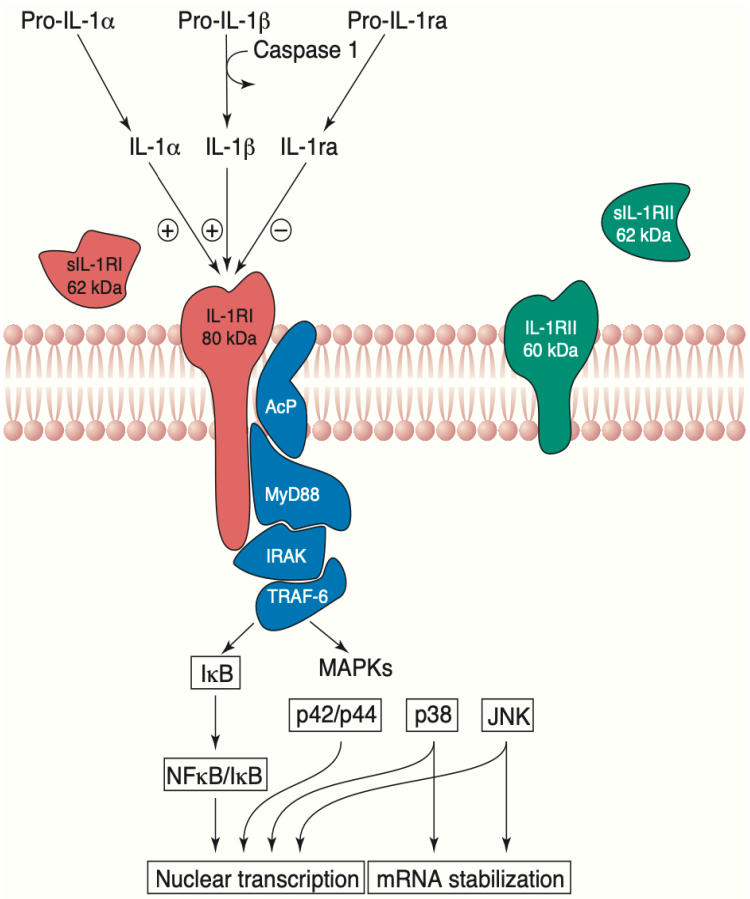

Figure 5: The IL-1 signaling pathway

After being cleaved into their mature form, interleukin (IL)-1α and IL-1β bind to interleukin 1 receptor type I (IL-1R1), which associates with an accessory protein (AcP). This interaction recruits the adaptor protein MyD88, leading to the activation of the protein kinases IRAK and TRAF-6, thereby triggering downstream signaling through the NF-κB and MAPK pathways, ultimately resulting in pro-inflammatory responses. Negative regulation of IL-1 signaling occurs through two mechanisms: (1) The interleukin-1 receptor antagonist (IL-1ra) binds to IL-1R1, blocking downstream signaling, and (2) interleukin 1 receptor type II (IL-1R2) binds IL-1α and IL-1β but lacks an intracellular domain, thereby acting as a decoy receptor to inhibit signaling.

Figure from Rothwell & Luheshi, 2000 [115]

1.6.2 IL-1 functions in the central nervous system

In the steady-state brain, IL-1 and IL-1R1 are expressed only at low levels [115-117]. Microglia are the main source of IL-1 in the brain in the absence of leukocyte infiltration, but IL-1 can also be produced by other CNS-resident cell types such as astrocytes [118]. IL-1 can provide feedback on the cell types producing it to further stimulate its own production [118]. However, IL-1 does not seem to stimulate microglia directly to produce IL-1, which rather occurs indirectly via the engagement of IL-1R1 on brain endothelial cells [114, 119, 120].

The expression of IL-1R1 in the brain at steady state seems to be restricted to certain brain regions and to specific cellular subpopulations, including endothelial, ependymal, and choroid plexus cells, as well as some subpopulations of neurons and astrocytes [119]. Lévesque *et al.* described IL-1R1 to be mainly expressed on endothelial cells of venules and veins that extend in the direction of the pial venous plexus, while they could not detect IL-1R1 expression on pericytes, astrocytes and neuron-glial antigen 2 (NG2)-expressing glia cells [121]. Recently, neuronal expression of IL-1R1 has been detected in discrete glutamatergic and serotonergic neuronal populations in specific brain regions [122]. Interestingly, in these neurons, IL-1R1 activation does not induce downstream NF-κB signaling but downregulates, among others, genes related to synaptic function via the recruitment of an alternatively spliced isoform of the IL-1R accessory protein called IL-1RAcPb [122].

Low physiological concentrations of IL-1 are involved in the regulation of normal brain function [123], e.g., IL-1 contributes to temperature regulation by altering neuronal sensitivity in the preoptic area of the hypothalamus, which is the temperature control center of the brain [114]. IL-1 also contributes to the regulation of neuroendocrine functions by stimulating ACTH and glucocorticoid responses [114]. Furthermore, several mechanism by which IL-1 can affect neuronal function have been described, such as regulation of synaptic structure, long-term potentiation and long-term depression, suggesting that IL-1 is involved in the regulation of neuroplasticity [123].

In disease conditions, such as in animal models of acute brain injury, Alzheimer's disease, Parkinson's disease, CNS autoimmunity, autism, anxiety disorder and MDD, the expression of IL-1 and other pro-inflammatory cytokines is induced [114]. Similarly, also in humans suffering from mental health diseases, IL-1 levels are elevated [123]. Increased expression of IL-1β in the brain seems to contribute to the progression of CNS diseases such as MS and neurodegenerative diseases [124]. For example, in the EAE model, the expression of IL-1R1 on brain endothelial cells and IL-1β secretion from infiltrating myeloid cells were required for

the establishment of disease [125]. Interestingly, even though IL-1 stimulates pro-inflammatory responses in astrocytes and microglia at least *in vitro* [116, 117, 126], the expression of IL-1R1 on these cell types was redundant for the development of EAE [125], highlighting the importance of BBB endothelial IL-1 signaling for the establishment of neuroinflammatory disease. Nevertheless, in the neuroinflammatory model of LPS preconditioning, repeated LPS injections induced microglial expression of IL-1R1 which contributed to the upregulation of IL-1β mRNA in the brain [120]. IL-1 signaling also contributes to the progression of pathology in other CNS diseases. For example, interfering with IL-1 signaling by administration of the IL-1 antagonist IL-1ra was beneficial in a stroke model [127] and in rodent models of depression [128, 129].

1.6.3 The role of IL-1 in BBB endothelial cells (BECs)

The direct effects of IL-1 on brain endothelial cells were mainly studied *in vitro*. Treatment of brain endothelial cell models with IL-1β induces a strong upregulation of ICAM-1 and VCAM-1, as well as the production of pro-inflammatory cytokines including IL-6, IL-8, GM-CSF, G-CSF and TNFα [121, 130-132]. In addition, IL-1β treatment reduces the expression of tight junction proteins, leading to an increased paracellular permeability [132, 133].

Similar to its *in vitro* effects, also in the EAE model, stimulation of IL-1R1 on endothelial cells induces the upregulation of ICAM-1 and VCAM-1 and promotes the subsequent infiltration of peripheral immune cells into the CNS [125, 134]. Therefore, mice lacking IL-1R1 in endothelial cells of the whole body had a greatly reduced EAE susceptibility [134]. Hauptmann *et al.* showed that IL-1R1 expression specifically on endothelial cells in the BBB is crucial for the development of EAE, with greatly reduced disease scores and reduced infiltration of peripheral immune cells in mice lacking IL-1R1 specifically in BBB endothelial cells (BECs) [125]. One of the mechanisms by which IL-1 signaling in BECs promotes EAE pathogenesis is by downregulating heme oxygenase 1 (HO-1) in the endothelial cells [125], a heme-catabolizing enzyme that is important for limiting tissue damage [135]. IL-1R1 on endothelial cells is also required for the induction of sickness behavior following IL-1β delivery into the brain ventricles, with sickness behavior being mediated by the induction of COX-2 in the endothelial cells [119]. Furthermore, endothelial IL-1R1 signaling mediates impairments in adult neurogenesis in the dentate gyrus following chronic overexpression of IL-1β in the hippocampus [119]. One mechanism by which IL-1β can increase BBB permeability *in vivo* is

by inducing the relocation of Cxcl12 from the abluminal to the luminal side of spinal cord endothelial cells, reflecting a mechanism that occurs during the induction phase of EAE [136].

Taken together, IL-1-mediated stimulation of IL-1R1 on BECs activates the downstream NF-κB and MAPK signaling pathways leading to the activation of the BECs. The activated BECs upregulate cell adhesion molecules and pro-inflammatory response genes such as COX-2, while downregulating the anti-inflammatory factor HO-1. In addition, BBB tightness is reduced, allowing for the infiltration of peripheral immune cells into the CNS in neuroinflammatory diseases such as the EAE model.

1.6.4 The actions of IL-1 in models of chronic stress

IL-1 is a key cytokine involved in the stress response, contributing to neuroinflammation and behavioral changes following chronic stress. Chronic stress induces IL-1β production both in the periphery and in the CNS, highlighting its importance in the stress response. IL-1β production by bone marrow-derived monocytes is induced during CSD stress [98]. Elevated levels of IL-1β were also detected in the spleen after foot shock stress [137] and in the serum following chronic restraint or chronic mild stress [138, 139]. Similarly, IL-1β production is upregulated in the brain during stress. CSD stress increases IL-1β mRNA across various brain regions [96, 140], while in the chronic mild stress model, IL-1β mRNA upregulation was observed in the hippocampus [141, 142]. Bone marrow-derived monocytes recruited to the brain vasculature during chronic stress may serve as a potential source of brain IL-1β [98]. However, they are unlikely to be the major source, as IL-1β mRNA levels remain elevated in CC chemokine receptor 2 (CCR2)-deficient mice, in which monocyte recruitment into the brain is blocked [96]. Instead, microglia are likely the primary source of brain IL-1β during chronic stress. This is supported by the finding that inhibiting microglia with minocycline blocks the induction of IL-1β mRNA expression in the hippocampus following foot shock stress [137]. Furthermore, multiple studies demonstrate increased IL-1β mRNA levels in microglia isolated from the brains of mice subjected to CSD stress [94, 97, 143-147].

IL-1β plays a crucial role in mediating stress-induced behavioral changes. IL-1R1 deficiency protects against certain stress-induced depression-like behaviors; however, different behavioral characteristics appear to be regulated differently. For instance, in the chronic mild stress model, IL-1R1 deficiency or overexpression of IL-1ra in the CNS prevented stress-induced social avoidance and anhedonia (measured by sucrose preference) [141]. In contrast, in CSD stress, IL-1R1-deficient mice were protected from stress-induced anxiety, sociability deficits and

working memory impairments but still exhibited social avoidance after stress [144, 148, 149]. The effects of IL-1 signaling on the stress response are mediated by its actions on different cell types. For instance, IL-1R1 expression in glutamatergic neurons is required for stress-induced sociability deficits and working memory impairments [149]. However, IL-1R1 expression on non-neuronal cells is needed for the stress-induced activation of microglia [140, 149]. In contrast, it remains controversial whether IL-1R1 is required at all for the stress-induced increase in circulating monocytes [97, 149].

BECs play a critical role in transmitting peripheral signals to the CNS, and endothelial IL-1R1 is important during the stress response. In CSD stress, IL-1R1 is upregulated on BECs and peripheral immune cells adhere to IL-1R1$^+$ blood vessels [98, 149]. This recruitment is absent in IL-1R1-deficient animals, likely due to the lack of stress-induced upregulation of ICAM-1 and VCAM-1 in these animals [149]. Endothelial cell-specific deletion of IL-1R1 using the tie2-Cre system protected against stress-induced anxiety and reduced microglial pro-inflammatory cytokine expression in a model of CSD stress [97]. These findings suggest that endothelial IL-1R1 participates in the chronic stress response by transmitting and amplifying peripheral signals to the CNS, contributing to neuroinflammation and behavioral changes. However, the exact mechanisms by which endothelial cells influence the stress response remain unclear. Notably, endothelial IL-1R1 deletion did not prevent peripheral inflammatory responses, as stress-induced increases in blood myeloid cells persisted in the absence of endothelial IL-1R1 [97].

In addition to IL-1β, IL-1α is also implicated in the stress response. IL-1α levels were increased in the prefrontal cortex and hippocampus of stressed animals [148, 150]. Injection of IL-1α into the brain before daily social defeat exacerbated social avoidance and HPA axis activation mediated by the stress exposure [150], while infusion of an IL-1α-neutralizing antibody before the social defeat blocked the development of social avoidance [148].

Mechanistically, in addition to promoting microglia activation, IL-1 signaling in the brain activates all the components of the HPA axis [151]. However, during severe restraint stress, IL-1R1 deficiency does not prevent stress-induced HPA axis activation [152], suggesting that additional mediators are involved in HPA axis activation during stress. Furthermore, IL-1R1 deficiency or treatment with IL-1ra prevents the stress-induced decrease in hippocampal neurogenesis [63, 141, 153], highlighting the role of IL-1 in the regulation of neurogenesis during stress. Taken together, IL-1 is a key mediator of the effects of chronic stress on the brain linking chronic stress to neuroinflammation and behavioral changes.

1.7 Mouse models of chronic stress and depression

Not all features of human depression can be fully replicated in animal models. While core symptoms such as helplessness, anhedonia, and behavioral despair are well-modeled in animals, others, like guilt and suicidality, remain uniquely human characteristics [154]. Most animal models of depression rely on the induction of a form of defeat or despair. This approach often triggers anxiety-like symptoms alongside depression-like behaviors, reflecting the frequent co-occurrence of anxiety and depression observed in humans [154]. Acute stress paradigms, such as the forced swim test (FST) or the learned helplessness model, are commonly used as tools to screen potential antidepressant compounds. However, these acute models do not properly reflect the pathology of MDD.

In contrast, models of chronic stress induce several behavioral abnormalities which reflect the behavioral alterations occurring in MDD. Given that exposure to stressful life events is a major risk factor for MDD, inducing depression-like behaviors in rodents through chronic stress provides a relevant simulation of the disorder's underlying causes. In the chronic unpredictable stress (CUS) or chronic variable stress (CVS) models, rodents are exposed to a variety of physical stressors (e.g., water deprivation, constant noise, damp bedding, restraint stress) in an unpredictable order over several weeks. However, many of these stressors are artificial and do not fully reflect the natural experience of stress as it occurs in rodents. In contrast, psychosocial stress models such as the CSD model leverage innate social behaviors to induce stress, offering a more etiologically valid approach [154]. Thus, the reliance on chronic stress to model depression-like behaviors in animals makes it inherently difficult to independently study stress and depression in animal models.

1.7.1 The mouse model of Chronic Social Defeat (CSD)

The CSD model, also known as repeated social defeat (RSD), is commonly used to induce depression-like behavior, including social avoidance, anxiety and anhedonia. Golden *et al.* developed a standardized protocol [155] in which C57BL/6 mice undergo repeated social defeats by a larger, aggressive CD-1 mouse, followed by psychological stress through visual and olfactory interaction with the CD-1 mouse. This protocol induces social avoidance behavior in most animals, while approximately one-third to half of the mice remain resilient to the social defeat and do not develop social avoidance [156]. Notably, social avoidance behavior induced by CSD responds exclusively to chronic, but not acute, antidepressant treatment, making the model particularly valuable for testing novel antidepressants [155].

In Golden *et al.*'s protocol, each daily defeat session lasts 5-10 minutes. After the defeat, the C57BL/6 experimental mouse and the CD-1 aggressor mouse are housed together in the home cage of the CD-1 mouse, separated by a divider allowing for visual and olfactory contact. This process is repeated daily for 10 consecutive days. Variations of this protocol exist, with defeat sessions lasting up to 2 hours per day in some cases. The duration of the overall protocol also varies, with some studies employing 6, 10, or 14 days of social defeat.

To avoid injuries, we consistently used the following protocol (Fig. 6): (1) On the first day of social defeat, the experimental C57BL/6 mouse is placed into the home cage of an aggressor CD-1 mouse. (2) The mice are closely monitored until 10 seconds of aggressive interaction occurs, at which point the mice are separated by a divider allowing for visual and olfactory contact. (3) After a 15-minute break, the C57BL/6 mouse is introduced into the home cage of a new CD-1 mouse for another 10 seconds of aggressive interaction. (4) A third social defeat session follows after another 15-minute break. (5) After the third defeat, the C57BL/6 mouse remains in the home cage of the final CD-1 aggressor, separated by the divider for 24 hours. This procedure is repeated daily for 10 days. Afterwards, experimental mice are single-housed and tested for depression-like behaviors. The classical behavioral test after social stress exposure is a social interaction (SI) test, which is used to classify the animals into "stress-susceptible" and "stress-resilient". Other behavioral tests commonly used include tests for anxiety-like behavior, despair, anhedonia, and cognitive function. In each CSD experiment, approximately 15-20 CD-1 mice were used, ensuring that each C57BL/6 mouse encountered the same CD-1 mouse no more than twice during the procedure. This rotation of aggressors is critical to prevent habituation.

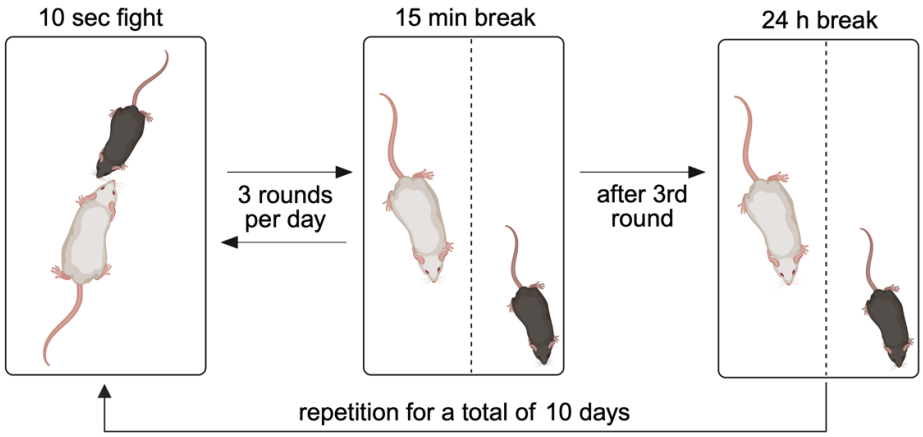

Figure 6: Our model of chronic social defeat (CSD) stress

Experimental C57BL/6 mice are placed into the home cage of an aggressor CD-1 mouse until 10 seconds of aggressive interaction occurred, after which they are separated by a divider allowing sensory interaction. After a 15-minutes break, the C57BL/6 mouse is introduced to a new CD-1 mouse for another 10 seconds of aggressive interaction, followed by a third social defeat after another 15-minutes break. After the final defeat, the C57BL/6 mouse remains in the cage of the last CD-1 aggressor, separated by the divider, for 24 hours. The procedure is repeated daily for 10 days.

1.8 Rationale of the study

The BBB, with endothelial cells as a central component, plays a vital role in maintaining CNS homeostasis by regulating the exchange of molecules and immune cells between the blood and CNS. The pro-inflammatory cytokine IL-1β is a key mediator of inflammatory responses in both the periphery and the CNS. Its receptor, IL-1R1, is primarily expressed by BECs in the steady-state CNS [119], but its expression is restricted to a small subset of these cells [121]. Interestingly, this subset increases under inflammatory conditions such as EAE, where it plays a crucial role in disease development [125].

Chronic stress is a major risk factor for depression, leading to systemic immune activation and neuroinflammation, both of which contribute to the development of depressive symptoms. IL-1β is a key mediator of stress-induced depression-like behavior in animal models of chronic stress [97, 141, 144, 148, 149]. Studies have shown that CSD stress induces IL-1R1 expression on BECs [98, 149], potentially contributing to BBB activation during stress. Interestingly, deletion of IL-1R1 on endothelial cells of the whole body was beneficial in CSD stress, where it prevented stress-induced anxiety behavior [97]. However, whether IL-1 acts specifically on BECs or peripheral endothelial cells during stress remains unclear.

Therefore, this study aims to investigate the role of IL-1 signaling in BECs during CSD and its impact on stress-induced behavioral changes. Using a transgenic mouse model with conditional deletion of IL-1R1 in BECs, this study addresses the following key questions:

1. What are the defining characteristics of IL-1R1$^+$ BECs, including their localization within the brain and activation status?
2. Does IL-1 signaling in BECs contribute to depression-like behavior following chronic social stress?
3. What mechanisms underlie the impact of IL-1 signaling in BECs on behavior?

The findings from this study aim to provide insights into the role of IL-1R1$^+$ BECs in BBB dysfunction, stress susceptibility *versus* resilience, as well as neuroinflammation, with the long-term goal of identifying therapeutic targets for stress-related disorders.

2 MATERIAL AND METHODS

2.1 Reagents, buffers, kits, and antibodies

Table 1: List of chemicals and reagents

Reagent	**Supplier**
Agarose	Biozym
AMPure XP Bead-Based Reagent	Beckman Coulter
BD Pharm Lyse™ Lysing Buffer	BD Biosciences
Bovine Serum Albumin (BSA)	PAN-Biotech
DAPI Fluoromount-G®	Thermo Fisher Scientific
DNase I	Sigma-Aldrich
Dulbecco's modified PBS (DPBS)	Thermo Fisher Scientific
Ethanol	Carl Roth
Ethylendiaminetetraacetic acid (EDTA)	Sigma-Aldrich
Fetal bovine serum (FBS)	Thermo Fisher Scientific
Gene ruler 100 bp DNA ladder	Thermo Fisher Scientific
Gibco® Hank's buffered saline solution (HBSS)	Thermo Fisher Scientific
Gibco® Hank's buffered saline solution (HBSS) with Ca^{2+} and Mg^{2+}	Thermo Fisher Scientific
GoTaq® qPCR Master Mix	Promega
Isoflurane	Abbvie
Isopropyl alcohol	Hedinger
Midori Green Advance DNA stain	Biozym
NaCl 0.9%	Braun
Olive oil	Sigma-Aldrich
Papain	Sigma-Aldrich
Paraformaldehyde (PFA) solution 4% in PBS	Santa Cruz Biotechnology
Percoll	Cytiva

Proteinase K	Roche
REDTaq® ReadyMix™	Sigma-Aldrich
ROTI® Histofix 4%	Carl Roth
Sucrose	Sigma-Aldrich
Tamoxifen	Sigma-Aldrich
Triton X-100	Sigma-Aldrich
TRIzol™ Reagent	Thermo Fisher Scientific
Tissue Freezing Medium	Jung
Trypan blue	Thermo Fisher Scientific
Fixable Viability Dye eFluor™ 780	Thermo Fisher Scientific

Table 2: List of buffers

Buffer	**Composition**
10x Ammonium-Chloride-Potassium (ACK) lysis buffer (pH 7.4)	150 mM NH_4Cl 100 mM $KHCO_3$ 10 mM EDTA
50x Tris-acetate-EDTA (TAE) buffer (pH 8.3)	2 M Tris 1 M acetic acid 50 mM EDTA pH 8.0
FACS buffer	PBS 2% FBS
MACS buffer	PBS 0.5% BSA 2 mM EDTA (pH 8)
Tails lysis buffer	10 mM Tris 5 mM EDTA (pH 8) 0.2% SDS 200 mM NaCl

Table 3: List of kits

Kit	Supplier
Agilent High Sensitivity DNA Kit	Agilent
Nextera XT DNA Library Prep Kit	Illumina
QuantiTect® Reverse Transcription Kit	Qiagen
ReliaPrep™ RNA Cell Miniprep System	Promega
SMART-Seq® v4 Ultra® Low Input RNA Kit for Sequencing	Takara Bio
CD31 MicroBeads	Miltenyi Biotec
CD11b MicroBeads	Miltenyi Biotec

Table 4: List of antibodies for different applications

Antibody	Conjugate	Clone	Host	Dilu-tion	Supplier	Applica-tion
InVivo MAb anti-mouse CD16/CD32		2.4G2	Rat	1:100	BioXCell	Blocking
CD11b	PE-Cy7	M1/70	Rat	1:1000	BioLegend	FACS
CD19	PerCP	6D5	Rat	1:400	BioLegend	FACS
CD31	PerCP-Cy5.5	390	Rat	1:100	BioLegend	FACS
CD31	FITC	MEC 13.3	Rat	1:100	BD Bioscience	FACS
CD45	BV510	30-F11	Rat	1:300	BioLegend	FACS
ICAM-1 (CD54)	Alexa647	YN1/1.4.7	Rat	1:200	BioLegend	FACS

IL-1R1 (CD121a)	PE	35F5	Rat	1:100	BD Bioscience	FACS
Ly6C	V450	AL-21	Rat	1:300	BD Bioscience	FACS
Ly6C	FITC	AL-21	Rat	1:300	BD Bioscience	FACS
Ly6G	PE	1A8	Rat	1:500	BioLegend	FACS
TCRβ	APC	H57-597	Arm. Hamster	1:500	BioLegend	FACS
VCAM-1 (CD106)	PE-Cy7	429 (MVCAM.A)	Rat	1:200	BioLegend	FACS
Iba-1	-	Poly-clonal	Rabbit	1:800	WAKO	IHC
GFAP	-	GA5	Mouse	1:100	Thermo Fisher Scientific	IHC
Anti-mouse IgG (H+L)	CF™ 488A	-	Donkey	1:800	Merck	IHC
Anti-rabbit IgG (H+L)	CF™ 594	-	Donkey	1:800	Merck	IHC

2.2 Mouse experiments

2.2.1 Mouse strains

Il1r1$^{fl/fl}$ mice [157] were crossed with *Slco1c1*-Cre^{ERT2} mice [158] to obtain IL-1R1$^{\Delta BEC}$ mice (Cre$^{+/-}$). Cre$^{-/-}$ littermates were used as wildtype-like controls (IL-1R1^{WT}). For flow cytometry, *Il1r1*-deficient mice (IL-1R1$^{-/-}$) were used as controls [159]. Transgenic mice were on a C57BL/6 background. C57BL/6JRj mice from Janvier labs were used as wildtype mice for the RNA sequencing experiment. CD-1 mice as aggressors for the CSD were obtained from Janvier labs. Only male mice were used in all experiments. All transgenic mice were bred at the Translational Animal Research Center (TARC) of the Johannes Gutenberg-University in Mainz. All mice were housed at the TARC under specific pathogen-free (SPF) conditions, with a 12 h light/dark cycle and unlimited access to food and water. All animal experiments were approved by the local administration (Landesuntersuchungsamt Koblenz; Aktenzeichen: G 20-1-071; G 20-17-057).

2.2.2 Tamoxifen treatment

0.4 g tamoxifen powder were added to 1 ml 99% ethanol and 19 ml olive oil to obtain a tamoxifen solution with a concentration of 20 mg/ml. Tamoxifen was dissolved by rotation for 48 h at 4°C. Mice were injected intraperitoneally with 100 µl of the solution (= 0.2 mg tamoxifen) at the age of 5-6 weeks on 5 consecutive days.

2.2.3 Chronic Social Defeat (CSD)

An experimental male C57BL/6 mouse was placed into the home cage of a male CD-1 aggressor mouse and their interaction was closely monitored. After 10 s of aggressive, physical interaction (social defeat of the C57BL/6 male by the CD-1 male), the two mice were physically separated by a grid allowing visual and sensory contact for 15 min. The social defeat was repeated with a new CD-1 aggressor mouse for 10 s followed by a separation for 15 min. After the third and last round of social defeat with the third CD-1 male, the two mice remained in the same cage separated by the divider for 24 h. The whole procedure was repeated on 10 consecutive days (in total, 30 rounds of social defeat). The mice were separated on day 11 and were single-housed during the behavioral tests. The behavioral tests were started after one day of rest after the end of the CSD.

The unstressed control mice were housed together with another C57BL/6 experimental male mouse in a cage separated by a divider allowing visual and sensory contact during the whole procedure and were handled daily to habituate them to the experimenter.

2.2.4 Behavioral tests

2.2.4.1 Social Interaction Test

The test was performed in a square arena with a small net enclosure on one side (diameter 10 cm, height 20 cm). The test mouse was first placed into the arena for 2.5 min with the net enclosure empty. Immediately afterwards, it was again placed into the arena for 2.5 min, now with an unknown CD-1 male in the net enclosure. The time the mouse interacted with either the empty net enclosure or the CD-1 mouse was recorded using the EthoVision XT software (Noldus, Wageningen, Netherlands) and the social interaction preference ("Social Interaction (SI) Ratio") was calculated.

2.2.4.2 Open Field Test

The test mouse was placed in a square arena and its behavior was recorded for 10 min. The total running distance of the mouse and its location during the test (center or arena border areas) were analyzed using the EthoVision XT software.

2.2.4.3 Elevated Plus Maze Test

The test mouse was placed into the center of a plus-shaped elevated arena (40 cm above the floor) that has two open and two closed arms with an area of 30 x 5 cm, which are connected by a central area of 5 x 5 cm. The behavior of the mouse was recorded for 10 min and the time the mouse spent in the open and closed arms was analyzed using the EthoVision XT software.

2.2.4.4 Forced Swim Test

The test mouse was placed into a glass cylinder (height 24 cm, diameter 13 cm) filled with water (water temperature 22°C) to a height of 15 cm and its movements were recorded for 6 min. “Immobility” was defined as a state in which the mouse floated on the water and made only minor movements with one paw to stabilize its position. The “immobility time” in the last 4 min of the 6-min test period was automatically quantified using the EthoVision XT software.

2.3 Cell Biology

2.3.1 Immune cell isolation from spleens for flow cytometry

Spleens of perfused mice were dissected and mechanically dissociated in FACS buffer by forcing the organ to pass through a 40 µm cell strainer. The cell suspension was centrifuged at 300 x g for 10 min at 4°C, the supernatant was removed and the cell pellet was resuspended in 1x ACK buffer for 4 min at room temperature to lyse the erythrocytes. The reaction was stopped by the addition of FACS buffer, the cells were pelleted by centrifugation at 300 x g for 10 min at 4°C and the cell pellet was used for flow cytometry.

2.3.2 BEC isolation for flow cytometry and Fluorescence-Activated Cell Sorting (FACS)

Mice were perfused post-mortem with 0.9% NaCl, the brains were dissected and cut into small pieces with a scalpel. The brains were digested with 1 mg/ml Papain and 100 µg/ml DNase I in HBSS (with Mg^{2+} and Ca^{2+}) by performing 3 cycles of mechanical dissociation with the GentleMACS homogenizer (Miltenyi, Bergisch Gladbach, Germany) with 10 min incubation steps at 37°C between the cycles. The reaction was stopped with FACS buffer, the cell suspension was filtered through a 70 µm cell strainer, centrifuged at 300 x g for 10 min at 4°C and the supernatant was discarded. The pellet was resuspended in 22% Percoll and transferred below a layer of HBSS for gradient centrifugation at 400 x g for 30 min at 15°C with lowest possible acceleration and no break. The supernatant was discarded, the cell pellet containing the endothelial cells was washed with FACS buffer, centrifuged at 300 x g for 10 min at 4°C, the supernatant was discarded and the cell pellet was used for flow cytometry stainings or for further preparation for FACS or RNA isolation.

2.3.3 Flow cytometry

The cell pellets obtained from the spleen or brain were resuspended in anti-mouse CD16/CD32 (5 µg/ml) in FACS buffer for 10-20 min at 4°C to block Fc receptors, washed with FACS buffer and centrifuged at 300 x g for 5 min at 4°C. Cells were stained with a master mix containing surface-binding antibodies and a viability dye (Fixable Viability Dye eFluor™ 780, 1:1000) in FACS buffer for 20-30 min at 4°C in the dark. Cells were washed with FACS buffer twice and were resuspended in 2% Roti Histofix for fixation overnight at 4°C. Samples were acquired at

a FACSCanto II (BD Bioscience, Franklin Lakes, USA) and analyzed with FlowJo™ v10 software (BD Bioscience, Franklin Lakes, USA).

2.3.4 Magnetic-Activated Cell Sorting (MACS) for enrichment of CD31$^+$ BECs or CD11b$^+$ microglia

To enrich for BECs, the cell pellet obtained in 2.3.2 was resuspended in 90 µl MACS buffer and 5 µl CD31 MicroBeads (Miltenyi Biotec, Bergisch Gladbach, Germany) were added. After incubation for 15 min at 4°C, the cells were washed with MACS buffer and centrifuged at 300 x g for 10 min at 4°C. The supernatant was discarded and the cell pellet was resuspended in 500 µl MACS buffer. The cell suspension was applied to a MS column in a OctoMACS separator (Miltenyi Biotec, Bergisch Gladbach, Germany), washed 2x with 500 µl MACS buffer, the MS column was removed from the OctoMACS separator and CD31$^+$ cells were eluted with 1 ml MACS buffer. The cell suspension was centrifuged at 300 x g for 10 min at 4°C, the supernatant was discarded and the cell pellet was further processed for FACS or was lysed in lysis buffer for RNA isolation.

To isolate CD11b$^+$ brain microglia, the flow-through from the BEC isolation was collected, centrifuged at 300 x g for 10 min at 4°C, and the cell pellet was resuspended in 90 µl MACS buffer and 10 µl CD11b MicroBeads (Miltenyi Biotec, Bergisch Gladbach, Germany). The same steps as before were performed, until CD11b$^+$ cells were eluted with 1 ml MACS buffer. The cell suspension was centrifuged at 300 x g for 10 min at 4°C, the supernatant was discarded and the cell pellet was lysed in lysis buffer for RNA isolation.

2.3.5 Fluorescence-Activated Cell Sorting (FACS) of IL-1R1$^+$ BECs

The enriched CD31$^+$ cells obtained in 2.3.4 were resuspended in anti-mouse CD16/CD32 (5 µg/ml) in FACS buffer for 10-20 min at 4°C to block Fc receptors, washed with FACS buffer and centrifuged at 300 x g for 5 min at 4°C. Cells were stained with a master mix containing surface-binding antibodies and a viability dye (Fixable Viability Dye eFluor™ 780, 1:1000) in FACS buffer for 30 min at 4°C in the dark. Cells were washed with FACS buffer twice and sorted at a FACSAria III (BD Bioscience, Franklin Lakes, USA) with a 100 µm nozzle directly into the lysis buffer containing RNase inhibitor from the SMART-Seq® v4 Ultra® Low Input RNA Kit for Sequencing (Takara, Kusatsu, Japan).

2.3.6 Whole blood staining for flow cytometry

Blood was collected post-mortem from the heart of the mice and mixed with heparin. Anti-mouse CD16/CD32 (0.5 µg per sample) was added to block Fc receptors and incubated for 20 min. at 4°C. Samples were washed with FACS buffer, centrifuged at 300 x g for 6 min at 4°C, the supernatant was discarded and the cell pellet was vortexed. Cells were stained with a master mix containing surface-binding antibodies and a viability dye (Fixable Viability Dye eFluor™ 780, 1:1000) in FACS buffer for 30 min at 4°C in the dark. Cells were washed twice with FACS buffer (centrifugation at 300 x g for 6 min at 4°C, supernatant was discarded, pellet was vortexed). The cells were then incubated with 1x BD Pharm Lyse™ Lysing Buffer for 8 min at room temperature in the dark to lyse the erythrocytes followed by two washing steps with FACS buffer.

2.3.7 Immunohistochemistry on frozen sections

Mice were perfused post-mortem with 0.9% NaCl, the brains were dissected, post-fixed in 4% PFA overnight at 4°C and cryoprotected in 30% sucrose. The tissue was embedded in Tissue Freezing Medium and stored at -20°C. Brains were cut with a cryostat into 30 µm-thick sections, were washed 3 times for 5 min at room temperature in 0.1% Triton X-100/1x PBS and afterwards permeabilized for 30 min in 0.3% Triton X-100/1x PBS at room temperature. After washing (3 times, 5 min), the sections were blocked for 1 h in blocking solution (5% BSA/0.1% Triton X-100/1x PBS) and then incubated with the primary antibody diluted in 1% BSA/0.1% Triton X-100/1x PBS overnight at 4°C. The sections were washed (3 times, 5 min) and incubated with the secondary antibody diluted in 1% BSA/0.1% Triton X-100/1x PBS for 1.5 h at room temperature. The tissue was washed (3 times, 5 min) and mounted with DAPI Fluoromount-G®. Images were acquired using a Keyence BZ-X810 fluorescence microscope with an objective magnification of 20x.

2.4 Molecular Biology

2.4.1 Genotyping: DNA isolation and Polymerase Chain Reaction (PCR)

Ear or toe biopsies were collected during marking of the mice at the recommended ages and were lysed overnight at 56°C in tail lysis buffer supplemented with 250 µg/ml proteinase K. An equal amount of isopropyl alcohol was added and after thorough mixing, the DNA was pelleted by centrifugation for 15 min at max. speed and room temperature. The supernatant was discarded, the pellet was washed with 70% ethanol and centrifuged for 10 min at max. speed at room temperature. The supernatant was again discarded and the DNA was dried at 37°C for 30 min. The DNA was dissolved in 200 µl distilled water at 56°C for 1-2 h and used for PCR.

For the PCR master mix, 5 µl of each primer (stock concentration: 100 µM) were added to 500 µl REDTaq® ReadyMix™ and the mix was filled up with water to a total volume of 950 µl. 1 µl of genomic DNA was added to 19 µl of this master mix in PCR tubes. PCR reactions were performed at annealing temperatures specific for the respective primer pairs. Primer sequences are listed in Table 5; 1260.1/2 primers were used to get a control band for the SLC-Cre^{ERT2} and IL-1R1-KO PCRs. Agarose gels were prepared by dissolving 6 g agarose in 300 ml 1x TAE buffer (2%) and 15 µl of Midori Green Advance DNA stain were added. Amplified DNA fragments were separated according to size using agarose gel electrophoresis at 130 V and visualized using UV light in the Gel Doc XR+ gel documentation system (Bio-Rad, Hercules, USA).

Table 5: List of genotyping primers

Primer	Primer sequence (5'-3')	Direction
SLC-Cre^{ERT2} fwd	GCT ATT CAT GTC TTG GAA GCC	sense
SLC-Cre^{ERT2} rev	CAG GTT CTT CTT GAC TTC ATC	anti-sense
1260.1 fwd	GAG ACT CTG GCT ACT CAT CC	sense
1260.2 rev	CCT TCA GCA AGA GCT GGG GAC	anti-sense
IL-1R1^{fl} fwd	CTA GTC TGG TGG AAC TTA CAT GC	sense
IL-1R1^{fl} rev	AAC TGA AAG CTC AGT TGT ATA CAG C	anti-sense
IL-1R1-KO fwd	CTA GTC TGG TGG AAC TTA CAT GC	sense
IL-1R1-KO rev	GTA CTA CTA TCT GGA AAG GTT GTG G	anti-sense

2.4.2 RNA isolation and quantification

RNA from whole brain tissue was isolated using Invitrogen™ TRIzol™ Reagent. In brief, 800 µl of TRIzol™ reagent were added to metal bead lysing matrix tubes (MP Biomedicals, Eschwege, Germany) and frozen brains were added. The mix was incubated at room temperature for 5 min, followed by homogenization using the FastPrep-24 homogenizer (MP Biomedicals, Eschwege, Germany). Tubes were centrifuged at 12,000 × g for 10 min at 4°C, the supernatant was transferred to a new tube and mixed with 200 µl of chloroform. After a 2–3 min incubation at room temperature, the mixture was centrifuged again at 12,000 × g for 15 minutes at 4°C. RNA was precipitated by mixing the supernatant with 400 µl of isopropyl alcohol and centrifuging at maximum speed for 10 min at 4°C. The supernatant was discarded, and the pellet was washed twice with 500 µl of 70% ethanol. Finally, the RNA pellet was dissolved in 100–150 µl of nuclease-free water by incubation for 10 min at 56°C.

RNA from MACS-isolated $CD31^+$ BECs and $CD11b^+$ microglia was isolated using the ReliaPrep™ RNA Cell Miniprep System (Promega, Madison, USA) following manufacturer's instructions. RNA concentrations were determined by measuring absorbance at 260 nm and 280 nm using the NanoQuant PlateTM (Tecan, Männedorf, Switzerland) at an Infinite M200 pro Tecan plate reader (Tecan, Männedorf, Switzerland).

2.4.3 Reverse transcription and quantitative real-time PCR (qPCR)

cDNA was synthesized with the QuantiTect® Reverse Transcription Kit (following manufacturers guidelines). cDNA was diluted 1:3 and subsequently used for quantitative real-time PCR (qPCR). qPCR reactions were performed in a total volume of 10 µl. For this, 1 µl of 5 µM-concentrated primers were pipetted into a 96-well plate and 1 µl cDNA as well as 8 µl GoTaq® qPCR Master Mix mixed with nuclease-free water and CXR reference dye were added. qPCR reactions were performed in the StepOnePlus™ Real-Time system (Thermo Fisher Scientific, Waltham, USA). Fold changes were calculated using the delta-delta CT method and normalized to controls. Hypoxanthin-Guanin-Phosphoribosyltransferase (*Hprt*) was used as reference housekeeping gene. Primers for *Gfap, Cd68, Cldn5, Il1b, Ccl2, Il6* and *Tnfa* were ordered as QuantiTect Primer Assays (Qiagen, Hilden, Germany). Primer sequence for *Lrg1* is shown in Table 6.

Table 6: List of qPCR primers

Primer	Primer sequence (5'-3')
Lrg1 fwd	CTGGGGTCTTGAGGACAGAC
Lrg1 rev	TTGAGATCCTGGAGGCTTCCTT

2.4.4 Next Generation Sequencing

For RNA sequencing of brain endothelial cells, 450 IL-1R1$^+$ endothelial cells were sorted into lysis buffer containing RNase inhibitor from the SMART-Seq® v4 Ultra® Low Input RNA Kit for Sequencing (Takara, Kusatsu, Japan). cDNA was synthesized directly from the lysed cells and purified using the SMART-Seq® v4 Ultra® Low Input RNA Kit for Sequencing and AMPure XP Bead-Based Reagent according to the manufacturer's instructions. cDNA concentrations were determined with the Qubit 2.0 fluorometer (Thermo Fisher Scientific, Waltham, USA) and quality was assessed on the Bioanalyzer 2100 (Agilent, Santa Clara, USA) with the Agilent's High Sensitivity DNA Kit. Libraries were prepared with the Nextera XT DNA Library Prep Kit from 1 ng cDNA according to the manufacturer's instructions and libraries were cleaned using the AMPure XP Bead-Based Reagent. Concentrations and quality were again determined as described before and libraries were sequenced with the NovaSeq™ 6000 Sequencing System (PE150) (Illumina, San Diego, USA) with reads of 150 nucleotides, using a paired-end library preparation. The raw output data was preprocessed according to the Illumina standard protocol.

2.5 Bioinformatic analysis

2.5.1 Statistics

Statistical analyses were performed with GraphPad Prism v10 software (GraphPad software, San Diego, USA). For comparison of four groups with two variables (genotype, stress group), two-way ANOVA with Bonferroni's multiple comparison correction was used. For comparison of three groups, one-way ANOVA with Tukey's multiple comparison correction was used. For comparison of two groups, unpaired two-tailed students t-test was used. All values are represented as mean ± standard error of the mean (SEM) and p-values were considered as significant with * $p<0.05$, ** $p<0.01$, *** $p< 0.001$ and **** $p<0.0001$.

2.5.2 Next Generation Sequencing data analysis

Quality control on the sequencing data was performed with the FastQC tool (version 0.11.8, https://www.bioinformatics.babraham.ac.uk/projects/fastqc/) and MultiQC (version v1.5). Reads were trimmed with the tool trim_galore (version 0.6.2) and aligned to the ENSEMBL Mus_musculus.GRCm39 reference genome. The corresponding annotation (ENSEMBL Mus_musculus.GRCm39.109) was also retrieved from ENSEMBL FTP website. The STAR aligner (version 2.6.1a) was used to perform mapping to the reference genome. Samples were quantified with Salmon (v.1.10.1) using the Gencode transcriptome (M27). The Salmon quantified output was used for further analysis in R (version 4.1.2). The exploration, modeling, and interpretation of the expression data followed the protocols defined by Ludt *et al.* [160]. Exploratory data analysis was performed with the pcaExplorer package (ver+cit). Differential expression analysis was performed with DESeq2 package (version 1.34.0), setting the false discovery rate (FDR) cutoff to 0.05. Accurate estimation of the effect sizes (described as log2 fold change) was performed using the apeglm shrinkage estimator (version 1.18.0) [161]. Further analyses included Gene Ontology pathway enrichment by goseq (version 1.46.0) and topGO (version 2.4.0), setting all expressed genes as background dataset, and were performed using the ideal package (version 1.18.1). The enrichment results were further processed with the GeneTonic package for visualization and summarizing (version 1.6.4) [162]. Gene expression profiles were plotted as heatmaps (color-coded standardized z-scores for the expression values, after regularized logarithm transformation) to enable comparison across samples.

3 RESULTS

3.1 IL-1R1$^+$ BECs form a small subset with high expression of ICAM-1 and VCAM-1

In the steady-state brain, endothelial cells are one of the primary cell types expressing IL-1R1 [119]. However, IL-1R1 expression appears to be limited to a subset of endothelial cells, that was estimated to comprise only 13% of BECs in the brain [121]. In the spinal cord under steady-state conditions, IL-1R1 is expressed by approximately 5% of BECs, a proportion that increases to approximately 20% shortly after EAE immunization [125].

Given the limited knowledge about the location and characteristics of IL-1R1-expressing BECs, we sought to further characterize this specific cellular subset. To achieve this, we isolated BECs from the brains of naïve mice and analyzed them using flow cytometry. BECs were identified as CD45$^-$ CD11b$^-$ CD31$^+$ Ly6C$^+$ cells and were further separated into IL-1R1$^-$ and IL-1R1$^+$ subsets (Fig. 7A). Consistent with previous findings [125], we found IL-1R1 to be expressed on around 5% of BECs. Next, we assessed the expression of the cellular adhesion molecules ICAM-1 and VCAM-1, commonly used as markers for BEC activation, in the IL-1R1$^-$ and IL-1R1$^+$ BEC subsets. A significantly higher proportion of IL-1R1$^+$ BECs expressed these markers, with 87.2 ± 7.8% of IL-1R1$^+$ BECs expressing ICAM-1 compared to only 12.8 ± 4.3% of IL-1R1$^-$ BECs, and 25.4 ± 6.3% of IL-1R1$^+$ BECs expressing VCAM-1 compared to only 1.2 ± 0.3% of IL-1R1$^-$ BECs (Fig. 7B+C). Additionally, the expression levels of these activation markers, measured as mean fluorescence intensity (MFI), were significantly higher in the IL-1R1$^+$ BEC subset (Fig. 7B+C).

Having established that IL-1R1$^+$ BECs represent a subset of brain endothelial cells with a distinctly activated phenotype, we sought to determine their specific location in the brain. Due to the lack of a suitable antibody against IL-1R1, we performed RNA in situ hybridization to detect *Il1r1* mRNA and found it to be expressed in various brain regions, including the cortex, hippocampus, and hypothalamus (data not shown; part of a Master's thesis). Furthermore, we observed *Il1r1* mRNA expression in blood vessels of varying sizes, ranging from just a few micrometers to approximately 100 micrometers in diameter (data not shown; part of a Master's thesis).

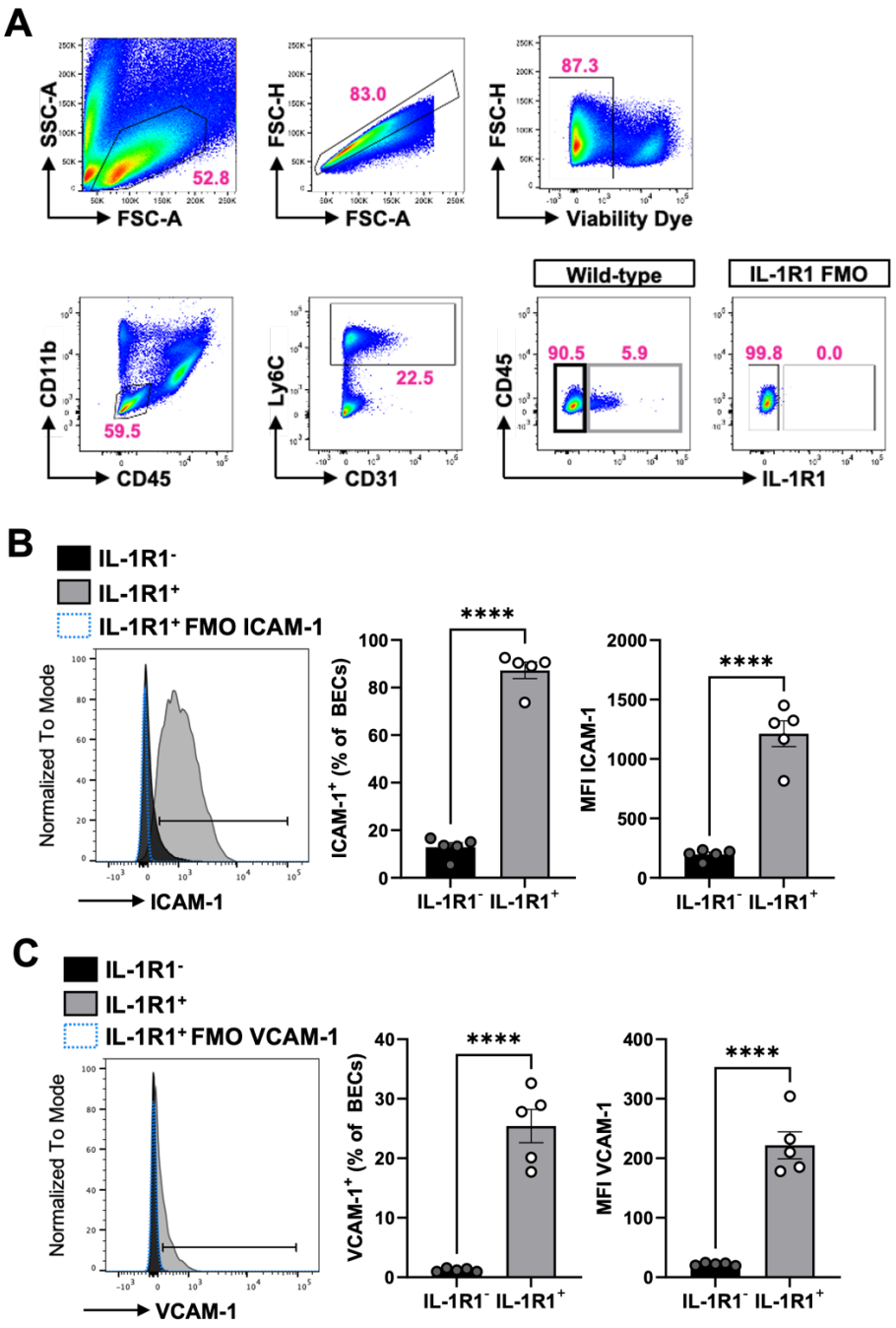

Figure 7: IL-1R1$^+$ BECs are a small subset in the brain with high levels of ICAM-1 and VCAM-1 expression

BECs from the brains of naïve wildtype-like mice were analyzed by flow cytometry. **(A)** Representative gating strategy to identify live CD45$^-$ CD11b$^-$ CD31$^+$ Ly6C$^+$ BECs. Based on the fluorescence minus one (FMO) control for IL-1R1, BECs were separated into IL-1R1$^-$ and IL-1R1$^+$ subsets. **(B)** Histogram showing the expression levels of ICAM-1 in IL-1R1$^-$ and IL-1R1$^+$ BEC subsets and in the FMO control for ICAM-1 (left). Percentages of ICAM-1$^+$ BECs (middle) and mean fluorescence intensity (MFI) for ICAM-1 (right) in IL-1R1$^-$ and IL-1R1$^+$ BEC subsets. **(C)** Histogram showing the expression levels of VCAM-1 in IL-1R1$^-$ and IL-1R1$^+$ BEC subsets and in the FMO control for VCAM-1 (left). Percentages of VCAM-1$^+$ BECs (middle) and MFI for VCAM-1 (right) in IL-1R1$^-$ and IL-1R1$^+$ BEC subsets. Each circle represents a single mouse. Data is represented as mean ± SEM. Statistical significance was determined by two-tailed unpaired Student's t-test. **** $p<0.0001$.

3.2 CSD drives IL-1R1 expression on BECs which is essential for their stress-induced activation

The percentage of IL-1R1-expressing BECs was increased during EAE, and IL-1R1 expression by BECs was required for EAE development [125]. Similarly, in a model of CSD involving severe 2-hour defeat sessions, upregulation of IL-1R1 in the vasculature was observed [98, 149]. Based on these findings, we aimed to confirm whether IL-1R1 expression is also upregulated on BECs in our CSD model. For this purpose, we subjected wildtype-like mice to CSD (Fig. 8A). Interestingly, similar to EAE, the percentage of IL-1R1$^+$ BECs was slightly increased by approximately 20% after CSD (Fig. 8B), indicating that IL-1R1 on BECs may play a role in the stress response.

Therefore, we decided to investigate the role of IL-1 signaling in the BBB during CSD by deleting IL-1R1 in BECs. We used mice of the *Slco1c1*-Cre^{ERT2} strain [158], in which a tamoxifen-inducible Cre recombinase is expressed under the *Slco1c1* promotor which is specifically expressed by endothelial cells in the BBB. We crossed *Slco1c1*-Cre^{ERT2} mice with *Il1r1*$^{fl/fl}$ mice [157]. After tamoxifen injection, we obtained Cre$^{+/-}$ IL-1R1$^{\Delta BEC}$ mice and Cre$^{-/-}$ littermates which were used as wildtype-like controls (IL-1R1^{WT}) (Fig. 8C). Flow cytometry analysis of BECs confirmed successful deletion of IL-1R1 in BECs with a reduction from 4.6 ± 0.4% IL-1R1$^+$ BECs in IL-1R1^{WT} mice to 1.3 ± 0.2% in IL-1R1$^{\Delta BEC}$ mice (Fig. 8D).

Next, we subjected IL-1R1$^{\Delta BEC}$ mice and IL-1R1^{WT} controls to CSD and analyzed their BECs by flow cytometry following the same gating strategy as before (Fig. 7A). Interestingly, the percentages of BECs expressing the activation markers ICAM-1 and VCAM-1 were increased in IL-1R1^{WT} mice after CSD, compared to unstressed controls of the same genotype (Fig. 8E+F). Exposure to CSD also induced increased expression levels (MFI) of ICAM-1 and VCAM-1 on BECs in IL-1R1^{WT} mice (Fig. 8E+F). These observations indicate that wildtype BECs become activated during chronic social stress. Notably, the deletion of IL-1R1 on BECs in IL-1R1$^{\Delta BEC}$ mice abrogated this CSD-induced BEC activation, with no differences in the percentages and MFI of ICAM-1 and VCAM-1 on BECs of IL-1R1$^{\Delta BEC}$ mice between unstressed controls and the CSD condition (Fig. 8E+F). This indicates that IL-1 signaling in BECs during CSD drives stress-induced BEC activation and confirms our previous finding that ICAM-1 and VCAM-1 are mainly expressed by IL-1R1$^+$ BECs. This can be explained by the fact that IL-1 signaling activates the NF-κB pathway, which directly upregulates the expression of ICAM-1 and VCAM-1, as shown in several *in vitro* studies using brain endothelial cell models [130-132].

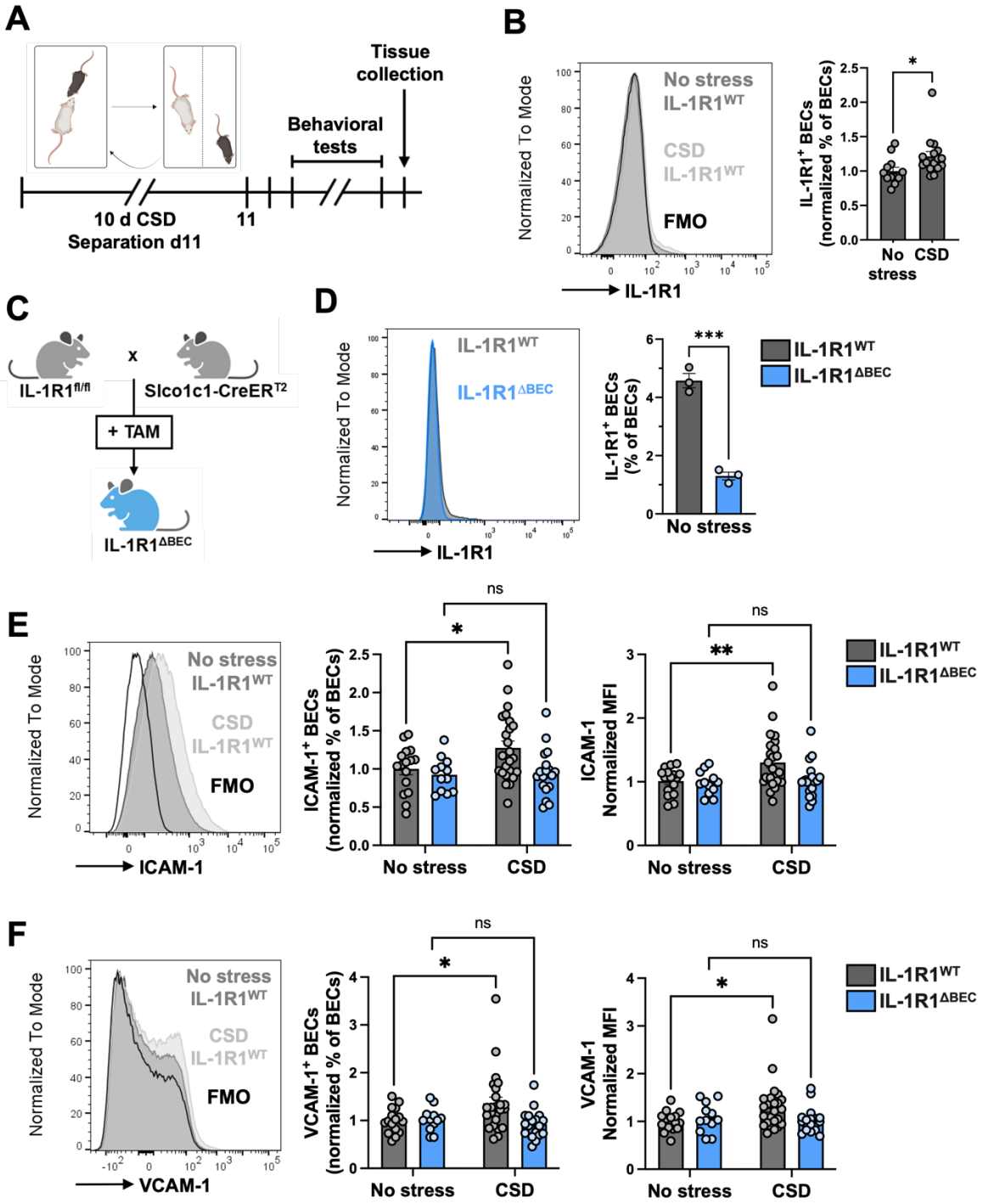

Figure 8: CSD drives IL-1R1 expression on BECs and IL-1R1 is required for stress-induced BEC activation

(A) Mice were exposed to 10 consecutive days of social defeat stress, followed by behavioral testing. BECs were collected for flow cytometry analysis 6-11 days after the end of CSD. **(B)** Histogram showing IL-1R1 expression measured by flow cytometry in BECs from unstressed and CSD-exposed wildtype-like mice and in the FMO control for IL-1R1 (left). Percentages of BECs expressing IL-1R1 normalized to the "No stress" condition (right). **(C)** IL-1R1$^{\Delta BEC}$ mice were generated by crossing *Slco1c1*-Cre^{ERT2} mice to *Il1r1*$^{fl/fl}$ mice. After tamoxifen injection, IL-1R1 is deleted specifically in BECs of IL-1R1$^{\Delta BEC}$ mice. **(D)** Histogram showing IL-1R1 expression measured by flow cytometry in BECs from unstressed IL-1R1$^{\Delta BEC}$ mice and IL-1R1^{WT} controls (left). Percentages of IL-1R1^{+} BECs in IL-1R1$^{\Delta BEC}$ mice and IL-1R1^{WT} controls confirming the deletion of IL-1R1 (right). **(E)** Histogram showing ICAM-1 expression measured by flow cytometry in BECs from unstressed and CSD-exposed wildtype-

like mice and in the FMO control for ICAM-1 (left). Percentages of BECs expressing ICAM-1 normalized to unstressed IL-1R1^{WT} controls (middle). MFI of ICAM-1 normalized to unstressed IL-1R1^{WT} controls (right). **(F)** Histogram showing VCAM-1 expression measured by flow cytometry in BECs from unstressed and CSD-exposed wildtype-like mice and in the FMO control for VCAM-1 (left). Percentages of BECs expressing VCAM-1 normalized to unstressed IL-1R1^{WT} controls (middle). MFI of VCAM-1 normalized to unstressed IL-1R1^{WT} controls (right). Each circle represents a single mouse. Data is represented as mean ± SEM. Statistical significance was determined by two-tailed unpaired Student's t-test (B, D) or two-way ANOVA with Bonferroni's multiple comparison correction (E, F). ns = non-significant, * $p<0.05$, ** $p<0.01$, *** $p<0.001$. Results in B, E and F are pooled from 3 independent experiments.

3.3 IL-1 signaling in BECs regulates CSD-induced depression-like behavior

The main hypothesis of this study was that IL-1 signaling in endothelial cells of the BBB influences the response to chronic social stress. This would be confirmed if IL-1R1$^{\Delta BEC}$ mice exhibit reduced susceptibility to CSD compared to their IL-1R1^{WT} littermates. CSD induces depression-like behavior characterized by the behavioral features of social avoidance, anxiety, and despair. To test our hypothesis, we therefore exposed IL-1R1$^{\Delta BEC}$ and IL-1R1^{WT} mice to CSD and analyzed their behavior in different behavioral tests. The key behavioral test following social stress exposure is the social interaction (SI) test, which is used to classify the animals into "stress-susceptible" and "stress-resilient". The SI test consists of two rounds: in the first round, the experimental mouse is placed in an empty arena, and in the second round, a novel CD-1 mouse is introduced (Fig. 9A). The SI test serves as the primary readout to evaluate the effectiveness of the CSD protocol, as it is specifically designed to assess social avoidance, a hallmark of the CSD model. The SI ratio is calculated as "time in interaction zone with CD-1 present divided by time in interaction zone without the CD-1". All mice with a SI ratio smaller than 1 are classified as "susceptible", since they show social avoidance after the CSD (they interacted more with the empty chamber than with the CD-1 mouse). All mice with a SI ratio larger than 1 are classified as "resilient", since, even after the CSD, they show a preference for the CD-1 mouse (Fig. 9B).

In our experiments, both, IL-1R1^{WT} and IL-1R1$^{\Delta BEC}$ mice developed social avoidance, with the levels of social interaction being markedly reduced in both genotypes after CSD in comparison to unstressed controls (Fig. 9B). However, upon separation into susceptible and resilient mice, it became apparent that more than half of the IL-1R1$^{\Delta BEC}$ mice (56.4 ± 28.8%) were resilient, compared to only one-third of the IL-1R1^{WT} mice (32.6 ± 18.7%, Fig. 9C). This indicates that IL-1 signaling in endothelial cells of the BBB indeed contributes to the establishment of social avoidance after chronic social stress.

Next, we assessed anxiety levels using the open field and elevated plus maze test. Surprisingly, exposure to CSD did not result in statistically significant anxiety behaviors in either genotype across both tests (Fig. 9D+E). Nevertheless, the time spent in the center of the open field tended to decrease in stressed IL-1R1^{WT} mice ($p = 0.0583$) but not in stressed IL-1R1$^{\Delta BEC}$ mice ($p = 0.3579$, Fig. 9D). In addition, the number of entries into the center zone of the open field tended to decrease only in stressed IL-1R1^{WT} mice ($p = 0.0745$, Fig. 9D) but not in stressed IL-1R1$^{\Delta BEC}$ mice ($p = 0.4246$, Fig. 9D). This indicates that IL-1 signaling in BECs could also play a role in the development of anxiety after CSD. Surprisingly, exposure to CSD also influenced the walking distance of IL-1R1^{WT} mice in the elevated plus maze with a decreased total distance in stressed IL-1R1^{WT} but not in stressed IL-1R1$^{\Delta BEC}$ mice (Fig. 9E). This was not observed in the open field test, where the distance was similar between genotypes and stress groups (Fig. 9D).

Finally, we also tested the mice in the forced swim test, a widely used model for assessing depression-like behaviors, including despair and anxiety. In this test, mice are placed into a water tank for six minutes, and the duration of floating, referred to as “immobility time”, is measured. Stressed IL-1R1^{WT} mice exhibited a significantly lower immobility time than unstressed IL-1R1^{WT} mice, while IL-1R1$^{\Delta BEC}$ mice were protected from this stress effect (Fig. 9F). Taken together, these findings indicate that IL-1 signaling in BECs plays a key role in inducing most stress-induced behavioral disturbances.

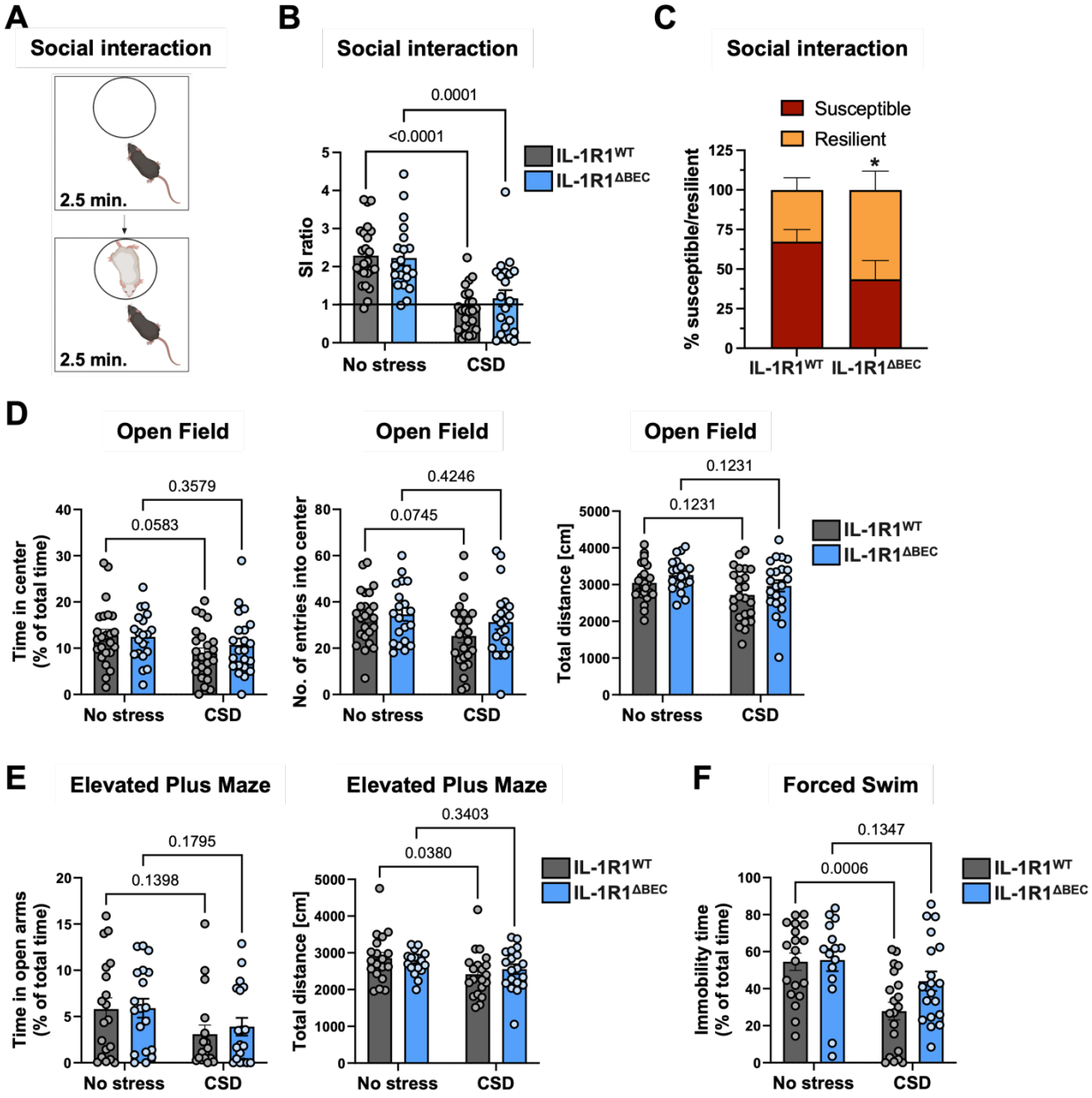

Figure 9: IL-1 signaling in BECs contributes to CSD-induced depression-like behavior

IL-1R1^{WT} and IL-1R1$^{\Delta BEC}$ mice were exposed to CSD and, after a one-day break, were tested in different behavioral tests. **(A)** In the first 2.5 min of the social interaction (SI) test, the experimental mouse is exposed to an empty arena, while in the second 2.5 min, a novel CD-1 mouse is present. The SI ratio is calculated as "time in interaction zone with CD-1 present divided by time in interaction zone without the target". **(B)** SI ratio of IL-1R1^{WT} and IL-1R1$^{\Delta BEC}$ mice without stress and after CSD. Line indicates separation of mice into susceptible (SI ratio < 1) and resilient (SI ratio > 1) groups**. (C)** Percentages of susceptible and resilient mice among IL-1R1^{WT} and IL-1R1$^{\Delta BEC}$ mice after CSD exposure. **(D)** Time in the center of an open field (left), number (no.) of entries into the center (middle), and total distance traveled (right) for IL-1R1^{WT} and IL-1R1$^{\Delta BEC}$ mice without stress and after CSD. **(E)** Time in the open arms of an elevated plus maze (left) and total distance traveled (right) for IL-1R1^{WT} and IL-1R1$^{\Delta BEC}$ mice without stress and after CSD. **(F)** Immobility time in the forced swim test for IL-1R1^{WT} and IL-1R1$^{\Delta BEC}$ mice without stress and after CSD. Each circle represents a single mouse. Data is represented as mean ± SEM. Statistical significance was determined by two-way ANOVA with Bonferroni's multiple comparison correction (B, D, E, F) or paired two-tailed t-test (C). * $p<0.05$. Results are pooled from 5 independent experiments.

3.4 The immune cell composition of spleen and blood is altered after CSD

Since we observed that IL-1R1 expression by BECs is required for CSD-induced behavioral disturbances, we wanted to confirm that peripheral immune activation occurs in our CSD model in order to determine potential sources of IL-1β acting on the BBB.

For this purpose, we isolated immune cells from the spleen and blood of unstressed and CSD-exposed IL-1R1^{WT} and IL-1R1$^{\Delta BEC}$ mice for flow cytometry analysis (Fig. 10A, D). In the spleen, the percentages of CD19^{+} B cells and TCR-β^{+} T cells were significantly decreased in stressed mice of both genotypes (Fig. 10B). In contrast, the percentages of Ly6G^{+} neutrophils were increased after CSD in both IL-1R1^{WT} and IL-1R1$^{\Delta BEC}$ mice, while the percentages of Ly6C^{high} monocytes were unaffected (Fig. 10B). Neutrophils were also significantly increased in number after CSD, while the number of B cells was not altered by stress and T cells were decreased in number only in stressed IL-1R1$^{\Delta BEC}$ mice (Fig. 10C). Taken together, these results indicate that CSD mostly induces an increase in neutrophils in the spleen, which leads to decreases in the percentages of other immune cells such as T cells and B cells.

In the blood, we only observed minor alterations in immune cell populations after CSD. Similar to the spleen, the percentages of B cells and T cells tended to decrease in stressed mice, while the percentages of neutrophils tended to increase after CSD, and the percentages of Ly6C^{high} monocytes were unaffected (Fig. 10E). However, the only statistically significant difference in the blood was the decrease in the percentage of B cells in stressed IL-1R1^{WT} mice compared to unstressed controls of the same genotype (Fig. 10E). Since neutrophils are known producers of IL-1β, their increase after CSD suggests them as one source of IL-1β acting on the BBB during chronic stress.

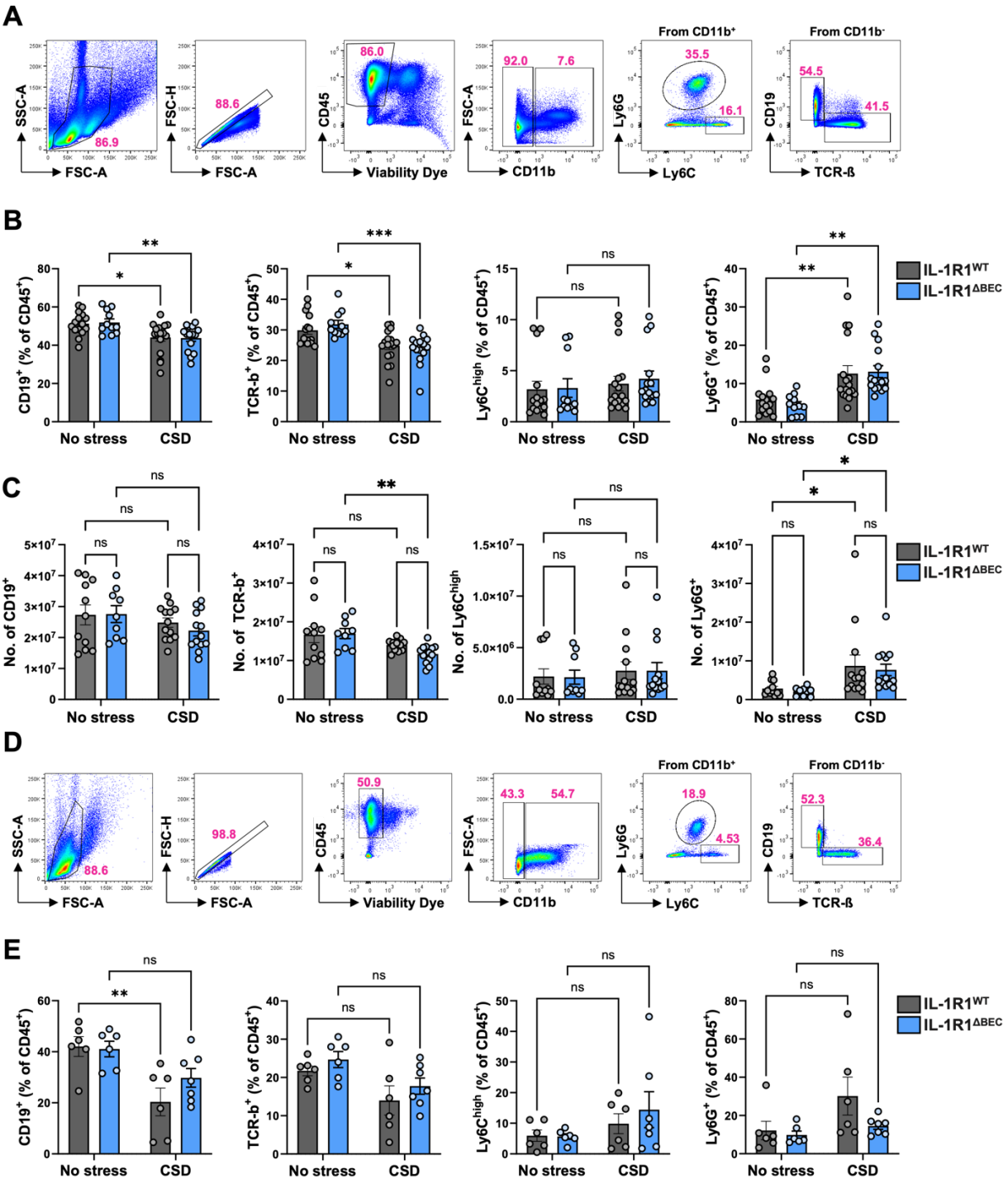

Figure 10: The peripheral immune cell composition is altered after CSD

IL-1R1^{WT} and IL-1R1$^{\Delta BEC}$ mice were exposed to CSD and the immune cells in spleen and blood were analyzed by flow cytometry 5-11 days after the end of the CSD (spleen) or 5-6 days after the end of the CSD (blood). **(A)** Gating strategy in the spleen: after gating on single, live, CD45^{+} immune cells, CD11b^{+} Ly6C^{high} monocytes, CD11b^{+} Ly6G^{+} neutrophils, CD11b^{-} CD19^{+} B cells, and CD11b^{-} TCR-β^{+} T cells were identified. **(B)** Percentages of B cells, T cells, monocytes, and neutrophils in the spleens of IL-1R1^{WT} and IL-1R1$^{\Delta BEC}$ mice without stress and after CSD. **(C)** Absolute numbers of B cells, T cells, monocytes, and neutrophils in the spleens of IL-1R1^{WT} and IL-1R1$^{\Delta BEC}$ mice without stress and after CSD. **(D)** Gating strategy in the blood: After gating on single, live, CD45^{+} immune cells, CD11b^{+} Ly6C^{high} monocytes, CD11b^{+} Ly6G^{+} neutrophils, CD11b^{-} CD19^{+} B cells, and CD11b^{-} TCR-β^{+} T cells were identified. **(E)** Percentages of B cells, T cells, monocytes, and neutrophils in the

blood of IL-1R1^{WT} and IL-1R1$^{\Delta BEC}$ mice without stress and after CSD. Each circle represents a single mouse. Data is represented as mean ± SEM. Statistical significance was determined by two-way ANOVA with Bonferroni's multiple comparison correction. ns = non-significant, * $p<0.05$, ** $p<0.01$, *** $p<0.001$. Results are pooled from 4 independent experiments (B, C) or from 2 independent experiments (E).

3.5 Immune cell infiltration into the brain is almost absent after CSD

Having established that IL-1 signaling in BECs contributes to stress-induced depression-like behavior, we sought to determine the mechanism by which BECs influence this behavior. The BEC activation markers ICAM-1 and VCAM-1, which were upregulated in wildtype-like BECs after CSD, are cell adhesion molecules that facilitate immune cell adhesion and subsequent infiltration into the CNS [85]. Peripheral immune cells entering the brain could influence resident CNS cells, such as microglia, astrocytes, and neurons through cytokine secretion. While some studies reported increased immune cell infiltration into the brain following CSD [96-99], contradictory observations were made in other studies [89, 93, 100].

To address these discrepancies, we analyzed immune cell infiltration in the brain after CSD using flow cytometry. The percentages of CD11b^{-} CD45^{high} infiltrates among all live brain cells were not affected by CSD in both genotypes (Fig. 11A, B). The percentages of CD11b^{+} CD45^{high} myeloid infiltrates tended to slightly increase after CSD in both genotypes, however, the increase observed was very minor and not statistically significant (Fig. 11A, B). Additionally, the percentages of Ly6C^{high} monocytes did not increase after CSD (Fig. 11C, D). This indicates that another mechanism apart from immune cell infiltration into the CNS must be responsible for the behavioral phenotypes observed after CSD.

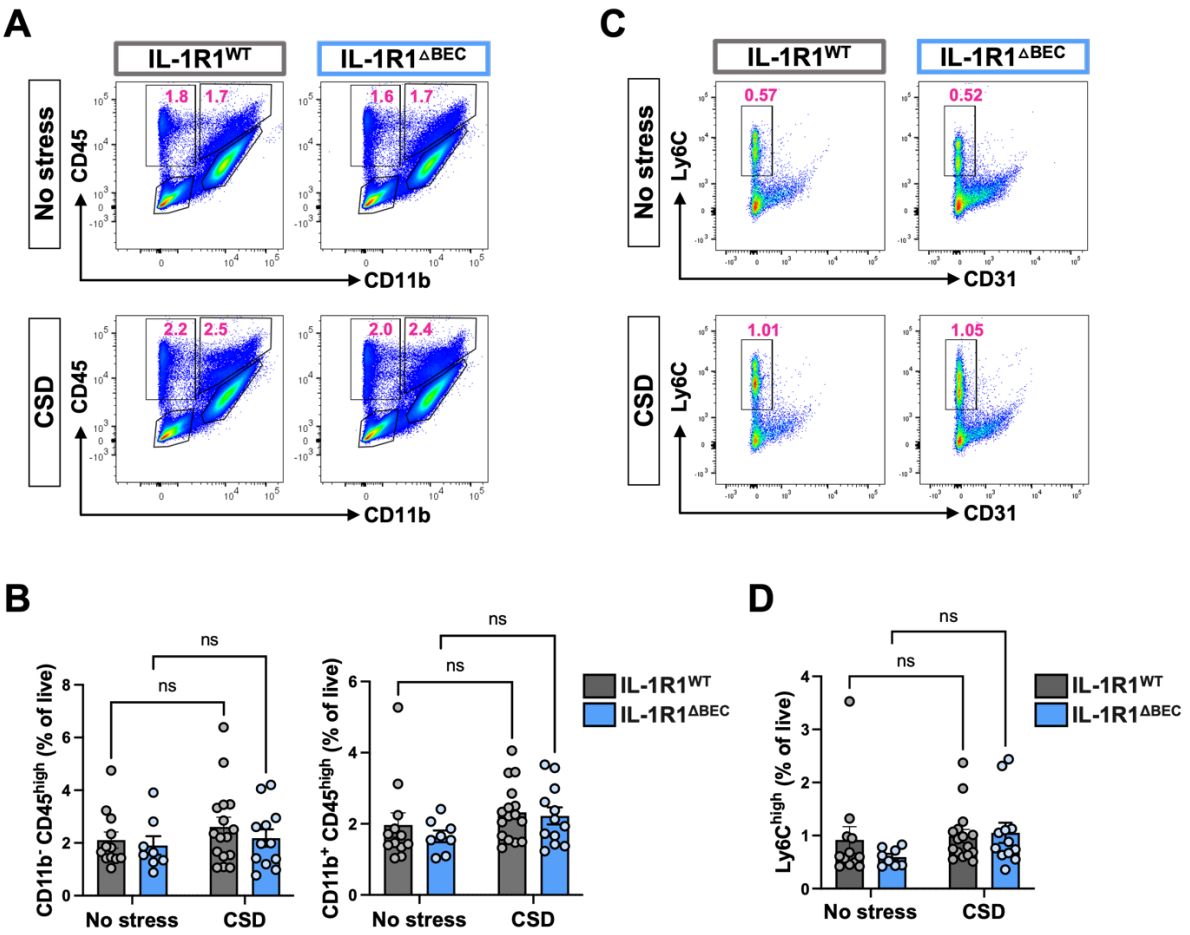

Figure 11: Infiltration of peripheral immune cells into the brain is almost absent after CSD

IL-1R1^{WT} and IL-1R1$^{\Delta BEC}$ mice were exposed to CSD and brain cells were analyzed by flow cytometry 6-11 days after the end of the CSD. **(A)** After gating on single, live cells, CD11b^{-} CD45^{high} and CD11b^{+} CD45^{high} infiltrates were identified. **(B)** Percentages of CD11b^{-} CD45^{high} and CD11b^{+} CD45^{high} infiltrates among all live cells in the brains of IL-1R1^{WT} and IL-1R1$^{\Delta BEC}$ mice without stress and after CSD. **(C)** After gating on single, live CD11b^{+} CD45^{high} cells, Ly6C^{high} monocytes were identified. **(D)** Percentages of Ly6C^{high} monocytes among all live cells in the brains of IL-1R1^{WT} and IL-1R1$^{\Delta BEC}$ mice without stress and after CSD. Each circle represents a single mouse. Data is represented as mean ± SEM. Statistical significance was determined by two-way ANOVA with Bonferroni's multiple comparison correction. ns = non-significant. Results are pooled from 3 independent experiments.

3.6 CSD does not induce neuroinflammation or altered microglia or astrocyte activation

Since IL-1 signaling in BECs during chronic stress did not affect the recruitment of peripheral immune cells into the CNS, we hypothesized that BECs could directly influence surrounding CNS cells such as microglia and astrocytes. To determine whether these cells were more activated after CSD, we isolated mRNA from the brains of unstressed and stressed IL-1R1^{WT} and IL-1R1$^{\Delta BEC}$ mice for quantitative PCR analysis. The expression levels of *glial fibrillary acidic protein (Gfap)*, an astrocyte marker upregulated in reactive astrocytes [163], were not altered by either CSD exposure or genotype (Fig. 12A). Similarly, the expression levels of *Cd68*, a phagocytosis marker upregulated in microglia during inflammation [164], were unchanged (Fig. 12A). We confirmed the lack of difference in microglia activation through a second experiment, in which we isolated CD11b^{+} brain microglia from both unstressed and stressed IL-1R1^{WT} and IL-1R1$^{\Delta BEC}$ mice by magnetic-activated cell sorting (MACS). Consistent with our initial findings, no differences in microglial *CD68* mRNA were observed (Fig. 12B). To further confirm the lack of astrogliosis and microglial activation at the protein level, we performed immunohistochemical staining for GFAP and the microglia marker ionized calcium-binding adaptor molecule 1 (Iba-1). Again, no evidence of altered astrocyte or microglial activation was detected in both the prefrontal cortex and the cortex above the hippocampus (Fig. 13A+B), supporting the conclusion that IL-1 signaling in BECs during CSD does not affect astrocyte or microglial activation.

To rule out potential differences in blood-brain barrier integrity, we analyzed the expression levels of *claudin-5* (*Cldn5*) mRNA, a key tight junction component, in the brains of both unstressed and stressed IL-1R1^{WT} and IL-1R1$^{\Delta BEC}$ mice. No differences were observed between genotypes or stress groups (Fig. 12C). However, it is important to note that this analysis was conducted on whole brain mRNA, which does not allow us to exclude region-specific variations in *Cldn5* expression, as reported in previous studies [89, 90]. Finally, to exclude potential neuroinflammatory changes during CSD, we compared the mRNA levels encoding for the pro-inflammatory cytokines IL-1β, CCL-2 and IL-6 between genotypes and stress groups. We found no significant differences in cytokine expression in total brain mRNA (Fig. 12D). Furthermore, no differences were observed in mRNA levels encoding for the pro-inflammatory cytokines IL-1β, CCL-2 and TNF-α directly in CD11b^{+} microglia isolated by MACS (Fig. 12E). Overall, these data suggest that CSD does not lead to neuroinflammation, significant changes in astrocyte or microglia activation, or alterations in the BBB.

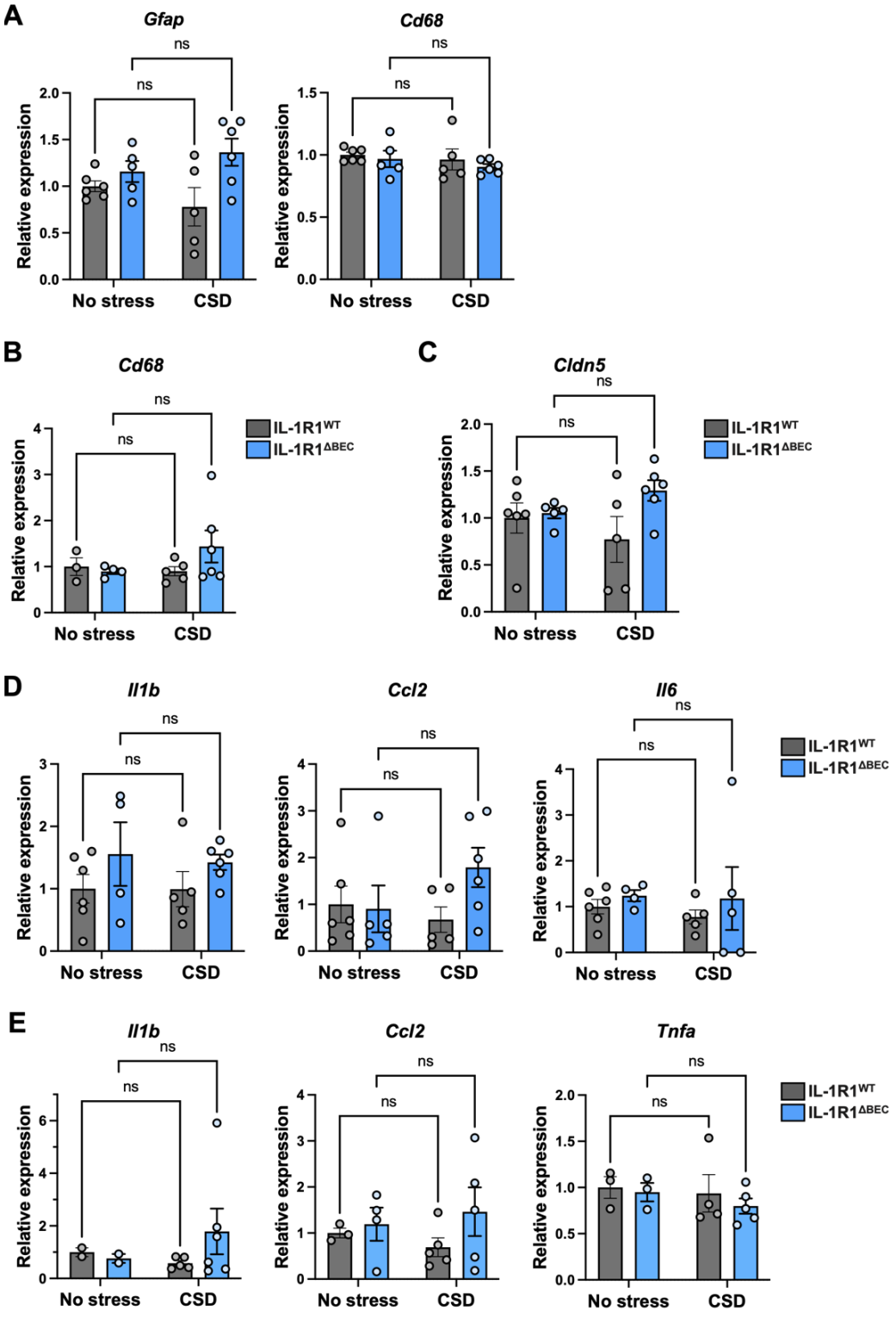

Figure 12: CSD does not induce neuroinflammation or changes in microglia or astrocyte activation

(A) Quantitative PCR with full brain mRNA isolated from IL-1R1^{WT} and IL-1R1$^{\Delta BEC}$ mice without stress and after CSD. **(B)** Quantitative PCR with mRNA from MACS-isolated CD11b^{+} brain microglia from IL-1R1^{WT} and IL-1R1$^{\Delta BEC}$ mice without stress and after CSD. **(C)** Quantitative PCR with full brain mRNA isolated from IL-1R1^{WT} and IL-1R1$^{\Delta BEC}$ mice without stress and after CSD. **(D)** Quantitative PCR with full brain mRNA isolated from IL-1R1^{WT} and IL-1R1$^{\Delta BEC}$ mice without stress and after CSD. **(E)** Quantitative PCR with mRNA from MACS-isolated CD11b^{+} brain microglia from IL-1R1^{WT} and IL-1R1$^{\Delta BEC}$ mice without stress and after CSD. All

data shown are mRNA levels normalized to *Hprt* and unstressed IL-1R1^{WT} controls. Samples for full brain mRNA were collected 5 days after the end of CSD. Samples for microglia mRNA were collected 4 days after the end of CSD. Each circle represents a single mouse. Data is represented as mean ± SEM. Statistical significance was determined by two-way ANOVA with Bonferroni's multiple comparison correction. ns = non-significant.

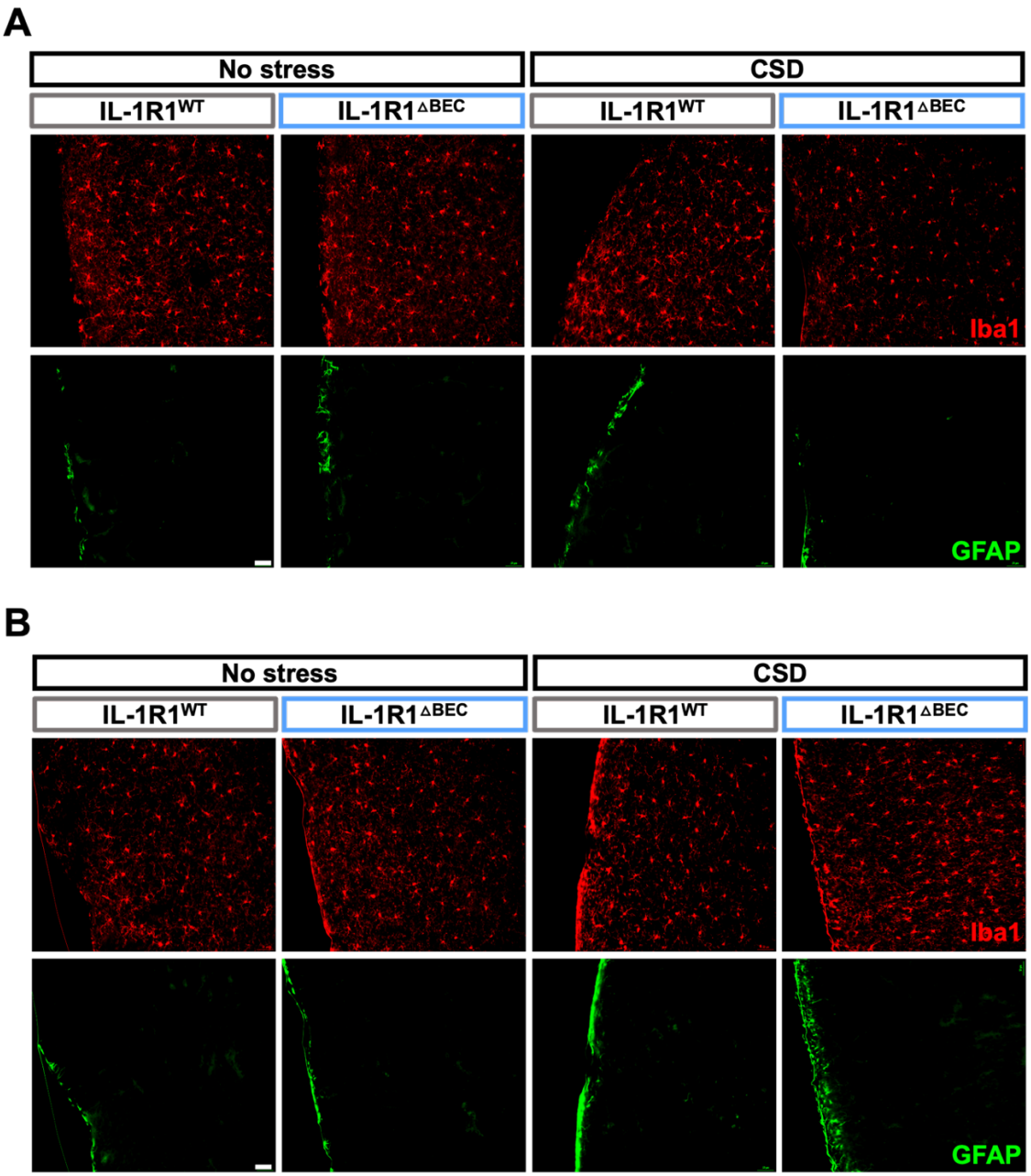

Figure 13: CSD does not induce astrogliosis or microglia activation

IL-1R1^{WT} and IL-1R1$^{\Delta BEC}$ mice were exposed to CSD and brain tissue was processed for immunohistochemistry 8 days after the end of CSD. Representative fluorescence images show staining for microglia (Iba-1, red) and astrocytes (GFAP, green) in the prefrontal cortex **(A)** and the cortex above the hippocampus **(B)**. Images were acquired using a Keyence BZ-X810 fluorescence microscope at 20x magnification. Scale bar = 50 µm.

3.7 RNA sequencing of IL-1R1$^+$ BECs of unstressed, resilient and susceptible mice after CSD

To determine the mechanism by which BECs influence behavior, we then performed a RNA sequencing experiment in which we compared the transcriptomes of IL-1R1$^+$ BECs isolated from unstressed, susceptible and resilient mice. This way, we aimed to identify regulators of stress resilience *versus* stress susceptibility in IL-1R1$^+$ BECs. We exposed wildtype mice to CSD and identified susceptible and resilient mice in the SI test (Fig. 14A+B). Resilient mice had a similar SI ratio as unstressed mice (2.1 ± 0.6 for unstressed; 2.0 ± 0.4 for resilient), while the SI ratio of susceptible mice was significantly decreased to 0.6 ± 0.2 (Fig. 14B). We isolated brain cells from these mice, followed by MACS of CD31$^+$ cells to enrich for BECs. We then used FACS to identify BECs as CD45$^-$ CD11b$^-$ Ly6C$^+$ CD31$^+$ single live cells (Fig. 14C). We also included an IL-1R1 knockout control mouse in the FACS analysis, which we used to determine which BECs expressed IL-1R1 (Fig. 14C), and we FACS-isolated 450 IL-1R1$^+$ BECs per sample for RNA sequencing.

We confirmed the purity of BECs in the RNA sequencing samples by plotting the normalized counts for endothelial cell markers and markers for other brain-resident cells (pericytes, astrocytes, neurons, oligodendrocytes and microglial cells) using markers published by Munji *et al*. [165] (Fig. 14D).

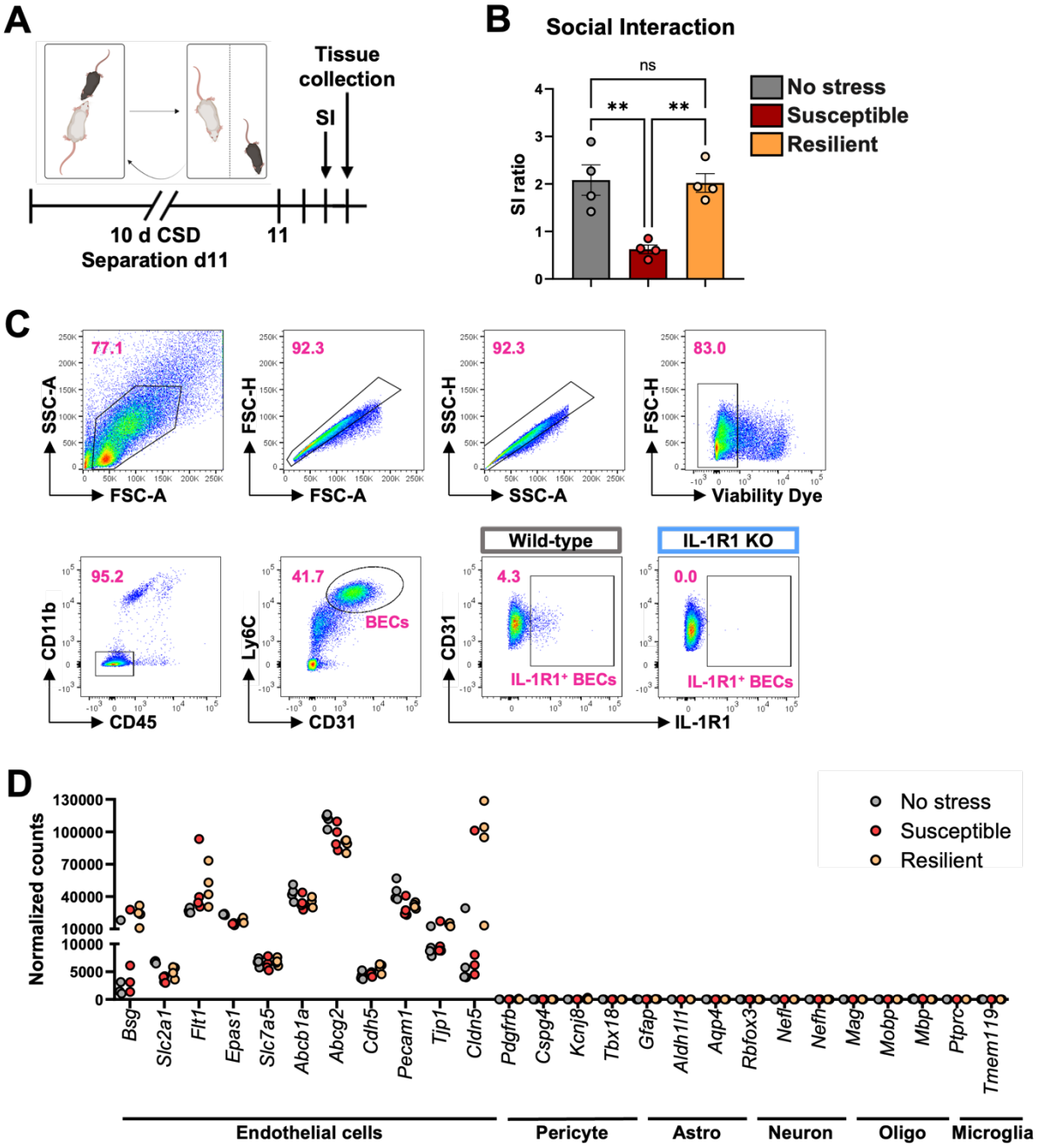

Figure 14: IL-1R1$^+$ BECs from the brains of unstressed, susceptible and resilient wildtype mice were FACS-isolated for transcriptome analysis

(A) Wildtype C57BL/6JRj mice were exposed to CSD, analyzed in the social interaction (SI) test, and brains were collected for BEC isolation. **(B)** SI ratios of unstressed, susceptible and resilient wildtype mice used for the RNA sequencing. **(C)** Representative gating strategy for the sorting of single, live, CD45$^-$ CD11b$^-$ Ly6C$^+$ CD31$^+$ IL-1R1$^+$ BECs. An IL-1R1 knockout (KO) mouse was included to determine the gate for the sorting of IL-1R1$^+$ BECs. **(D)** Normalized counts of marker genes for endothelial, pericyte, astrocyte (astro), neuron, oligodendrocyte (oligo) and microglia cell populations in the RNA sequencing data of sorted IL-1R1$^+$ BECs from the brains of unstressed, susceptible and resilient wildtype mice. Data in (B) is shown as mean ± SEM and statistical significance was determined by one-way ANOVA with Tukey's multiple comparison correction. ** $p<0.01$.

3.7.1 IL-1R1$^+$ BECs seem to be localized at postcapillary venules and venous sites of immune cell extravasation

As described earlier, with our approach of using RNA in situ hybridization to identify the blood vessel type and localization of *Il1r1* mRNA expression, we observed *Il1r1* mRNA across different brain regions and in blood vessels of varying sizes. To further define the blood vessel type in which IL-1R1$^+$ BECs are located, we plotted the normalized counts for endothelial cell genes that are specific for certain types of blood vessel from our transcriptome data. Figure 15A shows markers for capillary venular, capillary arteriolar, venous and arterial endothelial cells, as well as for interferon-activated endothelial cells. This cell population undergoes high transcriptional changes during neuroinflammation, as described by Fournier *et al.* [166]. Figure 15B shows markers for capillary venular, capillary arteriolar, venous and arterial endothelial cells, as well as for reactive endothelial venules (REVs), as described by Jeong *et al.* [167]. REVs are characterized by expression of adhesion molecules (*Icam1, Vcam1*) and *Vwf* and *Irf1*, known as endothelial cell activation/dysfunction markers [167].

The IL-1R1$^+$ BECs in our analysis mostly expressed markers for capillary venular and venous endothelial cells, as well as markers characteristic for REVs (Fig. 15A+B). This seems to be in line with the findings by Lévesque *et al.* who observed IL-1R1 expression mostly on venules and veins extending in the direction of the pial venous plexus [121]. Of note, the expression of these marker genes did not differ substantially between IL-1R1$^+$ BECs isolated from unstressed, susceptible or resilient mice (Fig. 15A+B). Jeong *et al.* allowed further exploration of their data using an online tool available at single-cell.mpi-muenster.mpg.de [167]. In line with our flow cytometry data, *Il1r1* was mostly co-expressed in endothelial cells expressing *Icam1* and *Vcam1* in Jeong *et al.*'s dataset, with *Il1r1* expression being limited to the cell population that was defined as REVs (Fig. 15C). Taken together, these results suggest that IL-1R1$^+$ endothelial cells are mostly located in smaller veins and postcapillary venules, which are also key sites in the vascular tree where immune cell extravasation into the CNS parenchyma occurs [168].

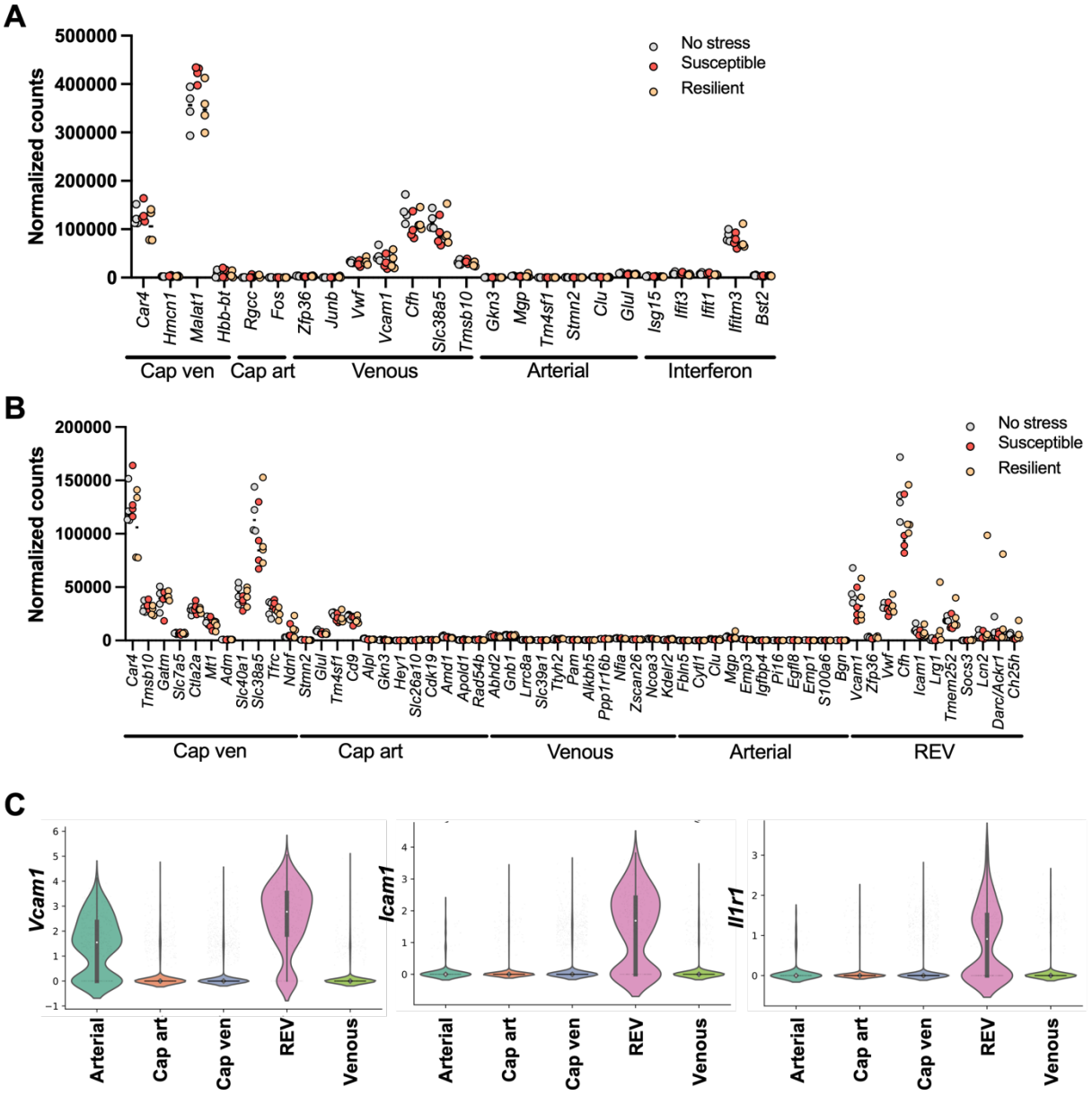

Figure 15: IL-1R1$^+$ BECs express capillary venular and venous endothelial cell markers and markers for reactive endothelial venules (REVs)

(A) Normalized counts of marker genes for capillary venular (Cap ven), capillary arteriolar (Cap art), venous, arterial and interferon-activated endothelial cells in FACS-isolated IL-1R1$^+$ BECs from unstressed, susceptible and resilient wildtype mice according to Fournier *et al.* [166]. **(B)** Normalized counts of marker genes for capillary venular, capillary arteriolar, venous and arterial endothelial cells, as well as for reactive endothelial venules (REVs), in FACS-isolated IL-1R1$^+$ BECs from unstressed, susceptible and resilient wildtype mice according to Jeong *et al.* [167]. **(C)** Expression of *Vcam1*, *Icam1* and *Il1r1* in the endothelial cell populations in the data set generated by Jeong *et al.* Graphs were generated at single-cell.mpi-muenster.mpg.de [167].

3.7.2 The transcriptome of IL-1R1$^+$ BECs differs substantially between unstressed, susceptible and resilient wildtype mice

To identify regulators of stress susceptibility *versus* stress resilience in BECs, we then compared the transcriptomes of IL-1R1$^+$ BECs isolated from unstressed, susceptible and resilient mice. Due to the experimental setup with three groups, the comparison of each group to the other two groups led to three different comparisons. We observed the largest number of differentially expressed genes (DEGs; adjusted p-value < 0.05; log2fold change < -0.6 or > 0.6) in the comparison "susceptible *vs.* no stress" (295 genes; 82 up, 213 down). 203 genes were differentially expressed in the comparison "resilient *vs.* no stress" (149 up, 54 down) and the smallest number of DEGs was observed in the comparison "resilient *vs.* susceptible" (99 genes; 89 up, 10 down) (Fig. 16A). To identify biological processes that the DEGs could be involved in, we performed a gene ontology (GO) term analysis. Figure 16B shows the top five GO terms with the lowest p-value for each of the three comparisons. The comparison "resilient *vs.* susceptible" mainly resulted in GO terms regarding the regulation of cell migration and cell adhesion. However, when analyzing the DEGs associated with each of these GO terms, the DEGs were mainly *Cx3cl1*, *Cx3Cr1* and *Trem2* for three out of the five GO terms questioning the importance of this observation (Fig. 16B). Since cell migration and cell adhesion are important processes during angiogenesis, the formation of new blood vessels, we nevertheless wanted to investigate potential differences in angiogenesis between the brains of unstressed, susceptible and resilient mice. We quantified the total area of blood vessels and assessed endothelial cell proliferation by Ki-67 staining. However, we did not detect differences in these two parameters, indicating that angiogenesis is not substantially altered in the brains of unstressed compared to susceptible and resilient mice (data not shown; part of a Master's thesis).

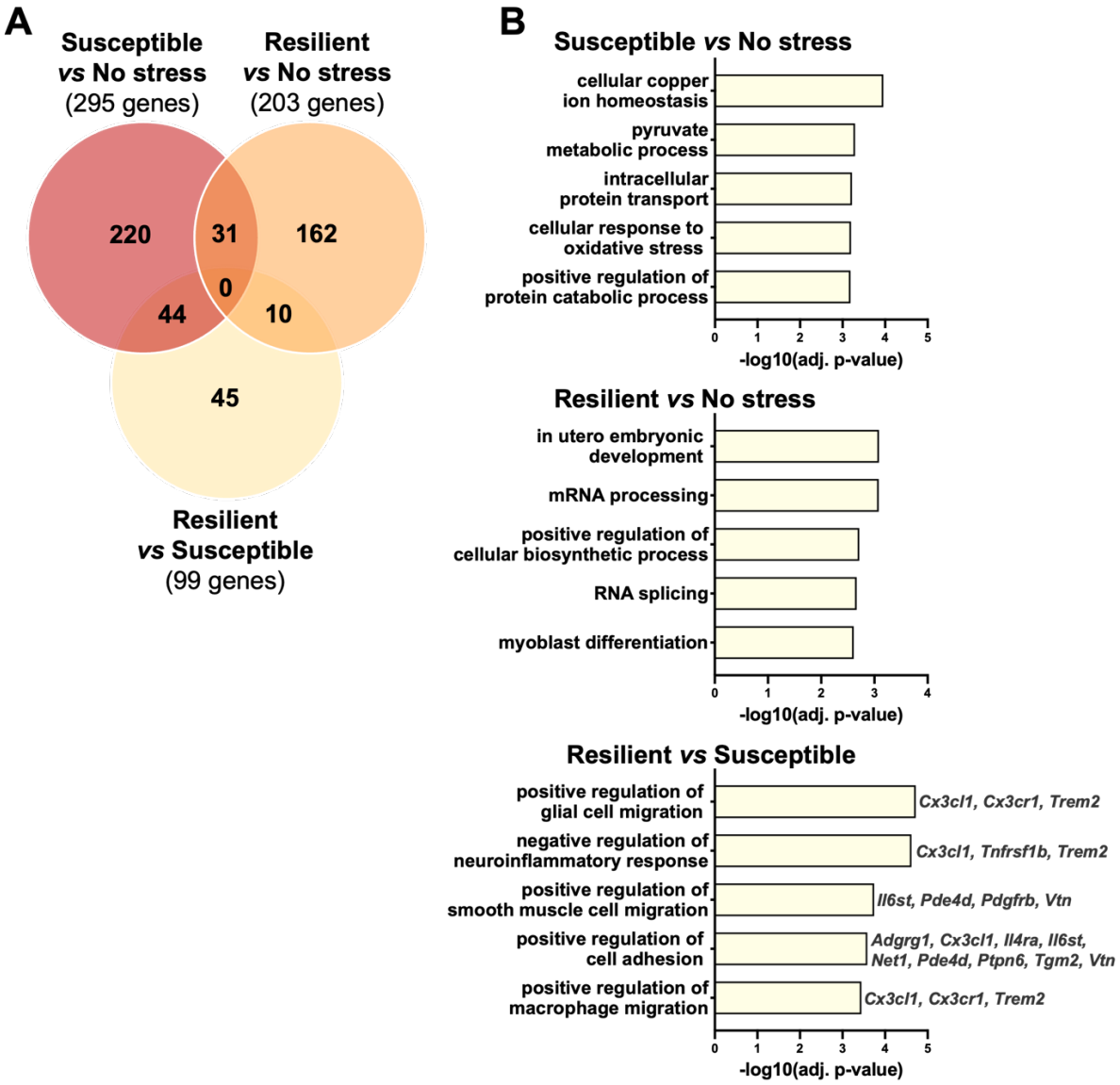

Figure 16: Transcriptome analysis of IL-1R1$^+$ BECs from unstressed, susceptible and resilient wildtype mice

(A) Numbers of differentially expressed genes (DEGs) for the 3 comparisons with adjusted p-value < 0.05 and log2fold change < -0.6 or > 0.6. Venn diagram shows numbers of shared DEGs. (B) Top 5 gene ontology (GO) terms with the lowest adjusted p-value for each comparison.

Next, we were interested in the individual DEGs and plotted the top 15 DEGs with the lowest adjusted p-value for each comparison in a heatmap (Fig. 17A). Notably, several genes appeared in the top 15 DEGs for two comparisons: *Fam205a2* was differentially expressed in both "resilient *vs.* no stress" and in "resilient *vs.* susceptible", while *Cx3cl1, Mfge8, Pfkl, Adgrg1, Paqr7, Tap2, Nucb1* and *Galnt4* were shared between "susceptible *vs.* no stress" and "resilient *vs.* susceptible" (Fig. 17A). Plotting the normalized counts for each of these genes revealed that *Fam205a2* was downregulated in BECs of resilient mice (Fig. 17B). However, its expression

levels were very low and varied substantially between individual samples. The other genes were all downregulated in BECs of susceptible mice (Fig. 17C). This selective downregulation in susceptible mice but not in resilient mice suggests these genes may play a role in mediating stress resilience. To explore this further, we examined their known functions. Among these genes, *Adgrg1*, encoding G-protein coupled receptor 56 (GPR56), stood out due to its established roles in both neuropsychiatric and vascular processes. For instance, *Adgrg1* knockdown in the mouse prefrontal cortex induced depression-like behaviors and its expression was downregulated in the prefrontal cortex of depressed individuals [169]. Additionally, GPR56 regulated angiogenesis in diabetic kidney disease together with leucine rich alpha-2-glycoprotein-1 (LRG1) [170]. Notably, *Lrg1* was among the top DEGs upregulated in the comparison "resilient *vs.* no stress" in our data set (adjusted p-value = 0.04). *Lrg1* is also commonly upregulated in BECs in several rodent models of BBB dysfunction [165] and following CSD stress [171, 172], suggesting it as an attractive target for further investigation.

Unfortunately, since it is only possible to isolate 500-1000 IL-1R1^{+} BECs from one brain, we were not able to verify the differential expression of the genes identified in the RNA sequencing in a second cohort of mice with another method, e.g., using quantitative PCR. Because of the promising literature about a potential role of LRG1 in BECs during CSD, as well as in other BBB dysfunction models, we nevertheless wanted to further investigate *Lrg1* expression in BECs after chronic stress. Therefore, we isolated total BECs, independent of their IL-1R1 expression, using MACS for CD31^{+} cells, and quantified *Lrg1* expression by quantitative PCR. Comparison of IL-1R1^{WT} and IL-1R1$^{\Delta BEC}$ mice without stress and after CSD revealed no significant differences in *Lrg1* expression in BECs (Fig. 18A). Similarly, *Lrg1* expression did not differ significantly between unstressed, susceptible and resilient wildtype-like mice (IL-1R1^{WT}) (Fig. 18B). However, it is important to note that the sample size for wildtype-like mice in this experiment was small, and these findings contradict previous studies that reported increased *Lrg1* expression in BECs after CSD [171, 172]. Therefore, larger sample sizes are needed to confirm these results and further investigation into LRG1's function in BECs during CSD stress would be important.

Interestingly, in the single-cell RNA sequencing data provided by Jeong *et al.* [167], accessible at single-cell.mpi-muenster.mpg.de, *Lrg1* expression was also restricted to the cell population defined as REVs. This pattern mirrors that of *Il1r1, Icam1* and *Vcam1,* suggesting that *Lrg1* may serve as an additional marker for REVs [167] (Fig. 18C).

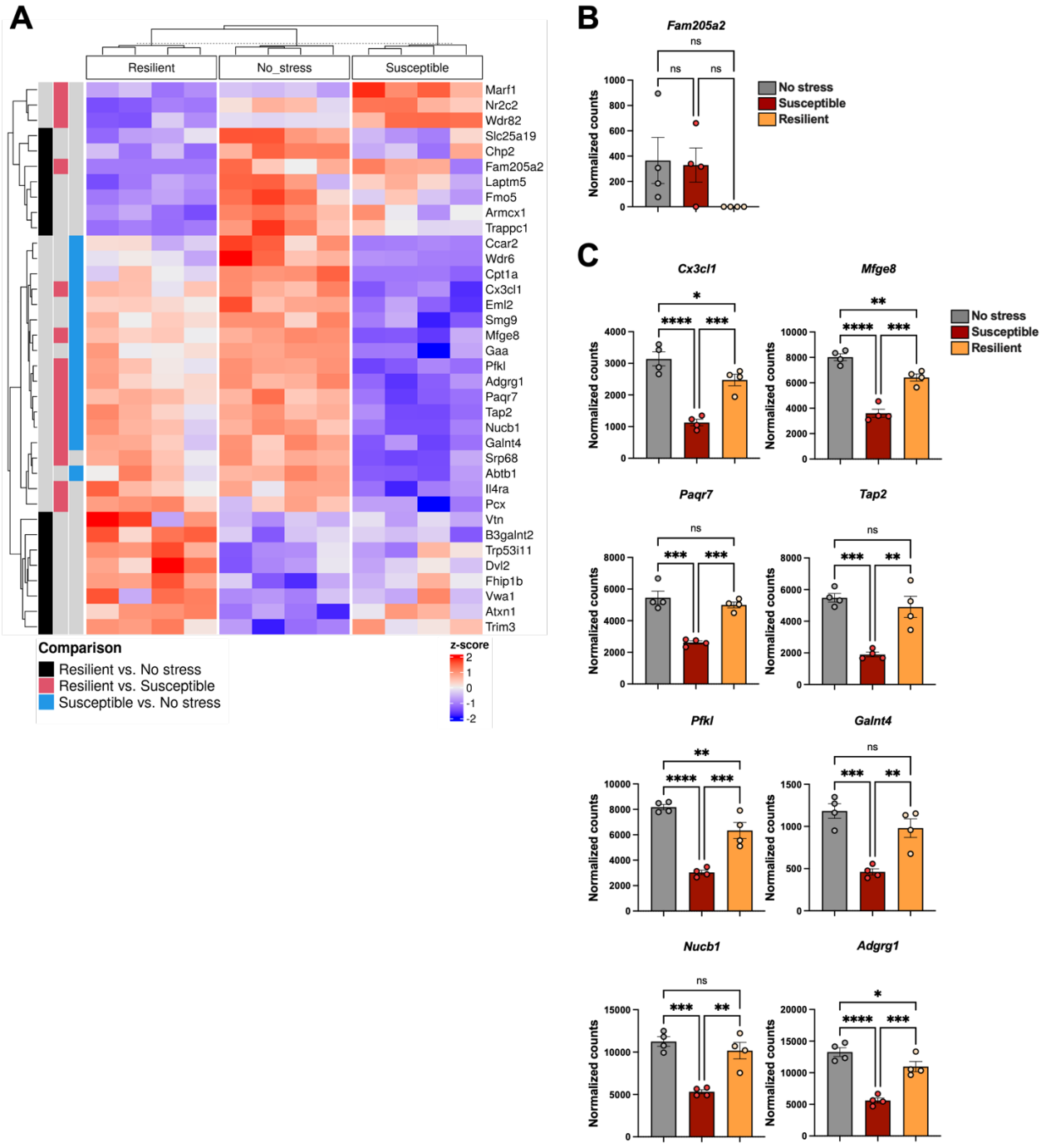

Figure 17: Differentially expressed genes (DEGs) in the transcriptome analysis of IL-1R1$^+$ BECs from unstressed, susceptible and resilient wildtype mice

(A) Heatmap showing the expression levels of the top 15 DEGs with the lowest adjusted p-value for the comparisons "Resilient *vs*. No stress", "Resilient *vs*. Susceptible" and "Susceptible *vs*. No stress". Each column represents an individual mouse. The colors on the left indicate the comparison(s), in which the gene was differentially expressed. **(B)** *Fam205a2* expression levels plotted as normalized counts in IL-1R1$^+$ BECs from unstressed, susceptible and resilient wildtype-like mice. **(C)** Normalized counts for genes downregulated in IL-1R1$^+$ BECs of susceptible mice compared to BECs of unstressed and resilient mice. Each circle represents a single mouse (B, C). Data is represented as mean ± SEM. Statistical significance was determined by one-way ANOVA with Tukey's multiple comparison correction. ns = non-significant, * $p<0.05$, ** $p<0.01$, *** $p<0.001$, **** $p<0.0001$.

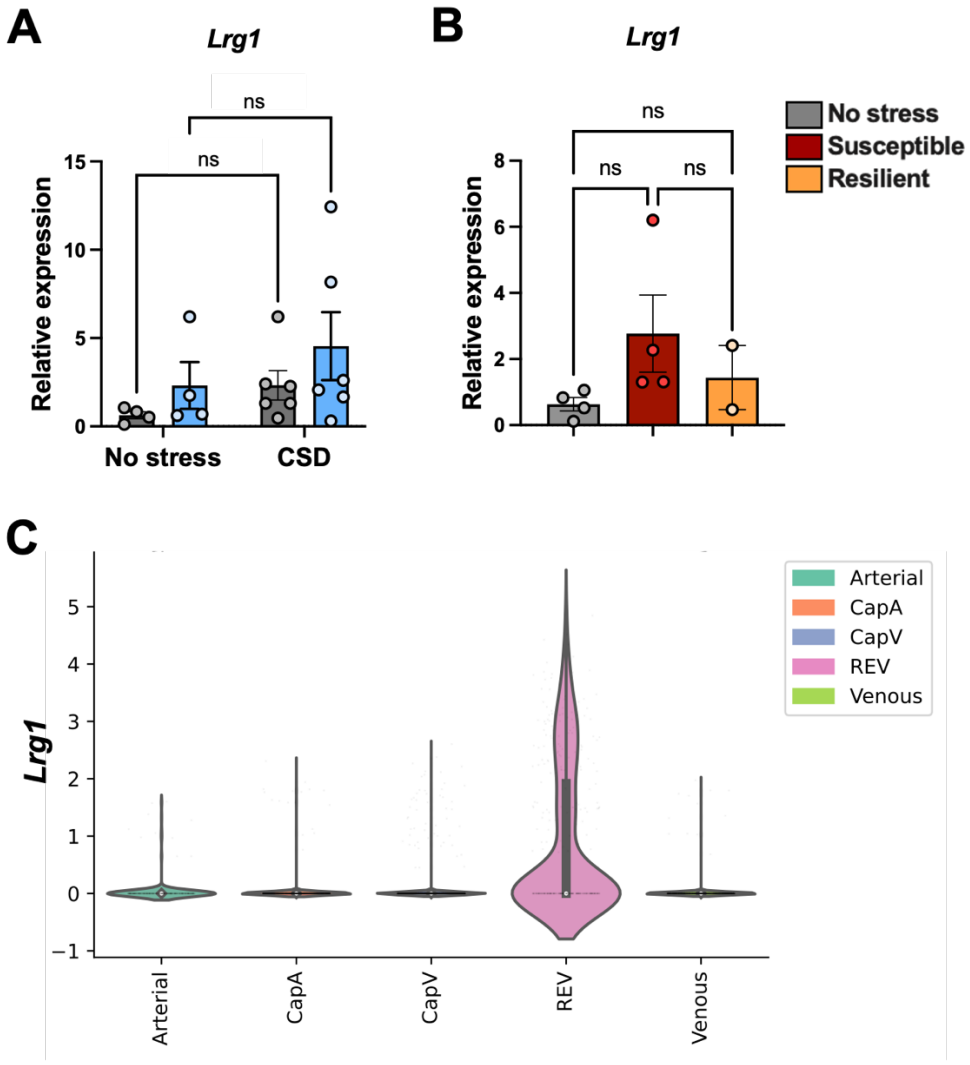

Figure 18: *Lrg1* expression in BECs at steady state and after CSD

(A) Quantitative PCR with mRNA from MACS-isolated CD31^{+} BECs from IL-1R1^{WT} and IL-1R1$^{\Delta BEC}$ mice without stress and after CSD. **(B)** Quantitative PCR with mRNA from MACS-isolated CD31^{+} BECs from unstressed, susceptible and resilient wildtype-like mice. **(C)** Expression of *Lrg1* in the endothelial cell populations in the data set generated by Jeong *et al.* Graphs were generated at single-cell.mpi-muenster.mpg.de [167]. Data in (A) are mRNA levels normalized to *Hprt* and unstressed IL-1R1^{WT} controls. Data in (B) are mRNA levels normalized to *Hprt* and unstressed controls. Each circle represents a single mouse. Data is represented as mean ± SEM. Statistical significance was determined by two-way ANOVA with Bonferroni's multiple comparison correction (A) or by one-way ANOVA with Tukey's multiple comparison correction (B). ns = non-significant.

4 DISCUSSION

IL-1R1 is expressed by only a small subset of BECs under steady-state conditions, but its expression increases significantly during neuroinflammation [125]. Similarly, CSD stress induces the upregulation of IL-1R1 on BECs [98, 149], contributing to BBB activation. While global deletion of IL-1R1 in endothelial cells alleviated stress-induced behavioral symptoms [97], it remains unclear to which extent IL-1 signaling specifically in BECs mediates these effects. Therefore, the main aim of this study was to investigate the role of IL-1 signaling in BECs during CSD and its contribution to depression-like behavior using the BEC-specific *Slco1c1*-Cre^{ERT2} mouse strain.

In this study, we showed that IL-1R1^{+} BECs are a small BEC subset with a distinctly activated phenotype, that is mainly localized in postcapillary venules and small veins. CSD stress induced IL-1R1 expression on BECs, which was essential for their activation. Conditional deletion of IL-1R1 in BECs mitigated CSD-induced behavioral changes, suggesting a key role for IL-1 signaling in mediating these stress effects. Further, IL-1 signaling in BECs influenced behavior independently of peripheral immune cell infiltration or neuroinflammation, suggesting alternative mechanisms are involved.

4.1 IL-1 signaling in BECs regulates CSD-induced depression-like behavior

4.1.1 IL-1 signaling in BECs contributes to CSD-induced social avoidance

It was previously shown that IL-1 signaling plays an important role in the development of stress-induced behavioral disturbances in several stress models. The effects of IL-1β are mediated through its actions on various cell types, including glutamatergic neurons as well as non-neuronal cells [149]. Interestingly, global IL-1R1 deficiency was shown to ameliorate certain stress-induced behaviors while having no effect on others. Furthermore, this seems to depend on the specific stress model used. For instance, IL-1R1 deficiency blocked stress-induced social avoidance after CMS [141], but not after CSD [148, 149]. In a study using the tie2-Cre system to delete IL-1R1 in endothelial cells throughout the body, IL-1R1 deletion prevented CSD-induced anxiety behavior, while social avoidance was not assessed in that study [97]. Since the tie2-Cre is expressed in endothelial cells of the whole body, we wanted to investigate the role of IL-1 signaling specifically in BECs in the context of CSD, a question that had not yet been addressed.

The SI test is the most critical tool for assessing stress susceptibility in the CSD model, as it allows to classify the mice into stress-susceptible and stress-resilient subgroups. In our study, when analyzing the SI ratio of the entire cohort of mice, CSD increased social avoidance in both IL-1R1^{WT} and IL-1R1$^{\Delta BEC}$ mice. However, upon separation of stressed mice into susceptible and resilient subgroups, we noticed that a significantly larger proportion of IL-1R1$^{\Delta BEC}$ mice was resilient to CSD-induced social avoidance compared to IL-1R1^{WT} mice. Notably, this phenotype differs from what was observed in the CMS model, where the whole group of IL-1R1 knockout animals tested showed higher levels of social interaction after stress compared to wildtype controls [141]. The phenotype observed in our study suggests that IL-1 signaling in BECs contributes to the development of social avoidance after CSD. However, it is likely that IL-1R1-mediated signaling in BECs represents only one of several mechanisms driving this behavior. This could explain why IL-1R1 deletion in BECs was only sufficient to prevent social avoidance in some, but not all, mice, as additional pathways and factors appear to be involved.

4.1.2 IL-1 signaling in BECs regulates CSD-induced behavioral dysfunction in the forced swim test

The strongest behavioral phenotype observed in our study was in the forced swim test. While IL-1R1^{WT} controls exhibited strongly reduced immobility after CSD, this stress-induced phenotype was blocked in IL-1R1$^{\Delta BEC}$ mice. This observation suggests that IL-1R1-mediated signaling in BECs is critical for the stress-induced behavioral abnormalities observed in the forced swim test. However, interpreting this reduction in immobility time is not straightforward.

The forced swim test was originally developed by Porsolt *et al.* in rats, and consisted of a 15-minute training session followed by a five-minute test session 24 hours later [173]. The adoption of immobility was interpreted as behavioral despair, since it reflects the animal's learned helplessness when escape is impossible. This interpretation was further supported by the observation that antidepressant treatments reduced immobility time, suggesting the forced swim test could be used as a tool to study despair or depression-like behavior [173]. Consequently, the forced swim test has been widely used to screen for antidepressant compounds, with immobility often described as "behavioral despair" or "depression-like behavior" [174].

However, this interpretation is the subject of significant debate, as the forced swim test lacks both face and construct validity to justify interpreting immobility as depression-like behavior

[175, 176]. Face validity assesses how well the neuropathological and behavioral traits of the human condition are mirrored in the animal model, while construct validity evaluates whether the methods used to induce the disease state accurately reflect its underlying mechanisms [155]. Given this limitation, alternative interpretations have been proposed in the literature. One suggestion is that the progressive immobility observed in the forced swim test is an adaptive coping strategy. The rodent transitions from active swimming to passive immobility in response to an inescapable situation, which might represent an evolutionarily advantageous strategy for saving energy [174, 175]. Another interpretation is that escape behavior in the forced swim test may be driven by anxiety [177]. Anyan and Amir [177] proposed this view based on their own findings, as well as those of Estanislau *et al.* [178], which demonstrated that rodents often exhibit an inverse correlation between depression-like and anxiety-like behaviors. Specifically, rodents that show depression-like behavior, as indicated by high immobility, exhibit low levels of anxiety. This inverse correlation is surprising, given that depression and anxiety frequently co-occur in human patients. Thus, it might be plausible that low immobility, indicated by high escape-directed behavior, reflects high levels of anxiety rather than reduced despair.

In summary, the interpretation of immobility time in the forced swim test remains highly debated. It is unclear whether high immobility represents behavioral despair, an energy-saving coping strategy, or low anxiety levels. Recognizing the complexity of the behavior assessed by the forced swim test, we therefore refrain from providing a definitive interpretation of our results. Instead, our main conclusion is that IL-1R1 deletion in BECs protects mice from the CSD-induced decrease in immobility time in the forced swim test, highlighting the role of IL-1 signaling in stress-induced behavioral changes.

4.1.3 Limitation of our CSD model for investigating stress-induced anxiety-like behavior

To assess anxiety-like behavior, we used the open field and the elevated plus maze test. Both tests rely on the innate aversion of mice to bright, open, and unfamiliar areas, which are perceived as dangerous [179, 180]. In the open field test, time spent in the center tended to decrease after CSD in both genotypes, although this effect did not reach statistical significance. Similarly, in the elevated plus maze, time spent in the open arms showed a trend toward reduction after CSD in both genotypes, again without reaching statistical significance. These results suggest that anxiety levels are only mildly elevated after CSD, if at all, which is somewhat unexpected given that CSD is generally known to induce anxiety-like behaviors. Of

note, some groups mainly used the light-dark preference test (LDPT) to measure anxiety-like behavior, a test that we did not use in our analysis. For instance, CSD induced anxiety-like behavior in the LDPT in wildtype-like controls, but not in IL-1R1-deficient animals [97, 144]. However, also in the open field test, anxiety-like behavior was observed after CSD [97]. Notably, these studies employed a more severe CSD protocol, with two-hour defeat sessions on six consecutive days [97, 144]. This protocol is substantially more severe than the one used in our study, which may account for the discrepancies between our results and theirs.

However, also a milder version of the CSD protocol, with defeats lasting five minutes daily, induced anxiety-like behavior in the LDPT [92, 181]. Similarly, in the elevated plus maze, anxiety-like behavior was observed in studies using CSD protocols with defeat sessions lasting 5 or 10 minutes per day [148, 156]. Nonetheless, these protocols may still be more severe than the one used in our study, which limited aggressive interactions to just 30 seconds per day.

Though not statistically significant, our data hint at a potential role of IL-1 signaling in BECs in the development of anxiety-like behaviors following CSD. Both, time spent in the center and the number of entries into the center of the open field tended to decrease mostly in IL-1R1^{WT} controls but not in IL-1R1$^{\Delta BEC}$ mice. This aligns with the previous finding that endothelial cell-specific deletion of IL-1R1 using the tie2-Cre system protected against stress-induced anxiety in both the open field test and the LDPT [97]. However, the tie2-Cre system was described to show minimal recombination in the brain [158], questioning whether the effects observed by Wohleb *et al.* using the tie2-Cre system [97] can be attributed specifically to the loss of IL-1R1 in BECs. To definitely clarify the role of IL-1 signaling in BECs for the development of anxiety after CSD, further studies using a more severe CSD protocol would therefore be necessary to ensure reliable induction of statistically significant anxiety-like behaviors.

4.2 CSD drives IL-1R1 expression on BECs which is essential for their stress-induced activation

Exposure to CSD induced the upregulation of IL-1R1 on BECs in our study, with approximately 20% more BECs expressing IL-1R1 after CSD compared to the unstressed condition. This aligns with previous studies, where IL-1R1 was upregulated across different brain regions after CSD, with this increased expression of IL-1R1 being limited to blood vessels [98, 149]. However, earlier studies did not clarify whether all BECs upregulate IL-1R1 expression levels after CSD or whether only a subset of BECs starts expressing the receptor. Using single-cell flow cytometry, we addressed this question and found that the proportion of IL-1R1^{+} BECs among all BECs was increased after CSD, while the expression levels of IL-1R1 in the total BEC population remained unchanged (MFI data not shown). This suggests that more BECs start expressing the IL-1R1 after CSD, rather than an overall increase in expression on the whole BEC population. It would be interesting to understand why only a subset of BECs starts expressing the IL-1R1 during CSD and what differentiates them from the cells which already express it at steady state and from the cells which remain IL-1R1^{-} even after CSD.

BECs were activated during the CSD exposure, indicated by the observed upregulation of the cell adhesion molecules ICAM-1 and VCAM-1 in wildtype-like BECs after CSD. A similar upregulation of ICAM-1 and VCAM-1 was already shown in a previous study, in which ICAM-1 expression was increased in some brain regions as early as one day after the first social defeat, while VCAM-1 upregulation was only observed after 6 days of social defeat [94]. We assessed the expression of the activation markers after completing both 10 days of CSD, as well as the behavioral tests. Our data show that BEC activation persists for at least 6 to 11 days after the end of CSD, suggesting that CSD exposure is indeed a strong and long-lasting stimulus for BEC activation.

Of note, stress-induced BEC activation was absent in IL-1R1$^{\Delta BEC}$ mice. This observation is consistent with *in vitro* studies showing that IL-1β is a strong inducer of ICAM-1 and VCAM-1 expression in BECs [121, 130-132]. This strongly suggests that increased IL-1 signaling during CSD is responsible for the phenotype observed. A similar observation was made in the EAE model, where endothelial IL-1R1 deletion abrogated ICAM-1 and VCAM-1 upregulation at disease onset [125, 134]. These findings highlight the important role of IL-1 signaling in driving BEC activation during chronic stress and suggest the interference with this pathway as a potential strategy to mitigate stress-induced neurovascular dysfunction.

4.3 Mechanisms by which IL-1R1$^+$ BECs could contribute to CSD-induced depression-like behavior

Having established that IL-1 signaling in BECs leads to their activation during CSD and that this contributes to CSD-induced behavioral disturbances, we aimed to identify the mechanisms behind this phenotype. Our RNA sequencing analysis identified the largest number of DEGs in the comparison between BECs from "susceptible *vs.* no stress" mice. This is consistent with the idea that susceptible mice experience greater stress-induced changes compared to resilient mice, because they were more affected by the stress exposure. However, we also identified 99 DEGs in the comparison of BECs from "resilient *vs*. susceptible" mice, which may include key regulators determining resilience *versus* susceptibility.

4.3.1 Angiogenesis as a potential mechanism for resilience

Among the top GO terms in the "resilient *vs*. susceptible" comparison were terms regarding the regulation of glia cell migration, smooth muscle cell migration and cell adhesion, all processes associated with angiogenesis. Furthermore, IL-1β is known to have pro-angiogenic effects on blood vessel formation [111]. However, our initial assessment of angiogenesis, based on quantification of blood vessel area and assessment of endothelial cell proliferation by Ki-67 staining (not shown here), did not reveal differences between unstressed, susceptible and resilient mice.

Interestingly, a study by Lehmann *et al.* identified angiogenesis as the dominant GO term in the gene expression analysis of BECs after 14 days of CSD [92]. The localization of angiogenesis markers overlapped with sites of vascular damage, where blood products had been deposited in the brain parenchyma [92]. Since angiogenesis is necessary for wound healing, enhanced angiogenesis after CSD could facilitate vascular repair [92], potentially contributing to better recovery in resilient mice and preventing the establishment of behavioral disturbances.

Several angiogenesis-associated genes were identified among the top DEGs in our analysis, namely *Lrg1*, *Adgrg1*, and *Mfge8.* Notably, *Lrg1* and *Adgrg1* were also among the genes associated with angiogenesis in Lehmann *et al.*'s data, where they were upregulated after 1, 7 and 14 days of CSD [92]. In our study, *Lrg1* was specifically upregulated in IL-1R1$^+$ BECs of resilient mice, while its expression levels were very low in BECs of unstressed and susceptible mice. *Lrg1* encodes LRG1, a multi-functional modulator of multiple signaling pathways [182]. LRG1 regulates TGF-β signaling by binding to endoglin, thereby promoting endothelial cell proliferation, migration and invasion [183]. Interestingly, *endoglin* (*Eng*), encoding a co-

receptor for TGF-β signaling, was also upregulated in IL-1R1$^+$ BECs of resilient mice. However, LRG1-induced neovascularization often results in disorganized and dysfunctional blood vessels [183], possibly due to disrupted interactions between endothelial cells and pericytes [184]. Additionally, LRG1 has anti-inflammatory effects in endothelial cells *in vitro* by negatively regulating TNF-α receptor signaling [185]. On the other hand, increased expression of *Lrg1* was implicated in several autoinflammatory disorders, though its specific function in these diseases remains unclear [182].

Upregulation of *Lrg1* in BECs was observed in various animal models of BBB disruption, namely in models of stroke, multiple sclerosis, traumatic brain injury and seizure [165]. We also confirmed *Lrg1* upregulation in BECs at the onset of EAE in an RNA sequencing data set previously published by our lab [186]. Interestingly, *Lrg1* was also upregulated in BECs from the prefrontal cortex and in whole-brain mRNA after CSD, though this study did not differentiate between susceptible and resilient mice [171]. In contrast, a separate study found *Lrg1* specifically upregulated in BECs from the nucleus accumbens of susceptible mice after CSD [172], contradicting our observation of its upregulation in resilient mice. To further validate our results, we performed a follow-up experiment in which we isolated CD31$^+$ BECs from the brains of unstressed, susceptible and resilient mice without distinguishing between IL-1R1$^+$ and IL-1R1$^-$ BECs. However, we could not detect significant differences in *Lrg1* expression in this analysis, likely also due to the small sample size. Whether this absence of a difference was due to the different cell population analyzed, namely all BECs *versus* only IL-1R1$^+$ BECs, needs to be further clarified. Therefore, future studies are needed to investigate the role of LRG1 in BECs, particularly in the context of chronic stress and neuroinflammatory diseases with BBB disruption. A conditional mouse model for targeted deletion of *Lrg1* in BECs could provide important insights and help to identify new promising therapeutic approaches.

Another angiogenesis-associated gene, *Adgrg1,* was one of the top downregulated genes in IL-1R1$^+$ BECs of susceptible mice. It encodes G-protein coupled receptor 56 (GPR56), a protein implicated in both vascular and neuropsychiatric processes. GPR56 inhibits angiogenesis in melanomas [187] and downregulates endothelial nitric oxide synthase in kidney endothelial cells [188]. *Adgrg1* downregulation in the prefrontal cortex was implicated in the pathogenesis of depression [169], and knockdown of *Adgrg1* in the prefrontal cortex induced depression-like behaviors in mice. Conversely, treatment with a GPR56 agonist alleviated stress-induced depression-like behaviors [169], underscoring its potential as a therapeutic target for neuropsychiatric disorders [189]. Given its dual roles in vascular function and depression,

and its downregulation specifically in IL-1R1$^+$ BECs of susceptible mice, further investigations into the role of GPR56 in BECs during chronic stress could be highly relevant.

Similarly, *Mfge8* was downregulated in IL-1R1$^+$ BECs of susceptible mice. *Mfge8* encodes milk fat globule-EGF factor 8 protein (MFG-E8), an integrin-binding protein localized in blood vessels. MFG-E8 supports VEGF-driven angiogenesis in adult mice and supports neovascularization following ischemia [190]. Moreover, MFG-E8 seems to contribute to vascular integrity by linking smooth muscle cells to elastic fibers in arteries [191]. Its downregulation in IL-1R1$^+$ BECs of susceptible mice suggests potential impairments in angiogenesis, further supporting the link between angiogenesis, vascular repair and resilience.

4.3.2 Genes with less characterized roles in BECs and stress resilience

In addition to angiogenesis-associated genes, other genes were also selectively downregulated in IL-1R1$^+$ BECs of susceptible mice. The function of these genes during CSD could be of great interest, since they might encode for potential mediators of stress resilience.

Cx3cl1 encodes CX3CL1, a chemokine that binds to its receptor CX3CR1 on monocytes and lymphocytes. Endothelial cells produce both a secreted form, which acts as a chemoattractant for immune cells, and a membrane-bound form, which facilitates immune cell adhesion. Importantly, IL-1 signaling induces CX3CL1 production in endothelial cells [192]. While *Cx3cl1* downregulation in IL-1R1$^+$ BECs of susceptible mice suggests reduced immune cell recruitment, we did not observe changes in immune cell infiltration in our analysis. Furthermore, if anything, we would expect increased immune cell infiltration in susceptible mice, making the effect of *Cx3cl1* downregulation unclear in this context.

Other downregulated DEGs in IL-1R1$^+$ BECs of susceptible mice included *Paqr7*, *Tap2*, *Pfkl*, *Nucb1*, and *Galnt4*, which have diverse roles. *Paqr7* encodes the membrane progesterone receptor alpha (mPRα), which has important functions in various reproductive tissues [193]. While its specific function in endothelial cells remains unclear, progesterone treatment induced mPRα-mediated relaxation of vascular smooth muscle cells *in vitro* [194]. *Tap2* encodes the transporter associated with antigen processing (TAP) 2, which forms a heterodimer with TAP1 to transport peptides into the endoplasmic reticulum during antigen presentation [195]. *Pfkl* encodes 6-phospho-fructokinase, liver type, the primary phosphofructokinase-1 isoform in immune cells, which participates in glycolysis [196]. *Nucb1* encodes nucleobindin-1, a secreted protein that regulates inflammation through interaction with COX-1 and COX-2 [197]. Lastly, *Galnt4* encodes N-acetylgalactosaminyl-transferase 4, an enzyme implicated in monocyte

adhesion and transmigration through the vascular wall [198]. While these genes have known functions in immunity and metabolism, their specific role in BECs during chronic stress remain unclear. Future studies should focus on unraveling their contributions to stress resilience and susceptibility.

Taken together, our findings identify *Lrg1*, *Adgrg1*, and potentially *Mfge8* as promising candidate genes for understanding the regulation of stress susceptibility *versus* resilience. All three genes are linked to endothelial cell function and angiogenesis, suggesting vascular repair as a potential mechanism contributing to stress resilience. Furthermore, dysregulation of *Lrg1* and *Adgrg1* was implicated in chronic stress, depression and BBB dysfunction, making them particularly relevant for further study. Investigating the function of these genes in BECs during chronic stress using conditional knockout models, along with more detailed analyses of their downstream mechanisms, could provide valuable insights into the interplay between vascular repair, inflammation, and stress resilience.

4.4 Characterization of IL-1R1$^+$ BECs in the steady-state brain

Since IL-1R1 is expressed by only a subset of BECs under steady-state conditions, we sought to further characterize these BECs regarding their marker expression and the type of blood vessel they are localized in. Our results showed that ICAM-1 and VCAM-1 expression was largely restricted to IL-1R1$^+$ BECs at steady state, while only a very small proportion of IL-1R1$^-$ BECs expressed these markers. Furthermore, the expression levels of ICAM-1 and VCAM-1 were substantially higher in IL-1R1$^+$ BECs compared to IL-1R1$^-$ BECs. This finding is consistent with data from a previous single-cell RNA sequencing study of BECs performed by Jeong *et al*., which found that *Il1r1*, *Icam1* and *Vcam1* were all co-expressed by the same BEC population, namely by reactive endothelial venules (REVs) [167]. REVs were described as a small, distinct BEC population characterized by the expression of *Icam1*, *Vcam1*, *Vwf* and *Irf1,* and were present in the brain both at steady state and at the peak of EAE [167]. GO term analysis of genes enriched in REVs identified processes involving inflammatory/immune responses, cell adhesion, and leukocyte migration and adhesion [167].

Conversely, Jeong *et al.* found that during LPS-induced inflammation, T cells first accumulated at ICAM-1$^+$ REVs before ICAM-1 was subsequently upregulated in other endothelial cells, suggesting that REVs may function as the initial entry point for immune cells during neuroinflammation [167]. This aligns with the established concept that immune cell infiltration into the CNS occurs predominantly at the level of postcapillary venules [75] and with the

observation that high levels of ICAM-1 on BECs are required for T cells to cross the BBB by transcellular diapedesis [199]. The strong co-expression of IL-1R1 with ICAM-1 and VCAM-1 in BECs in our study supports the hypothesis that IL-1R1 could serve as an additional REV marker and that IL-1R1$^+$ blood vessels likely act as key sites for immune cell entry during neuroinflammation. Further supporting this hypothesis, the deletion of IL-1R1 in BECs prior to EAE induction was shown to block immune cell infiltration and prevented disease onset [125]. Interestingly, IL-1 signaling in BECs not only induces *Icam1* and *Vcam1* expression *in vitro* [130-132], but also upregulates *Irf1* [200], another key REV marker. These findings suggest that IL-1R1 signaling may not only activate BECs during neuroinflammation but could also serve as a key upstream regulator of REV identity.

Interestingly, in addition to *Il1r1*, Jeong *et al.* also identified *Lrg1* as a REV marker, with its expression increasing in inflammatory BECs at the peak of EAE [167]. These observations further support the hypothesis that LRG1 in BECs could play a critical role in neuroinflammation, highlighting the need for further investigation into its function in BECs during chronic stress and BBB dysfunction.

Having characterized IL-1R1$^+$ BECs in terms of their marker expression, we next wanted to determine their precise localization within the vascular tree, as their position may provide further insights into their role during steady state and neuroinflammation. Endothelial cells exhibit a gradual change in marker expression along the vascular continuum, with distinct marker profiles distinguishing arterial, capillary, and venous subtypes [201]. To determine the vascular localization of IL-1R1$^+$ BECs, we analyzed their gene expression patterns and compared them to established markers for different blood vessel types identified in single-cell RNA sequencing studies of BECs [166, 167]. Our results revealed that IL-1R1$^+$ BECs predominantly expressed markers for capillary venular and venous endothelial cells, as well as for REVs. This localization pattern aligns with findings from Lévesque *et al.*, who observed IL-1R1 expression mostly on venules and veins extending in the direction of the pial venous plexus [121]. Consistently, Jeong *et al*. identified ICAM-1$^+$ REVs as a subset of venules ranging from 8 to 50 micrometers in diameter, representing a subpopulation of smaller venules, potentially postcapillary venules [167]. Further supporting this, Lévesque *et al.* observed that vessels smaller than 10 micrometers in diameter lacked IL-1R1 expression [121]. Additionally, IL-1R1 expression did not co-localize with α-smooth muscle actin [121], a marker of arterial and arteriolar smooth muscle cells, which are absent in veins, venules and capillaries [202].

Taken together, our findings, along with data from previous studies, strongly indicates that IL-1R1^{+} BECs are predominantly localized in smaller veins and venules, most likely postcapillary venules. These vessels are key sites for immune cell infiltration into the CNS during neuroinflammation, reinforcing the idea that IL-1R1^{+} BECs may play a crucial role in regulating neuroinflammatory processes.

4.5 Influence of CSD on neuroinflammation and microglia and astrocyte activation

One possible consequence of stress exposure is increased BBB permeability, allowing peripheral immune cells to enter the CNS. These cells could secrete cytokines and contribute to an inflammatory CNS milieu that may affect neuronal function. However, in this study, we found no statistically significant differences in immune cell infiltrates in the brains of IL-1R1^{WT} and IL-1R1$^{\Delta BEC}$ mice without stress and after CSD. This finding contradicts some previous studies in which increased proportions of infiltrating CD45^{high} peripheral immune cells were observed in the brain following CSD [96-99]. These studies, like ours, used flow cytometry to assess immune infiltration. However, this method does not allow to distinguish “real” infiltrates located in the CNS parenchyma from immune cells that perform immunosurveillance in the perivascular spaces and in the brain ventricles. Other studies found immune cells only in these border regions, namely in the perivascular spaces [89] and in the meninges and choroid plexus [100] following CSD, and a recent study even questioned whether CSD increases immune cell numbers in these areas at all [93]. These inconsistencies between studies raise the possibility that time point of analysis and differences in CSD severity may influence whether immune infiltration after CSD can be observed.

We assessed immune cell infiltration 6 to 11 days after the end of CSD. Furthermore, our CSD protocol includes 10 days of social defeat, while the protocol by the lab that consistently observed increased proportions of infiltrating CD45^{high} immune cells only involves 6 days of social defeat [96-98]. If infiltration occurs early during the stress response, the immune cells may have already left the brain or undergone apoptosis by the time of our analysis. Indeed, studies that observed increased immune infiltration after CSD reported that infiltrating monocytes persisted only for 8 to 10 days after the end of CSD [203].

In addition, we used a milder CSD protocol, with a total of 30-second defeat interactions per day, whereas studies consistently reporting immune infiltration used a much more severe protocol, involving 2-hour daily co-housing of three C57BL/6 mice with a CD-1 aggressor [96-

98]. This protocol not only induced immune infiltration into the CNS but also led to strong peripheral immune activation and splenomegaly, suggesting a much stronger systemic immune response [96-98]. Thus, it might be possible that injuries are required to induce strong peripheral inflammation to promote immune cell infiltration in the CSD model. Future studies should therefore clarify whether our less severe protocol was insufficient to induce immune cell infiltration into the CNS or whether the delay between the CSD and brain infiltrates analysis prevented detection of a potentially transient infiltration.

In line with our findings on the absence of immune infiltration into the CNS, we also observed only mild peripheral immune activation after CSD. The proportions and absolute numbers of $Ly6G^{+}$ neutrophils were increased in the spleens of both genotypes after CSD, while $Ly6C^{high}$ monocytes were not altered. This relatively weak immune response may again be due to the mild CSD protocol used or to the delayed timepoint of analysis 5 to 12 days after the end of CSD, as previous studies suggested that peripheral immune activation is rather transient.

BBB permeability is a key factor influencing immune cell infiltration into the CNS. Previous studies reported slight increases in BBB permeability after CSD, leading to the deposition of blood products in the brain parenchyma, which seemed to contribute to microglia activation during CSD [91-93]. We did not directly assess BBB permeability, but we measured mRNA levels of *Cldn5*, a critical tight junction molecule of the BBB. *Cldn5* expression did not differ between IL-1R1^{WT} and IL-1R1$^{\Delta BEC}$ mice without stress and after CSD. However, this analysis was performed using full-brain mRNA, whereas previous studies described *Cldn5* downregulation in a brain-region and sex-specific manner after CSD. In male mice, *Cldn5* expression was decreased in the nucleus accumbens and hippocampus of susceptible mice [89], while in female mice, it was decreased in the prefrontal cortex [90]. Therefore, in order to detect substantial differences in BBB permeability and tight junction molecule expression, a detailed analysis of separate stress-responsive brain regions would be required.

We also investigated the activation of CNS-resident cells during CSD by analyzing microglia and astrocyte responses. Immunohistochemical staining for Iba-1 and GFAP revealed no obvious signs of microglia or astrocyte activation in IL-1R1^{WT} or IL-1R1$^{\Delta BEC}$ mice after CSD. Additionally, mRNA levels of *Gfap* and *Cd68*, as well as pro-inflammatory cytokines in microglia, did not differ between groups. This contrasts with previous studies that reported increased microglia activation, indicated by increased Iba-1^{+} area, in different brain regions including the amygdala, prefrontal cortex, and hippocampus after CSD [144, 145]. However, the kinetics and duration of microglia activation during CSD are incompletely understood. In

one study, Iba-1 and CD68 signals were elevated in the prefrontal cortex 1.5 hours after CSD but returned to baseline within 4 hours [148]. Since we analyzed the brains several days after stress exposure, we cannot exclude the possibility that microglia and astrocytes were transiently activated and had already returned to a homeostatic state at the time of our analysis. An objective quantification of Iba-1 and GFAP signals in different brain regions, as well as an analysis at earlier timepoints, would help characterize the dynamics of CNS-resident immune activation following CSD.

Taken together, our findings suggest that the milder CSD protocol used in this study did not induce immune cell infiltration into the CNS, strong peripheral immune activation, or prolonged neuroinflammatory responses. However, the delayed timepoint of analysis may have prevented detection of transient inflammatory changes. Future studies should therefore investigate whether microglia activation and elevated levels of pro-inflammatory cytokines can be detected after CSD, as seen in patients with MDD [42, 44, 45]. This would help determine how well the CSD model replicates the neuroimmune alterations observed in MDD.

4.6 Conclusions and Outlook

This study highlights the critical role of IL-1 signaling in BECs in driving stress-induced behavioral changes and BBB activation during chronic stress. While our CSD model had limitations for assessing anxiety-like behavior, we showed that IL-1 signaling in BECs contributes to other stress-induced behavioral dysfunctions. Our RNA sequencing results suggest that angiogenesis and vascular repair could play a role in regulating stress susceptibility *versus* resilience, and identified LRG1, GPR56, and MFG-E8 as potential candidates for future research. Additionally, our findings propose IL-1R1 as a marker for REVs, and encourage future research into whether IL-1 signaling may help to regulate REV identity. Furthermore, IL-1R1 expression appears to define a subset of BECs with key roles in neuroinflammation.

Since IL-1α has also been implicated in the stress response, further studies should investigate the distinct roles of IL-1α and IL-1β in chronic stress and depression. Targeting IL-1 signaling in BECs may offer a promising approach to mitigate stress-induced neurovascular dysfunction. However, in this context, personalized strategies may be necessary, since this approach may only be beneficial for patients with elevated IL-1β levels. A deeper understanding of how inflammation contributes to depression could help guide the development of novel and effective immunotherapy-based treatments tailored to specific patient subgroups.

5 SUMMARY

Chronic stress is a major risk factor for depression, leading to systemic immune activation and neuroinflammation, both of which contribute to the development of depressive symptoms. The blood-brain barrier (BBB), with endothelial cells as a central component, plays a crucial role in maintaining central nervous system (CNS) homeostasis by regulating the exchange of molecules and immune cells between the blood and CNS. However, the precise impact of chronic stress on BBB function and whether BBB components contribute to the establishment of depression-like behavior following stress remain unclear. Interleukin-1 (IL-1), a key pro-inflammatory cytokine, plays a central role in the development of stress-induced behavioral changes. Its receptor, IL-1R1, is primarily expressed by BBB endothelial cells (BECs) in the CNS, but its expression is restricted to a small subset of these cells under steady-state conditions. Chronic social defeat (CSD) stress has been shown to upregulate IL-1R1 expression on BECs, potentially driving BBB activation during stress. Although systemic endothelial IL-1R1 deletion has been shown to alleviate stress-induced behavioral symptoms, it remains unclear whether IL-1 signaling specifically in BECs mediates these effects.

Using the *Slco1c1*-CreERT2 mouse strain to delete IL-1R1 selectively in BECs, this study aimed to investigate the role of IL-1 signaling in BECs during CSD and its contribution to depression-like behavior. Here, we show that IL-1 signaling in BECs is critical for mediating stress-induced behavioral dysfunction, as conditional deletion of IL-1R1 in BECs increased stress resilience and ameliorated behavioral changes following CSD. We found that IL-1R1^{+} BECs constitute a small, distinctly activated BEC subset under steady-state conditions. CSD stress further increased IL-1R1 expression on BECs, which was essential for their activation during stress. Notably, IL-1 signaling in BECs influenced behavior independently of peripheral immune cell infiltration or neuroinflammation, suggesting that alternative mechanisms are involved.

While IL-1 signaling is a well-established key regulator of chronic stress responses, our results demonstrate that this effect is specifically mediated through BECs, highlighting the importance of the BBB in the chronic stress response. Taken together, our findings suggest that targeting IL-1 signaling in BECs could be a promising strategy for mitigating stress-induced neurovascular dysfunction and its associated behavioral consequences.

6 ZUSAMMENFASSUNG

Chronischer Stress ist ein wichtiger Risikofaktor für die Entwicklung von Depressionen. Er bewirkt eine anhaltende Aktivierung des Immunsystems sowie Neuroinflammation, wodurch die Entstehung depressiver Symptome begünstigt wird. Die Blut-Hirn-Schranke (BHS) mit ihren Endothelzellen als zentralem Bestandteil steuert den Austausch von Molekülen und Immunzellen zwischen Blut und Zentralnervensystem (ZNS) und trägt somit maßgeblich zur Aufrechterhaltung des Gleichgewichts im ZNS bei. Allerdings ist bislang ungeklärt, wie chronischer Stress die Funktion der BHS beeinflusst und inwieweit ihre Bestandteile zur Entstehung depressiven Verhaltens nach Stress beitragen. Interleukin-1 (IL-1) ist ein wichtiges pro-entzündliches Zytokin mit einer zentralen Rolle in der Entstehung stressinduzierter Verhaltensstörungen. Sein Rezeptor, IL-1R1, wird im ZNS unter homöostatischen Bedingungen hauptsächlich von Endothelzellen der BHS exprimiert, jedoch nur von einem kleinen Anteil dieser Zellen. Es wurde gezeigt, dass „chronischer sozialer Niederlage“ (CSD)-Stress die IL-1R1-Expression in den BHS-Endothelzellen erhöht, was zur Aktivierung der BHS während Stress beitragen könnte. Die Deletion des IL-1R1 in Endothelzellen des gesamten Körpers konnte stressinduzierte Verhaltensstörungen teilweise verhindern. Allerdings ist bislang unklar, ob dieser Effekt durch IL-1-Signale speziell in Endothelzellen der BHS vermittelt wird.

Zur Klärung dieser Frage verwendeten wir das *Slco1c1*-CreERT2-Mausmodell, das die gezielte Deletion von IL-1R1 in BHS-Endothelzellen ermöglicht. Unsere Ergebnisse zeigen, dass IL-1-Signale in den Endothelzellen der BHS eine zentrale Rolle in der Entwicklung stressinduzierter Verhaltensstörungen spielen, denn die Deletion von IL-1R1 in diesen Zellen verringerte die CSD-induzierten Verhaltensstörungen signifikant. IL-1R1^{+} Endothelzellen bildeten unter homöostatischen Bedingungen eine kleine Zellpopulation mit aktiviertem Phänotyp. CSD führte zu einer verstärkten IL-1R1-Expression in diesen Zellen, die essenziell für ihre Aktivierung während CSD-Stress war. Interessanterweise beeinflusste der IL-1-Signalweg in BHS-Endothelzellen das Verhalten unabhängig von der Infiltration peripherer Immunzellen oder einer generellen Neuroinflammation, was auf andere involvierte Mechanismen hindeutet. Während die Rolle des IL-1-Signalwegs in chronischem Stress bereits etabliert war, zeigen unsere Ergebnisse, dass diese Effekte unter anderem über BHS-Endothelzellen vermittelt werden und unterstreichen die Bedeutung der BHS in der Regulation der Stressantwort. Unsere Ergebnisse legen nahe, dass die gezielte Modulation von IL-1-Signalen in BHS-Endothelzellen eine vielversprechende Strategie zur Verhinderung stressinduzierter BHS-Dysfunktionen und der damit verbundenen Verhaltensveränderungen darstellen könnte.

7 FIGURE INDEX

8 TABLE INDEX

9 REFERENCES

1. (2020) Global burden of 369 diseases and injuries in 204 countries and territories, 1990-2019: a systematic analysis for the Global Burden of Disease Study 2019. Lancet (London, England) 396: 1204-1222. DOI 10.1016/s0140-6736(20)30925-9

2. Whooley MA, Wong JM (2013) Depression and cardiovascular disorders. Annual review of clinical psychology 9: 327-354. DOI 10.1146/annurev-clinpsy-050212-185526

3. Arias-de la Torre J, Vilagut G, Ronaldson A, Serrano-Blanco A, Martín V, Peters M, Valderas JM, Dregan A, Alonso J (2021) Prevalence and variability of current depressive disorder in 27 European countries: a population-based study. The Lancet Public health 6: e729-e738. DOI 10.1016/s2468-2667(21)00047-5

4. Otte C, Gold SM, Penninx BW, Pariante CM, Etkin A, Fava M, Mohr DC, Schatzberg AF (2016) Major depressive disorder. Nature reviews Disease primers 2: 16065. DOI 10.1038/nrdp.2016.65

5. Nestler EJ, Barrot M, DiLeone RJ, Eisch AJ, Gold SJ, Monteggia LM (2002) Neurobiology of depression. Neuron 34: 13-25. DOI 10.1016/s0896-6273(02)00653-0

6. Krishnan V, Nestler EJ (2008) The molecular neurobiology of depression. Nature 455: 894-902. DOI 10.1038/nature07455

7. Li M, D'Arcy C, Meng X (2016) Maltreatment in childhood substantially increases the risk of adult depression and anxiety in prospective cohort studies: systematic review, meta-analysis, and proportional attributable fractions. Psychological medicine 46: 717-730. DOI 10.1017/s0033291715002743

8. Bromet E, Andrade LH, Hwang I, Sampson NA, Alonso J, de Girolamo G, de Graaf R, Demyttenaere K, Hu C, Iwata N, et al. (2011) Cross-national epidemiology of DSM-IV major depressive episode. BMC medicine 9: 90. DOI 10.1186/1741-7015-9-90

9. Lorant V, Deliège D, Eaton W, Robert A, Philippot P, Ansseau M (2003) Socioeconomic inequalities in depression: a meta-analysis. American journal of epidemiology 157: 98-112. DOI 10.1093/aje/kwf182

10. Yehuda R, Hoge CW, McFarlane AC, Vermetten E, Lanius RA, Nievergelt CM, Hobfoll SE, Koenen KC, Neylan TC, Hyman SE (2015) Post-traumatic stress disorder. Nature reviews Disease primers 1: 15057. DOI 10.1038/nrdp.2015.57

11. MacQueen G, Frodl T (2011) The hippocampus in major depression: evidence for the convergence of the bench and bedside in psychiatric research? Mol Psychiatry 16: 252-264. DOI 10.1038/mp.2010.80

12. Savitz J, Drevets WC (2009) Bipolar and major depressive disorder: neuroimaging the developmental-degenerative divide. Neuroscience and biobehavioral reviews 33: 699-771. DOI 10.1016/j.neubiorev.2009.01.004

13. Berton O, Nestler EJ (2006) New approaches to antidepressant drug discovery: beyond monoamines. Nat Rev Neurosci 7: 137-151. DOI 10.1038/nrn1846

14. Duman RS, Monteggia LM (2006) A neurotrophic model for stress-related mood disorders. Biol Psychiatry 59: 1116-1127. DOI 10.1016/j.biopsych.2006.02.013

15. Cuthbert BN (2014) The RDoC framework: facilitating transition from ICD/DSM to dimensional approaches that integrate neuroscience and psychopathology. World psychiatry : official journal of the World Psychiatric Association (WPA) 13: 28-35. DOI 10.1002/wps.20087

16. Ross RA, Foster SL, Ionescu DF (2017) The Role of Chronic Stress in Anxious Depression. Chronic Stress (Thousand Oaks) 1: 2470547016689472. DOI 10.1177/2470547016689472

17. Construct: Sustained Threat. *RDoC Classification.* NIMH2016.

18. Hammen C (2005) Stress and depression. Annual review of clinical psychology 1: 293-319. DOI 10.1146/annurev.clinpsy.1.102803.143938

19. McGonagle KA, Kessler RC (1990) Chronic stress, acute stress, and depressive symptoms. American journal of community psychology 18: 681-706. DOI 10.1007/bf00931237

20. Breslau N, Davis GC (1986) Chronic stress and major depression. Arch Gen Psychiatry 43: 309-314. DOI 10.1001/archpsyc.1986.01800040015003

21. Bruce ML, Hoff RA (1994) Social and physical health risk factors for first-onset major depressive disorder in a community sample. Social psychiatry and psychiatric epidemiology 29: 165-171. DOI 10.1007/bf00802013

22. Linsen F, Broeder C, Sep MSC, Verhoeven JE, Bet PM, Penninx B, Meijer OC, Vinkers CH (2023) Glucocorticoid Receptor (GR) antagonism as disease-modifying treatment for MDD with childhood trauma: protocol of the RESET-medication randomized controlled trial. BMC psychiatry 23: 331. DOI 10.1186/s12888-023-04830-9

23. McLaughlin KA, Green JG, Gruber MJ, Sampson NA, Zaslavsky AM, Kessler RC (2010) Childhood adversities and adult psychiatric disorders in the national comorbidity survey replication II: associations with persistence of DSM-IV disorders. Arch Gen Psychiatry 67: 124-132. DOI 10.1001/archgenpsychiatry.2009.187

24. Duman RS, Sanacora G, Krystal JH (2019) Altered Connectivity in Depression: GABA and Glutamate Neurotransmitter Deficits and Reversal by Novel Treatments. Neuron 102: 75-90. DOI 10.1016/j.neuron.2019.03.013

25. Godoy LD, Rossignoli MT, Delfino-Pereira P, Garcia-Cairasco N, de Lima Umeoka EH (2018) A Comprehensive Overview on Stress Neurobiology: Basic Concepts and Clinical Implications. Front Behav Neurosci 12: 127. DOI 10.3389/fnbeh.2018.00127

26. Irwin MR, Cole SW (2011) Reciprocal regulation of the neural and innate immune systems, England.

27. Spencer RL, Deak T (2017) A users guide to HPA axis research. Physiol Behav 178: 43-65. DOI 10.1016/j.physbeh.2016.11.014

28. Schramm E, Waisman A (2022) Microglia as Central Protagonists in the Chronic Stress Response. Neurology(R) neuroimmunology & neuroinflammation 9. DOI 10.1212/nxi.0000000000200023

29. Merkulov VM, Merkulova TI, Bondar NP (2017) Mechanisms of Brain Glucocorticoid Resistance in Stress-Induced Psychopathologies. Biochemistry Biokhimiia 82: 351-365. DOI 10.1134/s0006297917030142

30. Pariante CM, Miller AH (2001) Glucocorticoid receptors in major depression: relevance to pathophysiology and treatment. Biol Psychiatry 49: 391-404. DOI 10.1016/s0006-3223(00)01088-x

31. Mariotti A (2015) The effects of chronic stress on health: new insights into the molecular mechanisms of brain-body communication. Future science OA 1: Fso23. DOI 10.4155/fso.15.21

32. Perrin AJ, Horowitz MA, Roelofs J, Zunszain PA, Pariante CM (2019) Glucocorticoid Resistance: Is It a Requisite for Increased Cytokine Production in Depression? A Systematic Review and Meta-Analysis. Frontiers in psychiatry 10: 423. DOI 10.3389/fpsyt.2019.00423

33. Cattaneo A, Gennarelli M, Uher R, Breen G, Farmer A, Aitchison KJ, Craig IW, Anacker C, Zunsztain PA, McGuffin P, et al. (2013) Candidate genes expression profile associated with antidepressants response in the GENDEP study: differentiating between baseline 'predictors' and longitudinal 'targets'. Neuropsychopharmacology 38: 377-385. DOI 10.1038/npp.2012.191

34. Baumeister D, Akhtar R, Ciufolini S, Pariante CM, Mondelli V (2016) Childhood trauma and adulthood inflammation: a meta-analysis of peripheral C-reactive protein, interleukin-6 and tumour necrosis factor-α. Mol Psychiatry 21: 642-649. DOI 10.1038/mp.2015.67

35. Danese A, Caspi A, Williams B, Ambler A, Sugden K, Mika J, Werts H, Freeman J, Pariante CM, Moffitt TE, et al. (2011) Biological embedding of stress through inflammation processes in childhood. Mol Psychiatry 16: 244-246. DOI 10.1038/mp.2010.5

36. Bierhaus A, Wolf J, Andrassy M, Rohleder N, Humpert PM, Petrov D, Ferstl R, Eynatten Mv, Wendt T, Rudofsky G, et al. (2003) A mechanism converting psychosocial stress into mononuclear cell activation. Proceedings of the National Academy of Sciences of the United States of America 100: 1920–1925. DOI 10.1073/pnas.0438019100

37. Bierhaus A, Wolf J, Andrassy M, Rohleder N, Humpert PM, Petrov D, Ferstl R, von Eynatten M, Wendt T, Rudofsky G, et al. (2003) A mechanism converting psychosocial stress into mononuclear cell activation. Proc Natl Acad Sci U S A 100: 1920-1925. DOI 10.1073/pnas.0438019100

38. Heidt T, Sager HB, Courties G, Dutta P, Iwamoto Y, Zaltsman A, Zur Muhlen Cv, Bode C, Fricchione GL, Denninger J, et al. (2014) Chronic variable stress activates hematopoietic stem cells. Nature medicine 20: 754–758. DOI 10.1038/nm.3589

39. Niraula A, Wang Y, Godbout JP, Sheridan JF (2018) Corticosterone Production during Repeated Social Defeat Causes Monocyte Mobilization from the Bone Marrow, Glucocorticoid Resistance, and Neurovascular Adhesion Molecule Expression. The Journal of neuroscience : the official journal of the Society for Neuroscience 38: 2328–2340. DOI 10.1523/jneurosci.2568-17.2018

40. Busillo JM, Cidlowski JA (2013) The five Rs of glucocorticoid action during inflammation: ready, reinforce, repress, resolve, and restore. Trends in endocrinology and metabolism: TEM 24: 109-119. DOI 10.1016/j.tem.2012.11.005

41. Cruz-Topete D, Cidlowski JA (2015) One hormone, two actions: anti- and pro-inflammatory effects of glucocorticoids. Neuroimmunomodulation 22: 20-32. DOI 10.1159/000362724

42. Miller AH, Raison CL (2016) The role of inflammation in depression: from evolutionary imperative to modern treatment target. Nature reviews Immunology 16: 22-34. DOI 10.1038/nri.2015.5

43. Fleshner M, Frank M, Maier SF (2017) Danger Signals and Inflammasomes: Stress-Evoked Sterile Inflammation in Mood Disorders. Neuropsychopharmacology : official publication of the American College of Neuropsychopharmacology 42: 36–45. DOI 10.1038/npp.2016.125

44. Drevets WC, Wittenberg GM, Bullmore ET, Manji HK (2022) Immune targets for therapeutic development in depression: towards precision medicine. Nature reviews Drug discovery 21: 224-244. DOI 10.1038/s41573-021-00368-1

45. Enache D, Pariante CM, Mondelli V (2019) Markers of central inflammation in major depressive disorder: A systematic review and meta-analysis of studies examining cerebrospinal fluid, positron emission tomography and post-mortem brain tissue. Brain Behav Immun 81: 24-40. DOI 10.1016/j.bbi.2019.06.015

46. Khandaker GM, Pearson RM, Zammit S, Lewis G, Jones PB (2014) Association of serum interleukin 6 and C-reactive protein in childhood with depression and psychosis in young adult life: a population-based longitudinal study. JAMA Psychiatry 71: 1121-1128. DOI 10.1001/jamapsychiatry.2014.1332

47. Bell JA, Kivimäki M, Bullmore ET, Steptoe A, Carvalho LA (2017) Repeated exposure to systemic inflammation and risk of new depressive symptoms among older adults. Transl Psychiatry 7: e1208. DOI 10.1038/tp.2017.155

48. Lamers F, Milaneschi Y, Smit JH, Schoevers RA, Wittenberg G, Penninx B (2019) Longitudinal Association Between Depression and Inflammatory Markers: Results From the Netherlands Study of Depression and Anxiety. Biol Psychiatry 85: 829-837. DOI 10.1016/j.biopsych.2018.12.020

49. Carvalho LA, Torre JP, Papadopoulos AS, Poon L, Juruena MF, Markopoulou K, Cleare AJ, Pariante CM (2013) Lack of clinical therapeutic benefit of antidepressants is associated overall activation of the inflammatory system. J Affect Disord 148: 136-140. DOI 10.1016/j.jad.2012.10.036

50. Machado MO, Oriolo G, Bortolato B, Köhler CA, Maes M, Solmi M, Grande I, Martín-Santos R, Vieta E, Carvalho AF (2017) Biological mechanisms of depression following treatment with interferon for chronic hepatitis C: A critical systematic review. J Affect Disord 209: 235-245. DOI 10.1016/j.jad.2016.11.039

51. Chiu WC, Su YP, Su KP, Chen PC (2017) Recurrence of depressive disorders after interferon-induced depression. Transl Psychiatry 7: e1026. DOI 10.1038/tp.2016.274

52. Wray NR, Ripke S, Mattheisen M, Trzaskowski M, Byrne EM, Abdellaoui A, Adams MJ, Agerbo E, Air TM, Andlauer TMF, et al. (2018) Genome-wide association analyses identify 44 risk variants and refine the genetic architecture of major depression. Nature genetics 50: 668-681. DOI 10.1038/s41588-018-0090-3

53. Khandaker GM, Zammit S, Burgess S, Lewis G, Jones PB (2018) Association between a functional interleukin 6 receptor genetic variant and risk of depression and psychosis in a population-based birth cohort. Brain Behav Immun 69: 264-272. DOI 10.1016/j.bbi.2017.11.020

54. Wingo TS, Liu Y, Gerasimov ES, Gockley J, Logsdon BA, Duong DM, Dammer EB, Lori A, Kim PJ, Ressler KJ, et al. (2021) Brain proteome-wide association study implicates novel proteins in depression pathogenesis. Nat Neurosci 24: 810-817. DOI 10.1038/s41593-021-00832-6

55. Branchi I, Poggini S, Capuron L, Benedetti F, Poletti S, Tamouza R, Drexhage HA, Penninx B, Pariante CM (2021) Brain-immune crosstalk in the treatment of major depressive disorder. European neuropsychopharmacology : the journal of the European College of Neuropsychopharmacology 45: 89-107. DOI 10.1016/j.euroneuro.2020.11.016

56. Miller AH, Raison CL (2015) Are Anti-inflammatory Therapies Viable Treatments for Psychiatric Disorders?: Where the Rubber Meets the Road. JAMA Psychiatry 72: 527-528. DOI 10.1001/jamapsychiatry.2015.22

57. Raison CL, Rutherford RE, Woolwine BJ, Shuo C, Schettler P, Drake DF, Haroon E, Miller AH (2013) A randomized controlled trial of the tumor necrosis factor antagonist infliximab for treatment-resistant depression: the role of baseline inflammatory biomarkers. JAMA Psychiatry 70: 31-41. DOI 10.1001/2013.jamapsychiatry.4

58. Torres-Platas SG, Cruceanu C, Chen GG, Turecki G, Mechawar N (2014) Evidence for increased microglial priming and macrophage recruitment in the dorsal anterior cingulate white matter of depressed suicides. Brain, behavior, and immunity 42: 50–59. DOI 10.1016/j.bbi.2014.05.007

59. Zhu CB, Lindler KM, Owens AW, Daws LC, Blakely RD, Hewlett WA (2010) Interleukin-1 receptor activation by systemic lipopolysaccharide induces behavioral despair linked to MAPK regulation of CNS serotonin transporters. Neuropsychopharmacology 35: 2510-2520. DOI 10.1038/npp.2010.116

60. Neurauter G, Schröcksnadel K, Scholl-Bürgi S, Sperner-Unterweger B, Schubert C, Ledochowski M, Fuchs D (2008) Chronic immune stimulation correlates with reduced phenylalanine turnover. Current drug metabolism 9: 622-627. DOI 10.2174/138920008785821738

61. Moncrieff J, Cooper RE, Stockmann T, Amendola S, Hengartner MP, Horowitz MA (2022) The serotonin theory of depression: a systematic umbrella review of the evidence. Mol Psychiatry. DOI 10.1038/s41380-022-01661-0

62. Monje ML, Toda H, Palmer TD (2003) Inflammatory blockade restores adult hippocampal neurogenesis. Science (New York, NY) 302: 1760–1765. DOI 10.1126/science.1088417

63. Koo JW, Duman RS (2008) IL-1beta is an essential mediator of the antineurogenic and anhedonic effects of stress. Proc Natl Acad Sci U S A 105: 751-756. DOI 10.1073/pnas.0708092105

64. Iosif RE, Ekdahl CT, Ahlenius H, Pronk CJ, Bonde S, Kokaia Z, Jacobsen SE, Lindvall O (2006) Tumor necrosis factor receptor 1 is a negative regulator of progenitor proliferation in adult hippocampal neurogenesis. J Neurosci 26: 9703-9712. DOI 10.1523/jneurosci.2723-06.2006

65. Han QQ, Yu J (2014) Inflammation: a mechanism of depression? Neuroscience bulletin 30: 515-523. DOI 10.1007/s12264-013-1439-3

66. Warden D, Rush AJ, Trivedi MH, Fava M, Wisniewski SR (2007) The STAR*D Project results: a comprehensive review of findings. Current psychiatry reports 9: 449-459. DOI 10.1007/s11920-007-0061-3

67. Rush AJ, Trivedi MH, Wisniewski SR, Nierenberg AA, Stewart JW, Warden D, Niederehe G, Thase ME, Lavori PW, Lebowitz BD, et al. (2006) Acute and longer-term outcomes in depressed outpatients requiring one or several treatment steps: a STAR*D report. Am J Psychiatry 163: 1905-1917. DOI 10.1176/ajp.2006.163.11.1905

68. Marx W, Penninx B, Solmi M, Furukawa TA, Firth J, Carvalho AF, Berk M (2023) Major depressive disorder. Nature reviews Disease primers 9: 44. DOI 10.1038/s41572-023-00454-1

69. Karrouri R, Hammani Z, Benjelloun R, Otheman Y (2021) Major depressive disorder: Validated treatments and future challenges. World journal of clinical cases 9: 9350-9367. DOI 10.12998/wjcc.v9.i31.9350

70. Hare BD, Duman RS (2020) Prefrontal cortex circuits in depression and anxiety: contribution of discrete neuronal populations and target regions. Mol Psychiatry 25: 2742-2758. DOI 10.1038/s41380-020-0685-9

71. Wittenberg GM, Stylianou A, Zhang Y, Sun Y, Gupta A, Jagannatha PS, Wang D, Hsu B, Curran ME, Khan S, et al. (2020) Effects of immunomodulatory drugs on depressive symptoms: A mega-analysis of randomized, placebo-controlled clinical trials in inflammatory disorders. Mol Psychiatry 25: 1275-1285. DOI 10.1038/s41380-019-0471-8

72. Ransohoff RM, Engelhardt B (2012) The anatomical and cellular basis of immune surveillance in the central nervous system. Nature reviews Immunology 12: 623-635. DOI 10.1038/nri3265

73. Iliff JJ, Wang M, Liao Y, Plogg BA, Peng W, Gundersen GA, Benveniste H, Vates GE, Deane R, Goldman SA, et al. (2012) A paravascular pathway facilitates CSF flow through the brain parenchyma and the clearance of interstitial solutes, including amyloid β. Sci Transl Med 4: 147ra111. DOI 10.1126/scitranslmed.3003748

74. Louveau A, Smirnov I, Keyes TJ, Eccles JD, Rouhani SJ, Peske JD, Derecki NC, Castle D, Mandell JW, Lee KS, et al. (2015) Structural and functional features of central nervous system lymphatic vessels. Nature 523: 337-341. DOI 10.1038/nature14432

75. Engelhardt B, Vajkoczy P, Weller RO (2017) The movers and shapers in immune privilege of the CNS. Nature immunology 18: 123-131. DOI 10.1038/ni.3666

76. Profaci CP, Munji RN, Pulido RS, Daneman R (2020) The blood-brain barrier in health and disease: Important unanswered questions. J Exp Med 217. DOI 10.1084/jem.20190062

77. Daneman R, Prat A (2015) The blood-brain barrier. Cold Spring Harbor perspectives in biology 7: a020412. DOI 10.1101/cshperspect.a020412

78. Abbott NJ, Patabendige AA, Dolman DE, Yusof SR, Begley DJ (2010) Structure and function of the blood-brain barrier. Neurobiol Dis 37: 13-25. DOI 10.1016/j.nbd.2009.07.030

79. Biswas P, Canosa S, Schoenfeld D, Schoenfeld J, Li P, Cheas LC, Zhang J, Cordova A, Sumpio B, Madri JA (2006) PECAM-1 affects GSK-3beta-mediated beta-catenin phosphorylation and degradation. The American journal of pathology 169: 314-324. DOI 10.2353/ajpath.2006.051112

80. Graesser D, Solowiej A, Bruckner M, Osterweil E, Juedes A, Davis S, Ruddle NH, Engelhardt B, Madri JA (2002) Altered vascular permeability and early onset of experimental autoimmune encephalomyelitis in PECAM-1-deficient mice. J Clin Invest 109: 383-392. DOI 10.1172/jci13595

81. Nitta T, Hata M, Gotoh S, Seo Y, Sasaki H, Hashimoto N, Furuse M, Tsukita S (2003) Size-selective loosening of the blood-brain barrier in claudin-5-deficient mice. J Cell Biol 161: 653-660. DOI 10.1083/jcb.200302070

82. Armulik A, Genové G, Mäe M, Nisancioglu MH, Wallgard E, Niaudet C, He L, Norlin J, Lindblom P, Strittmatter K, et al. (2010) Pericytes regulate the blood-brain barrier. Nature 468: 557-561. DOI 10.1038/nature09522

83. Siddharthan V, Kim YV, Liu S, Kim KS (2007) Human astrocytes/astrocyte-conditioned medium and shear stress enhance the barrier properties of human brain

microvascular endothelial cells. Brain research 1147: 39-50. DOI 10.1016/j.brainres.2007.02.029

84. Heithoff BP, George KK, Phares AN, Zuidhoek IA, Munoz-Ballester C, Robel S (2021) Astrocytes are necessary for blood-brain barrier maintenance in the adult mouse brain. Glia 69: 436-472. DOI 10.1002/glia.23908

85. Engelhardt B, Ransohoff RM (2012) Capture, crawl, cross: the T cell code to breach the blood-brain barriers. Trends Immunol 33: 579-589. DOI 10.1016/j.it.2012.07.004

86. Bartholomäus I, Kawakami N, Odoardi F, Schläger C, Miljkovic D, Ellwart JW, Klinkert WE, Flügel-Koch C, Issekutz TB, Wekerle H, et al. (2009) Effector T cell interactions with meningeal vascular structures in nascent autoimmune CNS lesions. Nature 462: 94-98. DOI 10.1038/nature08478

87. Waisman A, Johann L (2018) Antigen-presenting cell diversity for T cell reactivation in central nervous system autoimmunity. J Mol Med (Berl) 96: 1279-1292. DOI 10.1007/s00109-018-1709-7

88. Samuels JD, Lotstein ML, Lehmann ML, Elkahloun AG, Banerjee S, Herkenham M (2023) Chronic social defeat alters brain vascular-associated cell gene expression patterns leading to vascular dysfunction and immune system activation. J Neuroinflammation 20: 154. DOI 10.1186/s12974-023-02827-5

89. Menard C, Pfau ML, Hodes GE, Kana V, Wang VX, Bouchard S, Takahashi A, Flanigan ME, Aleyasin H, LeClair KB, et al. (2017) Social stress induces neurovascular pathology promoting depression. Nature neuroscience 20: 1752–1760. DOI 10.1038/s41593-017-0010-3.

90. Dion-Albert L, Cadoret A, Doney E, Kaufmann FN, Dudek KA, Daigle B, Parise LF, Cathomas F, Samba N, Hudson N, et al. (2022) Vascular and blood-brain barrier-related changes underlie stress responses and resilience in female mice and depression in human tissue. Nature communications 13: 164. DOI 10.1038/s41467-021-27604-x

91. Lehmann ML, Weigel TK, Cooper HA, Elkahloun AG, Kigar SL, Herkenham M (2018) Decoding microglia responses to psychosocial stress reveals blood-brain barrier breakdown that may drive stress susceptibility. Scientific reports 8: 11240. DOI 10.1038/s41598-018-28737-8

92. Lehmann ML, Poffenberger CN, Elkahloun AG, Herkenham M (2020) Analysis of cerebrovascular dysfunction caused by chronic social defeat in mice. Brain Behav Immun 88: 735-747. DOI 10.1016/j.bbi.2020.05.030

93. Lehmann ML, Samuels JD, Kigar SL, Poffenberger CN, Lotstein ML, Herkenham M (2022) CCR2 monocytes repair cerebrovascular damage caused by chronic social defeat stress. Brain Behav Immun 101: 346-358. DOI 10.1016/j.bbi.2022.01.011

94. Sawicki CM, McKim DB, Wohleb ES, Jarrett BL, Reader BF, Norden DM, Godbout JP, Sheridan JF (2015) Social defeat promotes a reactive endothelium in a brain region-dependent manner with increased expression of key adhesion molecules, selectins and chemokines associated with the recruitment of myeloid cells to the brain. Neuroscience 302: 151–164. DOI 10.1016/j.neuroscience.2014.10.004

95. Brevet M, Kojima H, Asakawa A, Atsuchi K, Ushikai M, Ataka K, Inui A, Kimura H, Sevestre H, Fujimiya M (2010) Chronic foot-shock stress potentiates the influx of bone marrow-derived microglia into hippocampus. Journal of neuroscience research 88: 1890–1897. DOI 10.1002/jnr.22362

96. Wohleb ES, Powell ND, Godbout JP, Sheridan JF (2013) Stress-induced recruitment of bone marrow-derived monocytes to the brain promotes anxiety-like behavior. The Journal of

neuroscience : the official journal of the Society for Neuroscience 33: 13820–13833. DOI 10.1523/jneurosci.1671-13.2013

97. Wohleb ES, Patterson JM, Sharma V, Quan N, Godbout JP, Sheridan JF (2014) Knockdown of interleukin-1 receptor type-1 on endothelial cells attenuated stress-induced neuroinflammation and prevented anxiety-like behavior. The Journal of neuroscience : the official journal of the Society for Neuroscience 34: 2583–2591. DOI 10.1523/jneurosci.3723-13.2014

98. McKim DB, Weber MD, Niraula A, Sawicki CM, Liu X, Jarrett BL, Ramirez-Chan K, Wang Y, Roeth RM, Sucaldito AD, et al. (2018) Microglial recruitment of IL-1β-producing monocytes to brain endothelium causes stress-induced anxiety. Molecular psychiatry 23: 1421–1431. DOI 10.1038/mp.2017.64.

99. Ambrée O, Ruland C, Scheu S, Arolt V, Alferink J (2018) Alterations of the Innate Immune System in Susceptibility and Resilience After Social Defeat Stress. Front Behav Neurosci 12: 141. DOI 10.3389/fnbeh.2018.00141

100. Lehmann ML, Cooper HA, Maric D, Herkenham M (2016) Social defeat induces depressive-like states and microglial activation without involvement of peripheral macrophages. J Neuroinflammation 13: 224. DOI 10.1186/s12974-016-0672-x

101. Gudmundsson P, Skoog I, Waern M, Blennow K, Pálsson S, Rosengren L, Gustafson D (2007) The relationship between cerebrospinal fluid biomarkers and depression in elderly women. Am J Geriatr Psychiatry 15: 832-838. DOI 10.1097/JGP.0b013e3180547091

102. Greene C, Hanley N, Campbell M (2020) Blood-brain barrier associated tight junction disruption is a hallmark feature of major psychiatric disorders. Transl Psychiatry 10: 373. DOI 10.1038/s41398-020-01054-3

103. Dinarello CA (2018) Overview of the IL-1 family in innate inflammation and acquired immunity. Immunological reviews 281: 8-27. DOI 10.1111/imr.12621

104. Sims JE, March CJ, Cosman D, Widmer MB, MacDonald HR, McMahan CJ, Grubin CE, Wignall JM, Jackson JL, Call SM, et al. (1988) cDNA expression cloning of the IL-1 receptor, a member of the immunoglobulin superfamily. Science 241: 585-589. DOI 10.1126/science.2969618

105. Greenfeder SA, Nunes P, Kwee L, Labow M, Chizzonite RA, Ju G (1995) Molecular cloning and characterization of a second subunit of the interleukin 1 receptor complex. The Journal of biological chemistry 270: 13757-13765. DOI 10.1074/jbc.270.23.13757

106. (!!! INVALID CITATION !!! {})

107. Hannum CH, Wilcox CJ, Arend WP, Joslin FG, Dripps DJ, Heimdal PL, Armes LG, Sommer A, Eisenberg SP, Thompson RC (1990) Interleukin-1 receptor antagonist activity of a human interleukin-1 inhibitor. Nature 343: 336-340. DOI 10.1038/343336a0

108. McMahan CJ, Slack JL, Mosley B, Cosman D, Lupton SD, Brunton LL, Grubin CE, Wignall JM, Jenkins NA, Brannan CI, et al. (1991) A novel IL-1 receptor, cloned from B cells by mammalian expression, is expressed in many cell types. The EMBO journal 10: 2821-2832. DOI 10.1002/j.1460-2075.1991.tb07831.x

109. Mantovani A, Dinarello CA, Molgora M, Garlanda C (2019) Interleukin-1 and Related Cytokines in the Regulation of Inflammation and Immunity. Immunity 50: 778-795. DOI 10.1016/j.immuni.2019.03.012

110. Cohen I, Rider P, Carmi Y, Braiman A, Dotan S, White MR, Voronov E, Martin MU, Dinarello CA, Apte RN (2010) Differential release of chromatin-bound IL-1alpha discriminates

between necrotic and apoptotic cell death by the ability to induce sterile inflammation. Proc Natl Acad Sci U S A 107: 2574-2579. DOI 10.1073/pnas.0915018107

111. Dinarello CA (2009) Immunological and inflammatory functions of the interleukin-1 family. Annual review of immunology 27: 519-550. DOI 10.1146/annurev.immunol.021908.132612

112. Fu J, Wu H (2023) Structural Mechanisms of NLRP3 Inflammasome Assembly and Activation. Annual review of immunology 41: 301-316. DOI 10.1146/annurev-immunol-081022-021207

113. Lima TS (2023) Beyond an inflammatory mediator: Interleukin-1 in neurophysiology. Exp Physiol 108: 917-924. DOI 10.1113/ep090780

114. Liu X, Quan N (2018) Microglia and CNS Interleukin-1: Beyond Immunological Concepts. Frontiers in neurology 9: 8. DOI 10.3389/fneur.2018.00008

115. Rothwell NJ, Luheshi GN (2000) Interleukin 1 in the brain: biology, pathology and therapeutic target. Trends in neurosciences 23: 618-625. DOI 10.1016/s0166-2236(00)01661-1

116. Basu A, Krady JK, Levison SW (2004) Interleukin-1: a master regulator of neuroinflammation. J Neurosci Res 78: 151-156. DOI 10.1002/jnr.20266

117. Pinteaux E, Trotter P, Simi A (2009) Cell-specific and concentration-dependent actions of interleukin-1 in acute brain inflammation. Cytokine 45: 1-7. DOI 10.1016/j.cyto.2008.10.008

118. Shaftel SS, Griffin WS, O'Banion MK (2008) The role of interleukin-1 in neuroinflammation and Alzheimer disease: an evolving perspective. J Neuroinflammation 5: 7. DOI 10.1186/1742-2094-5-7

119. Liu X, Nemeth DP, McKim DB, Zhu L, DiSabato DJ, Berdysz O, Gorantla G, Oliver B, Witcher KG, Wang Y, et al. (2019) Cell-Type-Specific Interleukin 1 Receptor 1 Signaling in the Brain Regulates Distinct Neuroimmune Activities. Immunity 50: 317-333.e316. DOI 10.1016/j.immuni.2018.12.012

120. Nemeth DP, Liu X, McKim DB, DiSabato DJ, Oliver B, Herd A, Katta A, Negray CE, Floyd J, McGovern S, et al. (2022) Dynamic Interleukin-1 Receptor Type 1 Signaling Mediates Microglia-Vasculature Interactions Following Repeated Systemic LPS. J Inflamm Res 15: 1575-1590. DOI 10.2147/jir.S350114

121. Lévesque SA, Paré A, Mailhot B, Bellver-Landete V, Kébir H, Lécuyer MA, Alvarez JI, Prat A, de Rivero Vaccari JP, Keane RW, et al. (2016) Myeloid cell transmigration across the CNS vasculature triggers IL-1β-driven neuroinflammation during autoimmune encephalomyelitis in mice. J Exp Med 213: 929-949. DOI 10.1084/jem.20151437

122. Nemeth DP, Liu X, Monet MC, Niu H, Maxey G, Schrier MS, Smirnova MI, McGovern SJ, Herd A, DiSabato DJ, et al. (2024) Localization of brain neuronal IL-1R1 reveals specific neural circuitries responsive to immune signaling. J Neuroinflammation 21: 303. DOI 10.1186/s12974-024-03287-1

123. Nemeth DP, Quan N (2021) Modulation of Neural Networks by Interleukin-1. Brain Plast 7: 17-32. DOI 10.3233/bpl-200109

124. Mendiola AS, Cardona AE (2018) The IL-1β phenomena in neuroinflammatory diseases. J Neural Transm (Vienna) 125: 781-795. DOI 10.1007/s00702-017-1732-9

125. Hauptmann J, Johann L, Marini F, Kitic M, Colombo E, Mufazalov IA, Krueger M, Karram K, Moos S, Wanke F, et al. (2020) Interleukin-1 promotes autoimmune

neuroinflammation by suppressing endothelial heme oxygenase-1 at the blood-brain barrier. Acta Neuropathol 140: 549-567. DOI 10.1007/s00401-020-02187-x

126. Moynagh PN (2005) The interleukin-1 signalling pathway in astrocytes: a key contributor to inflammation in the brain. J Anat 207: 265-269. DOI 10.1111/j.1469-7580.2005.00445.x

127. McCann SK, Cramond F, Macleod MR, Sena ES (2016) Systematic Review and Meta-Analysis of the Efficacy of Interleukin-1 Receptor Antagonist in Animal Models of Stroke: an Update. Transl Stroke Res 7: 395-406. DOI 10.1007/s12975-016-0489-z

128. Huang QJ, Jiang H, Hao XL, Minor TR (2004) Brain IL-1 beta was involved in reserpine-induced behavioral depression in rats. Acta pharmacologica Sinica 25: 293-296

129. Koo JW, Duman RS (2009) Evidence for IL-1 receptor blockade as a therapeutic strategy for the treatment of depression. Current opinion in investigational drugs (London, England : 2000) 10: 664-671

130. Strozyk EA, Desch A, Poeppelmann B, Magnolo N, Wegener J, Huck V, Schneider SW (2014) Melanoma-derived IL-1 converts vascular endothelium to a proinflammatory and procoagulatory phenotype via NFκB activation. Exp Dermatol 23: 670-676. DOI 10.1111/exd.12505

131. O'Carroll SJ, Kho DT, Wiltshire R, Nelson V, Rotimi O, Johnson R, Angel CE, Graham ES (2015) Pro-inflammatory TNFα and IL-1β differentially regulate the inflammatory phenotype of brain microvascular endothelial cells. J Neuroinflammation 12: 131. DOI 10.1186/s12974-015-0346-0

132. Labus J, Häckel S, Lucka L, Danker K (2014) Interleukin-1β induces an inflammatory response and the breakdown of the endothelial cell layer in an improved human THBMEC-based in vitro blood-brain barrier model. J Neurosci Methods 228: 35-45. DOI 10.1016/j.jneumeth.2014.03.002

133. Wong D, Dorovini-Zis K, Vincent SR (2004) Cytokines, nitric oxide, and cGMP modulate the permeability of an in vitro model of the human blood-brain barrier. Experimental neurology 190: 446-455. DOI 10.1016/j.expneurol.2004.08.008

134. Li Q, Powell N, Zhang H, Belevych N, Ching S, Chen Q, Sheridan J, Whitacre C, Quan N (2011) Endothelial IL-1R1 is a critical mediator of EAE pathogenesis. Brain Behav Immun 25: 160-167. DOI 10.1016/j.bbi.2010.09.009

135. Martins R, Carlos AR, Braza F, Thompson JA, Bastos-Amador P, Ramos S, Soares MP (2019) Disease Tolerance as an Inherent Component of Immunity. Annual review of immunology 37: 405-437. DOI 10.1146/annurev-immunol-042718-041739

136. McCandless EE, Budde M, Lees JR, Dorsey D, Lyng E, Klein RS (2009) IL-1R signaling within the central nervous system regulates CXCL12 expression at the blood-brain barrier and disease severity during experimental autoimmune encephalomyelitis. J Immunol 183: 613-620. DOI 10.4049/jimmunol.0802258

137. Blandino P, Barnum CJ, Deak T (2006) The involvement of norepinephrine and microglia in hypothalamic and splenic IL-1beta responses to stress. Journal of neuroimmunology 173: 87–95. DOI 10.1016/j.jneuroim.2005.11.021

138. Grippo AJ, Francis J, Beltz TG, Felder RB, Johnson AK (2005) Neuroendocrine and cytokine profile of chronic mild stress-induced anhedonia. Physiol Behav 84: 697-706. DOI 10.1016/j.physbeh.2005.02.011

139. Mekaouche M, Givalois L, Barbanel G, Siaud P, Maurel D, Malaval F, Bristow AF, Boissin J, Assenmacher I, Ixart G (1994) Chronic restraint enhances interleukin-1-beta release in the basal state and after an endotoxin challenge, independently of adrenocorticotropin and corticosterone release. Neuroimmunomodulation 1: 292-299. DOI 10.1159/000097179

140. DiSabato DJ, Yin W, Biltz RG, Gallagher NR, Oliver B, Nemeth DP, Liu X, Sheridan JF, Quan N, Godbout JP (2022) IL-1 Receptor-1 on Vglut2 (+) neurons in the hippocampus is critical for neuronal and behavioral sensitization after repeated social stress. Brain, behavior, & immunity - health 26: 100547. DOI 10.1016/j.bbih.2022.100547

141. Goshen I, Kreisel T, Ben-Menachem-Zidon O, Licht T, Weidenfeld J, Ben-Hur T, Yirmiya R (2008) Brain interleukin-1 mediates chronic stress-induced depression in mice via adrenocortical activation and hippocampal neurogenesis suppression. Molecular psychiatry 13: 717–728. DOI 10.1038/sj.mp.4002055;

142. Wang YL, Han QQ, Gong WQ, Pan DH, Wang LZ, Hu W, Yang M, Li B, Yu J, Liu Q (2018) Microglial activation mediates chronic mild stress-induced depressive- and anxiety-like behavior in adult rats. J Neuroinflammation 15: 21. DOI 10.1186/s12974-018-1054-3

143. Ramirez K, Sheridan JF (2016) Antidepressant imipramine diminishes stress-induced inflammation in the periphery and central nervous system and related anxiety- and depressive-like behaviors. Brain, behavior, and immunity 57: 293–303. DOI 10.1016/j.bbi.2016.05.008

144. Wohleb ES, Hanke ML, Corona AW, Powell ND, Stiner LTM, Bailey MT, Nelson RJ, Godbout JP, Sheridan JF (2011) β-Adrenergic receptor antagonism prevents anxiety-like behavior and microglial reactivity induced by repeated social defeat. The Journal of neuroscience : the official journal of the Society for Neuroscience 31: 6277–6288. DOI 10.1523/jneurosci.0450-11.2011

145. Wohleb ES, Fenn AM, Pacenta AM, Powell ND, Sheridan JF, Godbout JP (2012) Peripheral innate immune challenge exaggerated microglia activation, increased the number of inflammatory CNS macrophages, and prolonged social withdrawal in socially defeated mice. Psychoneuroendocrinology 37: 1491–1505. DOI 10.1016/j.psyneuen.2012.02.003

146. Brachman RA, Lehmann ML, Maric D, Herkenham M (2015) Lymphocytes from chronically stressed mice confer antidepressant-like effects to naive mice. The Journal of neuroscience : the official journal of the Society for Neuroscience 35: 1530–1538. DOI 10.1523/jneurosci.2278-14.2015

147. Weber MD, McKim DB, Niraula A, Witcher KG, Yin W, Sobol CG, Wang Y, Sawicki CM, Sheridan JF, Godbout JP (2019) The Influence of Microglial Elimination and Repopulation on Stress Sensitization Induced by Repeated Social Defeat. Biological psychiatry 85: 667–678. DOI 10.1016/j.biopsych.2018.10.009

148. Nie X, Kitaoka S, Tanaka K, Segi-Nishida E, Imoto Y, Ogawa A, Nakano F, Tomohiro A, Nakayama K, Taniguchi M, et al. (2018) The Innate Immune Receptors TLR2/4 Mediate Repeated Social Defeat Stress-Induced Social Avoidance through Prefrontal Microglial Activation. Neuron 99: 464-479.e467. DOI 10.1016/j.neuron.2018.06.035

149. DiSabato DJ, Nemeth DP, Liu X, Witcher KG, O'Neil SM, Oliver B, Bray CE, Sheridan JF, Godbout JP, Quan N (2021) Interleukin-1 receptor on hippocampal neurons drives social withdrawal and cognitive deficits after chronic social stress. Mol Psychiatry 26: 4770-4782. DOI 10.1038/s41380-020-0788-3

150. Pearson-Leary J, Eacret D, Bhatnagar S (2020) Interleukin-1α in the ventral hippocampus increases stress vulnerability and inflammation-related processes. Stress 23: 308-317. DOI 10.1080/10253890.2019.1673360

151. Goshen I, Yirmiya R (2009) Interleukin-1 (IL-1): a central regulator of stress responses. Front Neuroendocrinol 30: 30-45. DOI 10.1016/j.yfrne.2008.10.001

152. Goshen I, Yirmiya R, Iverfeldt K, Weidenfeld J (2003) The role of endogenous interleukin-1 in stress-induced adrenal activation and adrenalectomy-induced adrenocorticotropic hormone hypersecretion. Endocrinology 144: 4453-4458. DOI 10.1210/en.2003-0338

153. Koo JW, Russo SJ, Ferguson D, Nestler EJ, Duman RS (2010) Nuclear factor-kappaB is a critical mediator of stress-impaired neurogenesis and depressive behavior. Proceedings of the National Academy of Sciences of the United States of America 107: 2669–2674. DOI 10.1073/pnas.0910658107

154. Krishnan V, Nestler EJ (2011) Animal models of depression: molecular perspectives. Curr Top Behav Neurosci 7: 121-147. DOI 10.1007/7854_2010_108

155. Golden SA, Covington HE, Berton O, Russo SJ (2011) A standardized protocol for repeated social defeat stress in mice. Nature protocols 6: 1183–1191. DOI 10.1038/nprot.2011.361.

156. Krishnan V, Han M-H, Graham DL, Berton O, Renthal W, Russo SJ, Laplant Q, Graham A, Lutter M, Lagace DC, et al. (2007) Molecular adaptations underlying susceptibility and resistance to social defeat in brain reward regions. Cell 131: 391–404. DOI 10.1016/j.cell.2007.09.018

157. Abdulaal WH, Walker CR, Costello R, Redondo-Castro E, Mufazalov IA, Papaemmanouil A, Rothwell NJ, Allan SM, Waisman A, Pinteaux E, et al. (2016) Characterization of a conditional interleukin-1 receptor 1 mouse mutant using the Cre/LoxP system. European journal of immunology 46: 912-918. DOI 10.1002/eji.201546075

158. Ridder DA, Lang M-F, Salinin S, Roderer J-P, Struss M, Maser-Gluth C, Schwaninger M (2011) TAK1 in brain endothelial cells mediates fever and lethargy. The Journal of experimental medicine 208: 2615–2623. DOI 10.1084/jem.20110398

159. Mufazalov IA, Regen T, Schelmbauer C, Kuschmann J, Muratova AM, Nikolaev A, Müller W, Pinteaux E, Waisman A (2016) Generation of a Novel T Cell Specific Interleukin-1 Receptor Type 1 Conditional Knock Out Mouse Reveals Intrinsic Defects in Survival, Expansion and Cytokine Production of CD4 T Cells. PLoS One 11: e0161505. DOI 10.1371/journal.pone.0161505

160. Ludt A, Ustjanzew A, Binder H, Strauch K, Marini F (2022) Interactive and Reproducible Workflows for Exploring and Modeling RNA-seq Data with pcaExplorer, Ideal, and GeneTonic. Curr Protoc 2: e411. DOI 10.1002/cpz1.411

161. Zhu A, Ibrahim JG, Love MI (2019) Heavy-tailed prior distributions for sequence count data: removing the noise and preserving large differences. Bioinformatics 35: 2084-2092. DOI 10.1093/bioinformatics/bty895

162. Marini F, Ludt A, Linke J, Strauch K (2021) GeneTonic: an R/Bioconductor package for streamlining the interpretation of RNA-seq data. BMC Bioinformatics 22: 610. DOI 10.1186/s12859-021-04461-5

163. Liddelow SA, Barres BA (2017) Reactive Astrocytes: Production, Function, and Therapeutic Potential. Immunity 46: 957-967. DOI 10.1016/j.immuni.2017.06.006

164. Jurga AM, Paleczna M, Kuter KZ (2020) Overview of General and Discriminating Markers of Differential Microglia Phenotypes. Frontiers in cellular neuroscience 14: 198. DOI 10.3389/fncel.2020.00198

165. Munji RN, Soung AL, Weiner GA, Sohet F, Semple BD, Trivedi A, Gimlin K, Kotoda M, Korai M, Aydin S, et al. (2019) Profiling the mouse brain endothelial transcriptome in health and disease models reveals a core blood-brain barrier dysfunction module. Nature neuroscience. DOI 10.1038/s41593-019-0497-x

166. Fournier AP, Tastet O, Charabati M, Hoornaert C, Bourbonnière L, Klement W, Larouche S, Tea F, Wang YC, Larochelle C, et al. (2023) Single-Cell Transcriptomics Identifies Brain Endothelium Inflammatory Networks in Experimental Autoimmune Encephalomyelitis. Neurology(R) neuroimmunology & neuroinflammation 10. DOI 10.1212/nxi.0000000000200046

167. Jeong HW, Diéguez-Hurtado R, Arf H, Song J, Park H, Kruse K, Sorokin L, Adams RH (2022) Single-cell transcriptomics reveals functionally specialized vascular endothelium in brain. eLife 11. DOI 10.7554/eLife.57520

168. Ransohoff RM, Kivisäkk P, Kidd G (2003) Three or more routes for leukocyte migration into the central nervous system. Nature reviews Immunology 3: 569-581. DOI 10.1038/nri1130

169. Belzeaux R, Gorgievski V, Fiori LM, Lopez JP, Grenier J, Lin R, Nagy C, Ibrahim EC, Gascon E, Courtet P, et al. (2020) GPR56/ADGRG1 is associated with response to antidepressant treatment. Nature communications 11: 1635. DOI 10.1038/s41467-020-15423-5

170. Fu J, Wei C, Zhang W, Schlondorff D, Wu J, Cai M, He W, Baron MH, Chuang PY, Liu Z, et al. (2018) Gene expression profiles of glomerular endothelial cells support their role in the glomerulopathy of diabetic mice. Kidney international 94: 326-345. DOI 10.1016/j.kint.2018.02.028

171. Yin W, Swanson SP, Biltz RG, Goodman EJ, Gallagher NR, Sheridan JF, Godbout JP (2022) Unique brain endothelial profiles activated by social stress promote cell adhesion, prostaglandin E2 signaling, hypothalamic-pituitary-adrenal axis modulation, and anxiety. Neuropsychopharmacology 47: 2271-2282. DOI 10.1038/s41386-022-01434-x

172. Dudek KA, Dion-Albert L, Lebel M, LeClair K, Labrecque S, Tuck E, Ferrer Perez C, Golden SA, Tamminga C, Turecki G, et al. (2020) Molecular adaptations of the blood-brain barrier promote stress resilience vs. depression. Proc Natl Acad Sci U S A 117: 3326-3336. DOI 10.1073/pnas.1914655117

173. Porsolt RD, Le Pichon M, Jalfre M (1977) Depression: a new animal model sensitive to antidepressant treatments. Nature 266: 730-732. DOI 10.1038/266730a0

174. de Kloet ER, Molendijk ML (2016) Coping with the Forced Swim Stressor: Towards Understanding an Adaptive Mechanism. Neural plasticity 2016: 6503162. DOI 10.1155/2016/6503162

175. Molendijk ML, de Kloet ER (2019) Coping with the forced swim stressor: Current state-of-the-art. Behav Brain Res 364: 1-10. DOI 10.1016/j.bbr.2019.02.005

176. Commons KG, Cholanians AB, Babb JA, Ehlinger DG (2017) The Rodent Forced Swim Test Measures Stress-Coping Strategy, Not Depression-like Behavior. ACS Chem Neurosci 8: 955-960. DOI 10.1021/acschemneuro.7b00042

177. Anyan J, Amir S (2018) Too Depressed to Swim or Too Afraid to Stop? A Reinterpretation of the Forced Swim Test as a Measure of Anxiety-Like Behavior. Neuropsychopharmacology 43: 931-933. DOI 10.1038/npp.2017.260

178. Estanislau C, Ramos AC, Ferraresi PD, Costa NF, de Carvalho HM, Batistela S (2011) Individual differences in the elevated plus-maze and the forced swim test. Behav Processes 86: 46-51. DOI 10.1016/j.beproc.2010.08.008

179. Seibenhener ML, Wooten MC (2015) Use of the Open Field Maze to measure locomotor and anxiety-like behavior in mice. Journal of visualized experiments : JoVE: e52434. DOI 10.3791/52434

180. Kraeuter AK, Guest PC, Sarnyai Z (2019) The Elevated Plus Maze Test for Measuring Anxiety-Like Behavior in Rodents. Methods Mol Biol 1916: 69-74. DOI 10.1007/978-1-4939-8994-2_4

181. Lehmann ML, Weigel TK, Poffenberger CN, Herkenham M (2019) The Behavioral Sequelae of Social Defeat Require Microglia and Are Driven by Oxidative Stress in Mice. J Neurosci 39: 5594-5605. DOI 10.1523/jneurosci.0184-19.2019

182. Camilli C, Hoeh AE, De Rossi G, Moss SE, Greenwood J (2022) LRG1: an emerging player in disease pathogenesis. Journal of biomedical science 29: 6. DOI 10.1186/s12929-022-00790-6

183. Wang X, Abraham S, McKenzie JAG, Jeffs N, Swire M, Tripathi VB, Luhmann UFO, Lange CAK, Zhai Z, Arthur HM, et al. (2013) LRG1 promotes angiogenesis by modulating endothelial TGF-β signalling. Nature 499: 306-311. DOI 10.1038/nature12345

184. O'Connor MN, Kallenberg DM, Camilli C, Pilotti C, Dritsoula A, Jackstadt R, Bowers CE, Watson HA, Alatsatianos M, Ohme J, et al. (2021) LRG1 destabilizes tumor vessels and restricts immunotherapeutic potency. Med 2: 1231-1252.e1210. DOI 10.1016/j.medj.2021.10.002

185. Pang KT, Ghim M, Liu C, Tay HM, Fhu CW, Chia RN, Qiu B, Sarathchandra P, Chester AH, Yacoub MH, et al. (2021) Leucine-Rich α-2-Glycoprotein 1 Suppresses Endothelial Cell Activation Through ADAM10-Mediated Shedding of TNF-α Receptor. Frontiers in cell and developmental biology 9: 706143. DOI 10.3389/fcell.2021.706143

186. Johann L, Soldati S, Müller K, Lampe J, Marini F, Klein M, Schramm E, Ries N, Schelmbauer C, Palagi I, et al. (2023) A20 regulates lymphocyte adhesion in murine neuroinflammation by restricting endothelial ICOSL expression in the CNS. J Clin Invest 133. DOI 10.1172/jci168314

187. Yang L, Chen G, Mohanty S, Scott G, Fazal F, Rahman A, Begum S, Hynes RO, Xu L (2011) GPR56 Regulates VEGF production and angiogenesis during melanoma progression. Cancer Res 71: 5558-5568. DOI 10.1158/0008-5472.Can-10-4543

188. Wu J, Wang Z, Cai M, Wang X, Lo B, Li Q, He JC, Lee K, Fu J (2023) GPR56 Promotes Diabetic Kidney Disease Through eNOS Regulation in Glomerular Endothelial Cells. Diabetes 72: 1652-1663. DOI 10.2337/db23-0124

189. Qi W, Guan W (2024) GPR56: A potential therapeutic target for neurological and psychiatric disorders. Biochem Pharmacol 226: 116395. DOI 10.1016/j.bcp.2024.116395

190. Silvestre JS, Théry C, Hamard G, Boddaert J, Aguilar B, Delcayre A, Houbron C, Tamarat R, Blanc-Brude O, Heeneman S, et al. (2005) Lactadherin promotes VEGF-dependent neovascularization. Nat Med 11: 499-506. DOI 10.1038/nm1233

191. Larsson A, Peng S, Persson H, Rosenbloom J, Abrams WR, Wassberg E, Thelin S, Sletten K, Gerwins P, Westermark P (2006) Lactadherin binds to elastin--a starting point for medin amyloid formation? Amyloid 13: 78-85. DOI 10.1080/13506120600722530

192. Imaizumi T, Yoshida H, Satoh K (2004) Regulation of CX3CL1/fractalkine expression in endothelial cells. J Atheroscler Thromb 11: 15-21. DOI 10.5551/jat.11.15

193. Thomas P (2008) Characteristics of membrane progestin receptor alpha (mPRalpha) and progesterone membrane receptor component 1 (PGMRC1) and their roles in mediating rapid progestin actions. Front Neuroendocrinol 29: 292-312. DOI 10.1016/j.yfrne.2008.01.001

194. Pang Y, Thomas P (2018) Progesterone induces relaxation of human umbilical cord vascular smooth muscle cells through mPRα (PAQR7). Mol Cell Endocrinol 474: 20-34. DOI 10.1016/j.mce.2018.02.003

195. Mantel I, Sadiq BA, Blander JM (2022) Spotlight on TAP and its vital role in antigen presentation and cross-presentation. Mol Immunol 142: 105-119. DOI 10.1016/j.molimm.2021.12.013

196. Amara N, Cooper MP, Voronkova MA, Webb BA, Lynch EM, Kollman JM, Ma T, Yu K, Lai Z, Sangaraju D, et al. (2021) Selective activation of PFKL suppresses the phagocytic oxidative burst. Cell 184: 4480-4494.e4415. DOI 10.1016/j.cell.2021.07.004

197. Leung AK, Ramesh N, Vogel C, Unniappan S (2019) Nucleobindins and encoded peptides: From cell signaling to physiology. Adv Protein Chem Struct Biol 116: 91-133. DOI 10.1016/bs.apcsb.2019.02.001

198. Ye Z, Guo H, Wang L, Li Y, Xu M, Zhao X, Song X, Chen Z, Huang R (2022) GALNT4 primes monocytes adhesion and transmigration by regulating O-Glycosylation of PSGL-1 in atherosclerosis. J Mol Cell Cardiol 165: 54-63. DOI 10.1016/j.yjmcc.2021.12.012

199. Abadier M, Haghayegh Jahromi N, Cardoso Alves L, Boscacci R, Vestweber D, Barnum S, Deutsch U, Engelhardt B, Lyck R (2015) Cell surface levels of endothelial ICAM-1 influence the transcellular or paracellular T-cell diapedesis across the blood-brain barrier. European journal of immunology 45: 1043-1058. DOI 10.1002/eji.201445125

200. Harikumar KB, Yester JW, Surace MJ, Oyeniran C, Price MM, Huang WC, Hait NC, Allegood JC, Yamada A, Kong X, et al. (2014) K63-linked polyubiquitination of transcription factor IRF1 is essential for IL-1-induced production of chemokines CXCL10 and CCL5. Nature immunology 15: 231-238. DOI 10.1038/ni.2810

201. Vanlandewijck M, He L, Mäe MA, Andrae J, Ando K, Del Gaudio F, Nahar K, Lebouvier T, Laviña B, Gouveia L, et al. (2018) A molecular atlas of cell types and zonation in the brain vasculature. Nature 554: 475-480. DOI 10.1038/nature25739

202. Carare RO, Bernardes-Silva M, Newman TA, Page AM, Nicoll JA, Perry VH, Weller RO (2008) Solutes, but not cells, drain from the brain parenchyma along basement membranes of capillaries and arteries: significance for cerebral amyloid angiopathy and neuroimmunology. Neuropathology and applied neurobiology 34: 131-144. DOI 10.1111/j.1365-2990.2007.00926.x

203. Witcher KG, Yin W, Sheridan JF, Godbout JP (2019) Reply to: Microglia, Monocytes, and the Recurrence of Anxiety in Stress-Sensitized Mice. Biol Psychiatry 85: e69-e70. DOI 10.1016/j.biopsych.2019.01.026

204. Shirai, Y. (1921) On the transplantation of the rat sarcoma in adult heterogenous animals. Jap Med World 1 (1921): 14-15.

10 ACKNOWLEDGEMENTS

This work has been supported by the computing infrastructure provided by the Core Facility Bioinformatics at the University Medical Center Mainz.

11 EIDESSTATTLICHE VERSICHERUNG

Hiermit versichere ich, dass ich die von mir vorgelegte Dissertation angefertigt, die benutzten Quellen und Hilfsmittel vollständig angegeben und die Stellen der Arbeit, einschließlich Tabellen und Abbildungen, die andere Werke im Wortlaut oder dem Sinn nach entnommen sind, in jedem Einzelfall als Entlehnung kenntlich gemacht habe; dass diese Dissertation noch keiner anderen Fakultät oder Universität zur Prüfung vorgelegen hat, dass sie noch nicht veröffentlicht worden ist, sowie dass ich eine solche Veröffentlichung vor Abschluss des Promotionsverfahrens nicht vornehmen werde. Die Bestimmungen dieser Promotionsordnung sind mir bekannt. Die von mir vorgelegte Dissertation ist von Herrn Prof. Dr. Ari Waisman betreut worden.

Mainz, Februar 2025 Eva Charlotte Schramm-Hermann

12 CURRICULUM VITAE

13 PUBLICATIONS

Schramm E, Becker V, Palagi I, Müller M, Rösler T, Durak F, Ebering A, Karram K, von Stebut E, Schmeisser MJ, Waisman A. Constitutive expression of the deubiquitinating enzyme CYLD does not affect microglia phenotype or function in homeostasis and neuroinflammation. *J Mol Med (Berl)*. 2024. doi: 10.1007/s00109-024-02489-7. PMID: 39302418.

Johann L, Soldati S, Müller K, Lampe J, Marini F, Klein M, **Schramm E**, Ries N, Schelmbauer C, Palagi I, Karram K, Assmann JC, Khan MA, Wenzel J, Schmidt MH, Körbelin J, Schlüter D, van Loo G, Bopp T, Engelhardt B, Schwaninger M, Waisman A. A20 regulates lymphocyte adhesion in murine neuroinflammation by restricting endothelial ICOSL expression in the CNS. *J Clin Invest*. 2023. doi: 10.1172/JCI168314. PMID: 37856217.

Schramm E, Waisman A. Microglia as Central Protagonists in the Chronic Stress Response. *Neurol Neuroimmunol Neuroinflamm*. 2022. doi: 10.1212/NXI.0000000000200023. PMID: 36357946.

Frenis K, Helmstädter J, Ruan Y, **Schramm E**, Kalinovic S, Kröller-Schön S, Bayo Jimenez MT, Hahad O, Oelze M, Jiang S, Wenzel P, Sommer CJ, Frauenknecht KBM, Waisman A, Gericke A, Daiber A, Münzel T, Steven S. Ablation of lysozyme M-positive cells prevents aircraft noise-induced vascular damage without improving cerebral side effects. *Basic Res Cardiol.* 2021. doi: 10.1007/s00395-021-00869-5. PMID: 33929610.

Jordão MJC, Sankowski R, Brendecke SM, Sagar, Locatelli G, Tai YH, Tay TL, **Schramm E**, Armbruster S, Hagemeyer N, Groß O, Mai D, Çiçek Ö, Falk T, Kerschensteiner M, Grün D, Prinz M. Single-cell profiling identifies myeloid cell subsets with distinct fates during neuroinflammation. *Science*. 2019. doi: 10.1126/science.aat7554. PMID: 30679343.

Rubbenstroth D, Peus E, **Schramm E**, Kottmann D, Bartels H, McCowan C, Schulze C, Akimkin V, Fischer N, Wylezich C, Hlinak A, Spadinger A, Großmann E, Petersen H, Grundhoff A, Rautenschlein S, Teske L. Identification of a novel clade of group A rotaviruses in fatally diseased domestic pigeons in Europe. *Transbound Emerg Dis. 2019*. doi: 10.1111/tbed.13065. PMID: 30407742.